UNIVERSITY OF LONDON THESIS

Degree PhD Year 2007 Name of Author ZENNER, Helen Laura

The Biogenesis of Weibel-Palade Bodies

Helen Laura Zenner

A thesis submitted to the University of London for the degree of Doctor of Philosophy

October 2007

MRC Laboratory for Molecular Cell Biology
University College London
Gower Street
London WC1E 6BT

ProQuest LLC
789 East Eisenhower Parkway
P.O. Box 1346
Ann Arbor, MI 48106-1346

Declaration

I, Helen Laura Zenner, confirm that the work presented in this thesis is my own. Where information has been derived from other sources, I confirm that this has been indicated in the thesis.

Abstract

Weibel-Palade bodies (WPB) are the secretory lysosome-related organelles (LRO), of endothelial cells. The storage of both P-selectin and von Willebrand factor in the WPB means the organelles play key roles in both inflammation and haemostasis respectively. The storage of the VWF as tubules is responsible for the unique elongated shape of WPB, and, in turn, the organisation as tubules is essential to its release as functional platelet binding strings upon stimulation.

Whilst the functional importance of VWF tubulation is thus clear, the relationship between tubules and biogenesis has not been studied. This relationship has been investigated using the relatively new technique of high pressure freezing (HPF) and freeze substitution (FS) followed by electron microscopy to consider biogenesis at the ultrastructural level. Use of this technique indicates that tubules are able to form within the trans-Golgi network (TGN). The WPB then remain attached to the TGN by a membranous stalk and become filled with tubules. The VWF tubules in the immature WPB are disordered but during maturation there is a dramatic increase in the spatial organisation of the tubules and in organelle electron density. Another maturation step the WPB undergo is removal of unwanted material, indicated by the presence of clathrin-coated buds on the WPB. Additionally, the use of HPF-FS has raised questions concerning the role of the cytoskeleton in the formation of WPB and the machinery required for the scission of the WPB from the TGN. Preliminary experiments indicate that the actin cytoskeleton, Myosin VI, FAPP and dynamin may be involved in the biogenesis at the TGN.

Finally, since the WPB are described as LROs, it seems possible that a similar machinery may be involved in their biogenesis to other LROs. Hermansky-Pudlak syndrome (HPS) is an example of disease that affects LROs. The symptoms of the patients can be explained by defects in melanosome and platelet dense granules respectively. However, knocking down the HPS proteins that form the biogenesis of lysosome-related organelles complexes (BLOC) two and three in endothelial cells has no effect on the biogenesis of WPB.

Acknowledgements

Firstly, I would like to thank Dan, my supervisor, for allowing me to develop my own ideas, but always providing support and advice throughout my PhD (and, of course, for allowing me to remain in the lab after I asked him if I could inherit the lab if anything should happen to him!)

Within the Cutler lab, there are other two people who have, in particular, made an enormous contribution to my thesis: Winnie, who taught me most of what I know and always being there to give me advice and Tom, who as well as keeping me laughing, has continually been ready to lend a hand and provide guidance; it has been a pleasure to share the HPS's with you! In addition I would like to thank Kim for not deserting me for her record label, Marnie for the glory bench, 'Technical' Tim for always giving 'detailed' advice, 'little' Dan for lending me his bench at weekends and Krupa for the random facts and career advice.

Thanks also to Lucy and Greg for starting the high pressure freezing project and allowing me to join them. Furthermore, my journey into the EM world would not have been possible without Jemima, who was always willing to do 'a quick bit of sectioning' and providing advice throughout the HPF saga.

My PhD would not have been half as much fun without my PhD year; Andy, Doug, Emma, Sean, Silene and Tom. Also, thanks to my two desk mates in the LMCB, Aron and Catherine for not minding being interrupted with 'quick' questions or my messy desk. Thanks to Ale, my compatriot in the Cutler lab, for always being on hand for those emergencies that require chocolate or alcohol and of course for all of the invitations to dinner.

Thanks to my parents for always supporting the decisions I have made and for, at times, pretending to know what I am talking about when I ring to tell them about an exciting result I have had. Finally, thanks to Miguel for putting up with me whilst I wrote this thesis and the ImageJ macro!

Table of Contents

1 INTRODUCTION 12

1.1 VON WILLEBRAND FACTOR 12

1.1.1 Von Willebrand disease 13

1.1.2 Biosynthesis of VWF 14

1.1.3 Multimerisation and tubulation 16

1.2 BIOGENESIS FROM THE TGN 19

1.2.1 A role for AP-1 in the earliest stage of biogenesis 19

1.2.2 A role for the cytoskeleton? 19

1.2.3 Scission from the Golgi 22

1.3 RECRUITMENT OF PROTEINS TO WPB 24

1.3.1 Recruitment of P-selectin 24

1.3.2 Recruitment of other proteins at the TGN 25

1.3.3 Delivery of proteins post-TGN 26

1.4 EXOCYTOSIS OF WPB 28

1.4.1 Activators of exocytosis 28

1.4.2 Molecular Machinery 29

1.5 LRO AND DISEASE 30

1.5.1 Hermansky-Pudlak syndrome 31

1.5.2 BLOC proteins 32

1.5.3 BLOC1 34

1.5.4 BLOC-2 35

1.5.5 BLOC-3 37

1.5.6 Double and triple mutants 38

1.5.7 BLOCs are not required for all LRO biogenesis 38

1.6 OBJECTIVES 39

2 MATERIALS AND METHODS 40

2.1 CELL CULTURE 40

2.1.1 Cell lines and maintenance 40

2.1.2 Freezing and thawing cultured cells 40

2.1.3 Transient transfections 40

2.1.4 Microinjection 41

2.1.5 Inhibitor studies 42

2.1.6 Immunofluorescence microscopy 43

2.1.7 Timelapse microscopy 44

2.2 ELECTRON MICROSCOPY 45

2.2.1 High pressure freezing 45

2.2.2 *Freeze substitution* 45
2.2.3 *Electron microscopy* 46
2.3 MOLECULAR BIOLOGY 47
2.3.1 *Polymerase chain reaction* 47
2.3.2 *Restriction digests* 47
2.3.3 *Agarose gel electrophoresis* 47
2.3.4 *Extraction of DNA from agarose gels* 48
2.3.5 *Ligations* 48
2.3.6 *Transformation of E.coli by 'heat shock'* 48
2.3.7 *Bacterial DNA preps* 49
2.3.8 *HPS3 construct* 49
2.3.9 *RNA extraction* 49
2.3.10 *Reverse transcription* 49
2.3.11 *DNA quantitation* 50
2.3.12 *Real time PCR* 50
2.4 BIOCHEMISTRY 51
2.4.1 *Secretion assay* 51
2.4.2 *ELISA* 52
2.4.3 *SDS polyacrylamide gel electrophoresis* 52
2.4.4 *Western blotting* 53
2.4.5 *Co-immunoprecipitations* 54
2.5 COMPUTATIONAL SOFTWARE 55

3 HIGH PRESSURE FREEZING AND WPB 56

3.1 INTRODUCTION 56
3.2 RESULTS 59
3.2.1 *Tubulation in the TGN* 61
3.2.2 *Stalk-like structures maintain the connection between the forming WPB and the TGN* 62
3.2.3 *The relationship between the tubules and membrane in immature WPB is complex* 65
3.2.4 *Maturation: a second role for clathrin?* 68
3.2.5 *Cargo concentration in the mature WPB* 70
3.2.6 *An alternative organelle* 74
3.2.7 *Fusion of WPB* 75
3.2.8 *Disruption of tubules* 80
3.3 DISCUSSION 82
3.3.1 *Tubule formation* 83
3.3.2 *Clathrin coating* 83
3.3.3 *Tubules and the membrane* 85
3.3.4 *Maturation* 86

3.3.5 *Fusion and flexion* ... 87
3.3.6 *Use of HPF in analysis of WPB formation* ... 88

4 FORMATION OF WPB AT THE TGN ... 89

4.1 INTRODUCTION ... 89
4.2 RESULTS ... 90
4.2.1 *Co-localisation between TGN, cytoskeleton and WPB* ... 90
4.2.2 *Formation of recombinant WPB* ... 92
4.2.3 *Microtubules and the biogenesis of WPB* ... 95
4.2.4 *Actin and the biogenesis of WPB* ... 97
4.2.5 *Motor proteins and WPB biogenesis* ... 99
4.2.6 *Hip1R and WPB biogenesis* ... 106
4.2.7 *Regulation of budding and scission* ... 107
4.2.8 *Scission from the Golgi* ... 109
4.2.8.1 PKD and WPB ... 110
4.2.8.2 Dynamin-2 and Scission from the TGN ... 113
4.3 DISCUSSION ... 115
4.3.1 *The cytoskeleton and the biogenesis of WPB* ... 115
4.3.2 *Actin motors and the biogenesis of WPB* ... 116
4.3.3 *Hip1R and the biogenesis of WPB* ... 117
4.3.4 *Regulation of scission* ... 117
4.3.5 *Scission from the Golgi* ... 118
4.3.6 *Roles for other proteins at the TGN* ... 119

5 HERMANSKY-PUDLAK SYNDROME AND WPB ... 120

5.1 INTRODUCTION ... 120
5.2 RESULTS ... 123
5.2.1 *BLOC-2 localisation* ... 124
5.2.2 *BLOC-2 knockdown and association of membrane proteins* ... 128
5.2.3 *BLOC-2 knockdown and exocytosis* ... 134
5.2.4 *BLOC-2 and AP-3 double knockdown* ... 138
5.2.5 *BLOC-3 knockdown & the recruitment of WPB-specific membrane-associated proteins* ... 139
5.2.6 *BLOC-3 and exocytosis* ... 143
5.2.7 *BLOC-3, LAMP-1 and CD63* ... 143
5.2.8 *BLOC-2 and BLOC-3 double knockdown* ... 145
5.3 DISCUSSION ... 147
5.3.1 *HPS3 and clathrin* ... 147
5.3.2 *BLOC-2 is not involved in WPB biogenesis* ... 148
5.3.3 *The function of BLOC-3 in endothelial cells* ... 148
5.3.4 *LRO – the differences* ... 149

5.3.5 Use of siRNA *150*

6 SUMMARY AND DISCUSSION **151**

6.1 HIGH PRESSURE FREEZING AND WPB BIOGENESIS 151

6.2 FORMATION OF WPB AT THE TGN 154

6.3 HERMANSKY-PUDLAK SYNDROME, WPB AND OTHER LRO 156

7 APPENDIX **158**

7.1 APPENDIX I 158

7.2 APPENDIX II 159

List of Figures

Figure 1.1 The formation of tubules and their importance in VWF function. 18
Figure 1.2 The biogenesis of WPB. 28
Figure 3.1 Cultures of HUVECs prepared for conventional transmission EM after chemical fixation give hints of the early biogenesis itinerary of WPB. 58
Figure 3.2 The membrane of the WPB is wrapped directly around VWF tubules in EM images after chemical fixation. 59
Figure 3.3 Use of HPF-FS results in better preservation of HUVEC. 61
Figure 3.5 WPB remain attached to the TGN by membranous stalks and the tubules may be important in ensuring that premature scission doesn't take place. 64
Figure 3.6 The tubules in immature WPB are disordered and are able to contact each other or the membrane along their long axis. 66
Figure 3.7 The width of the WPB is determined by the number of tubules incorporated. 67
Figure 3.8 Clathrin has a dual role in the biogenesis of WPB 69
Figure 3.9 Mature WPB are more electron-dense than immature WPB and the relationship between the tubules and between the tubules and membrane is less complex. 71
Figure 3.10 A low power view of an endothelial cell showing both immature and mature WPB. 72
Figure 3.11 Mature WPB are, on average, narrower than immature WPB. 73
Figure 3.12 Elongated structures that have no obvious tubular structure are also found in HUVEC. 75
Figure 3.13 The mature WPB are longer and have a bigger surface area than immature WPB. 76
Figure 3.14 WPB appear to undergo homotypic fusion. 77
Figure 3.15 WPB may be able to undergo homotypic fusion. 79
Figure 3.16 WPB are able to bend at sharp angles as tubules within the organelle break. 80
Figure 3.17 Monensin treated WPB. 81
Figure 3.18 DTT treated WPB have narrower tubules than untreated WPB. 82
Figure 4.1 VWF and tubulin co-localise next to the MTOC and in the cell periphery. 91
Figure 4.2 Limited co-localisation between VWF and actin. 92
Figure 4.3 WPB are able to form at 20℃ 93
Figure 4.4 Incubation of cells at 18℃ or 21℃ does not lead to an accumulation of VWF in the TGN. 94
Figure 4.5 WPB formation is not dependent on microtubules. 96
Figure 4.6 WPB formation is not dependent on the activity of kinesin. 97

Figure 4.7 Actin is involved in the formation of WPB. 98
Figure 4.8 Reduction in VWF-GFP positive WPB after cytochalasin D treatment. 99
Figure 4.7 Myosin II activity is not required for the formation of WPB. 100
Figure 4.8 Myosin VI may play a role in the biogenesis of WPB. 102
Figure 4.9 Myosin VI may play a role in the formation of pseudo-WPB in HEK293 cells. 103
Figure 4.10 Only 50% of cells expressing Myosin VI tail-only and VWF are able to make WPB. 104
Figure 4.11 Some limited co-localisation between Rab8-GFP and VWF, but expression of Rab8Q67L has no effect on biogenesis of WPB. 105
Figure 4.12 Depletion of Hip1R has no effect on release of VWF from HUVEC. 107
Figure 4.13 FAPP may play a role in the regulation of scission of WPB. 109
Figure 4.14 Localisation of PKD-kinase dead to the Golgi results in a failure to make elongated WPB. 111
Figure 4.15 Stimulated release of VWF is reduced in HEK293 cells expressing VWF and PKD kinase dead, compared with wild type. 112
Figure 4.16 Dynamin 2 may be required for scission of WPB from the TGN. 114
Figure 5.1 Knockdown of BLOC-1 results in a greater than two-fold reduction in stimulated release. 120
Figure 5.2 Recruitment of membrane proteins to WPB. 122
Figure 5.3 HPS3-GFP is cytosolic and does not colocalise with VWF-positive WPB. 125
Figure 5.4 Expression of mutant HPS3 construct lacking the clathrin binding domain has no effect on the biogenesis of WPB. 127
Figure 5.5 HPS3 does not interact with clathrin in endothelial cells. 128
Figure 5.6 Nucleofection of HPS3-1 siRNA causes a loss of WPB from HUVEC. 129
Figure 5.7 Knockdown of HPS3 results in a 50% reduction of WPB in HUVEC 130
Figure 5.8 HPS3 knockdown in HUVEC has no effect on the localisation of membrane proteins. 132
Figure 5.9 HPS5 does not play a role in the localisation WPB membrane proteins. 133
Figure 5.10 HPS6 does not play a role in the localisation of WPB membrane proteins. 134
Figure 5.11 Depletion of BLOC-2 has no effect on stimulated release of VWF. 136
Figure 5.12 BLOC-2 depletion has no effect on localisation of WPB membrane proteins. 137
Figure 5.13 Knockdown of BLOC-2 and AP-3 together has no additional effect on delivery of CD63. 138
Figure 5.14 WPB membrane proteins are localised normally in the absence of HPS1. 140
Figure 5.15 WPB membrane proteins are localised normally in the absence of HPS4. 141

List of Tables

Table 1.1 Proteins and complexes associated with Hermansky-Pudlak syndrome. 31

Table 2.1 Details of constructs used in this study. 41

Table 2.2 Details of siRNA oligos used in this study. 42

Table 2.3 List of inhibitors used in this study and their working concentration. 43

Table 2.4 List of primary antibodies used in this study. 44

Table 2.5 List of secondary antibodies used for immunofluorescence in this study 44

Table 2.6 Composition of epon used for embedding. 46

Table 2.7 Primers used to make HPS3-GFP. 49

Table 2.8 Primers used in the real time PCR. 50

Table 2.9 Cycling conditions used for real time PCR 51

Table 2.10 Constituents of polyacrylamide resolving and stacking gels. 53

Table 2.11 List of antibodies used for Western blotting and immunoprecipitation. 54

Table 5.1 % knockdown of HPS mRNA compared to cells mock transfected. 124

1 Introduction

Weibel-Palade bodies (WPB) were discovered in 1964 by Ewald Weibel and George Palade. They described "a hitherto unknown rod-shaped cytoplasmic component which consists of a bundle of fine tubules, enveloped by a tight fitting membrane," using electron microscopy of endothelial cells lining small arteries in a variety of organs in both rat and human (Weibel and Palade, 1964). However, they could not ascribe a function to the structure they described. Current understanding is that the organelle is important for storing components involved in both haemostasis and inflammation, due to the presence of two proteins stored in the WPB, von Willebrand factor (VWF) and P-selectin respectively. Other proteins incorporated into the WPB also have roles to play in these processes, but the aforementioned proteins are best-understood. The storage of VWF and P-selectin in WPB is required for a rapid release following secretagogue stimulation. However, whilst these proteins are absolutely required for the function of WPB; it is other proteins and additional features such as the presence of the tetraspanin CD63, plus the low intra-organellar pH that they share with lysosomes and other specialized post-Golgi organelles, that lead them to be classified in the family of lysosome-related organelles (LRO). Examples of other LRO are melanosomes, platelet dense granules, platelet alpha granules and secretory lysosomes such as the lytic granules present in cytotoxic T lymphocytes (CTL). The biogenesis of WPB is, therefore, likely to require some of the same components involved in the biogenesis of other LRO, as well as some components unique to WPB.

1.1 Von Willebrand factor

In 1982, Wagner et al. demonstrated that von Willebrand factor (VWF), a previously described haemostatic protein, is localised to WPB using both immunofluorescence and electron microscopy (Wagner et al., 1982). However, it is only recently that the fundamental importance of this protein in forming WPB has been demonstrated by its ability to drive the formation of pseudo-WPB in non-endothelial cell lines such as HEK293 and AtT20 cells (Blagoveshchenskaya et al., 2002; Michaux et al., 2003;

Wagner et al., 1991). These pseudo-WPB recruit the membrane proteins characteristic of WPB (which will be described in more detail later in the text) and are responsive to secretagogue. VWF plays a role in both primary and secondary haemostasis: The former by binding platelets at the site of injury, by interaction with the high molecular forms of VWF as platelet-capturing strings of up to 100 micrometres (Dong et al., 2002), to form an unstable platelet clump and the latter by the low molecular weight forms acting as a chaperone to another haemostatic protein, Factor VIII, which is part of the protease cascade necessary for formation of a stable clot (Lollar, 1991; Lollar et al., 1988). It is the high molecular weight forms that are stored within the WPB.

1.1.1 Von Willebrand disease

Certain mutations in von Willebrand factor cause Von Willebrand disease, a haemorrhagic condition described by Dr. von Willebrand in 1926 and initially referred to as pseudohaemophilia. It is characterised by prolonged bleeding times, mucocutaneous bleeding and has an estimated prevalence of up to 1% in some human populations. The disease can be divided into three types, Type 1, 2 and 3 (Sadler and Gralnick, 1994). The most common form is Type 1, accounting for roughly 70% of VWD, which is characterised by a reduced level of VWF in the blood. The mutations in VWF, normally substitutions, result in increased ER retention and proteasomal degradation. Type 2 accounts for 30% of VWD and broadly describes all the patients suffering from qualitative defects, and is subdivided further into categories A, B, M and N, as well as Vincenza variant, with super-high molecular weight multimers. Like Type 1, most mutations are substitutions and the defects include reduced binding to Factor VIII (2N), reduced binding to platelets (2A and 2M) or increased binding to platelets (2B and Vincenza). Type 3 VWD is the most severe form of the disease but accounts for only 1-2% of all cases. It is characterised by an almost complete lack of plasma VWF, as a result of rearrangements and deletion in the VWF gene, sometimes leading to retention of the protein in the ER. The study of VWF patients has contributed to the elucidation of the roles for the various domains of VWF (Michaux and Cutler, 2004). Some of these domains are required for the correct storage of VWF in WPB, whilst

others play critical roles in binding platelets and collagen upon exocytosis, as discussed later.

1.1.2 Biosynthesis of VWF

VWF is a large multimeric glycoprotein of approximately 350kDa, in its monomeric form. It is synthesised as a precursor called pre-pro-VWF. The precursor consists of a 22-aa signal sequence, a 741-aa propeptide and a 2050-aa mature VWF protein. It can be divided into the signal sequence, and domains D1-D2-D'-D3-A1-A2-A3-A4-D4-B-C1-C2, of which D1-D2 comprise the propeptide and subsequent domains make up the mature VWF monomer (Michaux and Cutler, 2004). In addition the protein is extensively modified as it passes through the secretory pathway.

As with any secretory protein, the pre-pro-VWF first enters the ER at which point the signal sequence is cleaved. The pro-VWF is then modified with the addition of N-linked oligosaccharides and formation disulfide bonds, leading to C-terminal dimerisation (Titani et al., 1986; Voorberg et al., 1991). Studies by Tjernberg et al. (2004) identified the residues important for dimerisation. They expressed the C2671Y, C2739Y, and C2754W mutants of VWF in HEK293T cells and demonstrated they are unable to form pseudo-WPB (Tjernberg et al., 2004). C-terminal dimerisation is required for efficient exit from the ER and deletion of this region leads degradation from the ER, whereas when expressed alone the C-terminal is able to dimerise and exit the ER (Voorberg et al., 1991).

Upon exit, VWF enters the Golgi where it undergoes further glycosylation and sulfation, at either termini. These modifications are found at binding sites for heparin, collagen type I, platelet glycoprotein (GP) Ib, factor VIIIC in the N-terminus and platelet GP IIb and IIa in the C-terminus (Ruggeri, 2007). Mutations in genes responsible for the addition of these moieties as well as mutations in the glycosylation and sulfation sites themselves can cause VWD. Indeed it is perhaps unsurprising given that 20% of the mass of the VWF is made up of oligosaccharide that glycosylation so important for the

function of VWF (Millar and Brown, 2006; Vlot et al., 1998). Generally, glycosylation is found to: protect VWF from proteolytic cleavage, maintain the multimeric structure and to be required for interactions with platelets and collagen. There are 12 N-linked oligosaccharide chains and 10 O-linked oligosaccharide chains (Titani et al., 1986). The N-linked chains terminate with a sialic acid, and it is the addition of this carbohydrate moiety that is particularly important (Samor et al., 1982). As long ago as 1976, Gralnick et al. found that a reduction in sialylation of VWF was associated with VWD (Gralnick et al., 1976). More recently a mouse with a genetic lesion inactivating the ST3Gal IV sialytransferase was found to have increased bleeding times and a dramatic reduction in the half-life of VWF in the circulation, from 4.5 hours in the case of wild type VWF to 1.9 hours for VWF from the homozygous ST3Gal IV mouse (Ellies et al., 2002).

It is surmised that the cleavage of the propeptide from mature VWF occurs in the trans-Golgi network (TGN). VWF is cleaved after residue 763, C-terminal to a consensus R-S-K-R site (Wise et al., 1988). Furin, the candidate enzyme for this event, is located in the TGN (Wise et al., 1991). In addition to cleavage, multimerisation is also thought to occur in the TGN (Federici et al., 1989; Vischer and Wagner, 1994). Extensive multimerisation leads to the formation of the high molecular weight VWF multimers, between 500-20,000 kDa. These multimers are required for its haemostatic function, since high molecular weight multimers are particularly efficient in platelet binding (Federici et al., 1989). The disulfide bridges form between the cysteine residues in the D3 domain of the mature VWF and the cysteine residues in both the D1-D2 domains of the propeptide. The propeptide acts as a guide to ensure that the adjacent VWF dimers are aligned correctly (Rosenberg et al., 2002). Mutations in both the propeptide, R273W, and in the mature VWF, C788R, cause both Type 1 and Type 3 VWD, resulting in only dimers and low molecular weight multimers being present in the plasma, whereas these mutations do not prevent storage (Allen et al., 2000a; Allen et al., 2000b; Michaux et al., 2003). The critically important association between propeptide and mature VWF is dependent on an acidic pH and high calcium concentration, conditions that prevail in the TGN (Mayadas and Wagner, 1989; Wagner et al., 1986).

1.1.3 Multimerisation and tubulation

Y87S is a mutation found in patients with VWD. The mutation occurs in the pro-region of VWF and affects multimerisation (Rosenberg et al., 2002). Consequently Y87S patients have a preponderance of dimers in plasma. However, although it prevents multimerisation it does not prevent the storage of VWF, in granular structures in AtT-20 cell model and in VWF null canine endothelial cells, this indicates that multimerisation is not a required for storage (Haberichter et al., 2005; Rosenberg et al., 2002). This confirms an earlier finding of Mayadas and Wagner; they introduced a mutant that prevents multimerisation, but it was still stored (Mayadas and Wagner, 1992). In addition, Michaux et al. 2006 find that expression of either the propeptide or mature VWF is able to trigger the formation of round VWF positive structures in HEK293 cells (Michaux et al., 2006a). This is contradicted by data from Habericter and co-workers indicating that only the propeptide is occasionally stored when expressed alone in the canine VWD cells (Haberichter et al., 2003). The authors show however, that if the propeptide is fused to another protein, C3α in this case, it is sufficient to induce storage of both proteins.

Recently it has been shown that it is the tubulation of VWF that is responsible for the characteristic elongated shape of the WPB (Michaux et al., 2006a; Wagner et al., 1991). Characterisation of a series of deletion mutants indicated that the D1-A1 domains, which include the propeptide and the region of the mature VWF that interacts with the propeptide, are necessary and sufficient to promote elongation of WPB, though the VWF stored in the resultant structures lacks much of the haemostatic function. This research also highlighted the importance of the pH-dependent interaction between the propeptide and mature VWF in elongation. However, despite multimerisation being dependent on this same interaction it does not play a role in elongation. This was shown in three ways, firstly there a dramatic rounding of post-Golgi WPB following treatment with monensin. Monensin treatment disrupts the pH dependent interaction between the propeptide and the mature protein (Wagner et al., 1985), but since the disulfide bonds have already formed, this treatment cannot affect multimerisation. Conversely, disruption of disulfide bonds using DTT has no effect of the shape of the WPB

(Michaux et al., 2006a). Finally, the expression of two human variants of VWF, R273W and C788R, which have almost identical multimerisation defects, results, in the case of the former, in an almost total abolition in elongation, whilst the latter has no significant effect on WPB shape (Michaux et al., 2003). The importance of the interaction for both processes explains why many of the mutations affecting multimerisation also effect elongation, for example Y87S.

Tubulation and multimerisation both have functional importance. The tubulation may allow for the 100-fold compaction of the VWF required for string formation and efficient storage. Multimerisation is presumably necessary to allow for effective unfurling of the VWF strings that have high affinity binding sites for the platelet glycoproteins, Ib and IIb/IIIa (Federici et al., 1989; Haberichter et al., 2005; Michaux et al., 2006a). Interestingly, this high degree of organisation doesn't preclude movement around the cell since the tubules are able to break at the points that the organelle forms hinges (Zenner et al., 2007). A schematic diagram outlining the biosynthesis of VWF, from the domain structure to the formation of tubules and then the packaging of the VWF tubules into the WPB to the formation of strings upon exocytosis is outlined in Figure 1.1 (with permission from Michaux and Cutler).

However, not all of the VWF is fated to be incorporated into WPB and undergo regulated release. Whilst the highest molecular weight multimers, which have high affinity binding sites for the platelet glycoproteins, are incorporated into the WPB, the lower molecular weight VWF is constitutively secreted. The pool of constitutively released VWF consists of partially cleaved dimeric and low molecular weight multimers. It has been suggested that up to 95% of VWF is secreted by the constitutive pathway (Mayadas et al., 1989), although this is controversial, with others claiming that released VWF derives only from the WPB that comprise the storage pool (Tsai et al., 1991). A role for the low molecular weight multimers in acting as a chaperone for Factor VIII, may suggest that the former is correct. However, deregulation of WPB exocytosis, resulting in uncontrolled release of very pro-thrombotic high molecular weight multimers into the bloodstream, could have severe haemostatic consequences,

hence the regulation and storage in WPB is of the upmost importance.

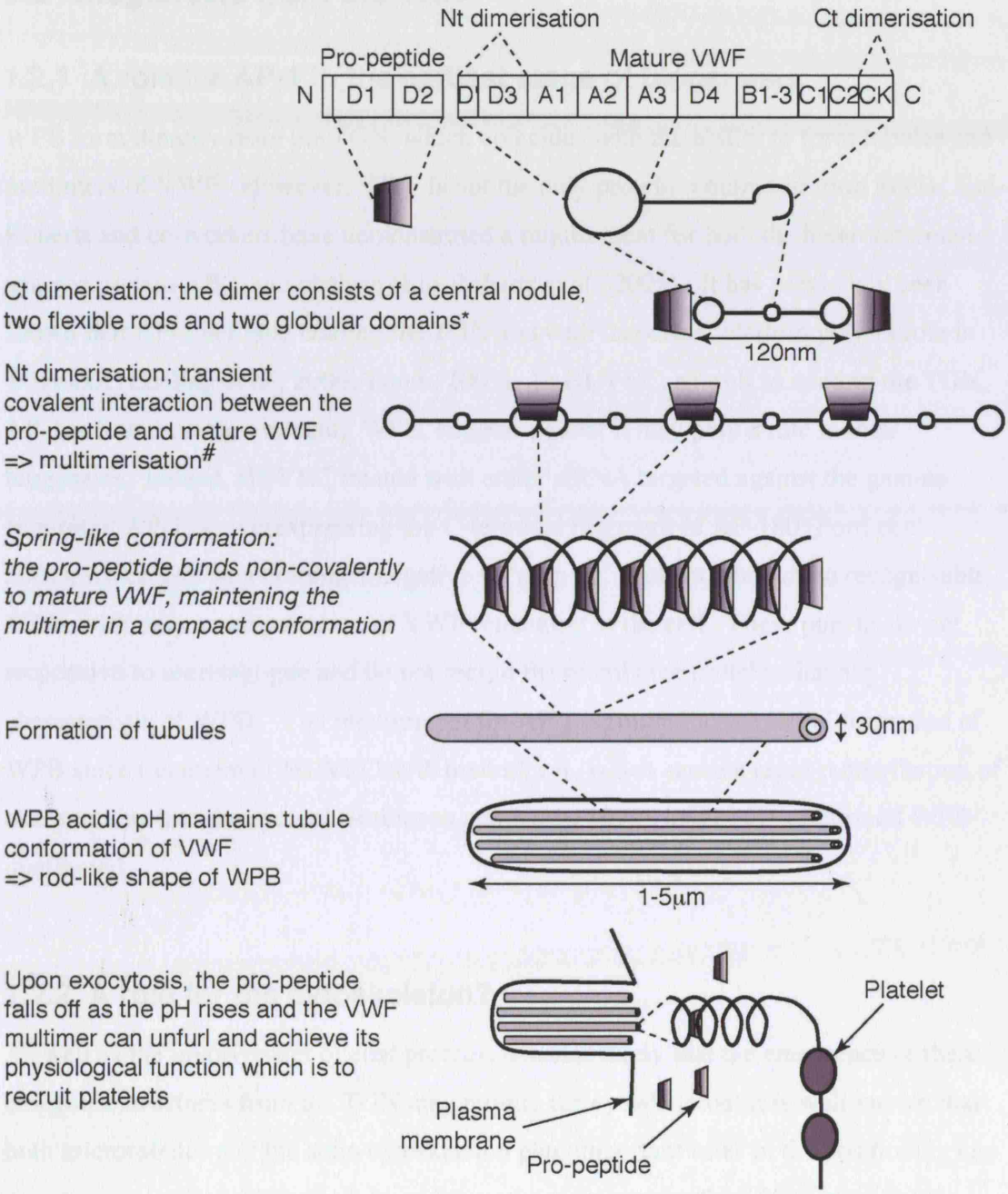

Figure 1.1 ***The formation of tubules and their importance in VWF function.***

Text in italics indicates hypothesis from Michaux et al. (2006). * from Fowler et al.,

1985; # from Purvis and Sadler, 2004).

1.2 Biogenesis from the TGN

1.2.1 A role for AP-1 in the earliest stage of biogenesis

WPB form directly from the TGN, which coincides with the ability to form tubules and multimers of VWF. However, VWF is not the only protein required to form WPB. Lui-Roberts and co-workers have demonstrated a requirement for both the heterotetrameric adaptor protein AP-1 and clathrin (Lui-Roberts et al., 2005). It has previously been shown that AP-1 is found coating the TGN and with its partner clathrin plays a role in TGN exit (Edeling et al., 2006; Traub, 2005). In HUVEC, as well as coating the TGN, AP-1 is found on the emerging WPB, suggesting that it may play a role in their biogenesis. Indeed, HUVEC treated with either siRNA targeted against the gamma subunit of AP-1 or overexpressing the C-terminal fragment of AP-180 (Ford et al., 2001), which acts as a dominant negative to 'mop up' clathrin, contain no recognisable WPB, with only small punctuae of VWF remaining in the cell. These puncta are not responsive to secretagogue and do not recruit the membrane proteins that are characteristic of WPB. The requirement for AP-1 is limited to the initial formation of WPB since treatment of HUVEC with brefeldin A, which cause a rapid redistribution of coat proteins into the cytosol (Robinson and Kreis, 1992), leaves the preformed WPB unaffected.

1.2.2 A role for the cytoskeleton?

As well as the involvement of coat proteins it seems likely that the emergence of these elongated structures from the TGN may require the cytoskeleton. It is well known that both microtubules and the actin cytoskeleton play important roles in the positioning and maintenance of Golgi cisternae, in addition vimentin intermediate filaments can also associate with Golgi membrane, though the role they play is somewhat less clear (Egea et al., 2006; Rios and Bornens, 2003; Stamnes, 2002; Thyberg and Moskalewski, 1999; Toivola et al., 2005).

Extended treatment of cultured cells with the microtubule depolymerising drug nocodazole, results in fragmentation of the Golgi into functional 'mini stacks' at ER exit sites, since the spatial relationship between ER, the intermediate compartment and the Golgi is disrupted (Rogalski and Singer, 1984; Thyberg and Moskalewski, 1999). In contrast, the treatment of cells with actin toxins have more subtle effects on Golgi morphology only noticeable at the EM level: Treatment with the actin depolymerising drugs such as cytochalasin D and Latruculin A induce swelling of the Golgi, whereas treatment with the actin filament-stabilising drug jasplakinolide results in fragmentation of the stack (Lazaro-Dieguez et al., 2006). The actin depolymerising drug also results in an increase in the pH of the Golgi, although, of only approximately 0.23 units in the case of cytochalasin D (Lazaro-Dieguez et al., 2006). Both microtubules and the actin cytoskeleton also play a role in the emergence of transport structures from the TGN.

Formation of tubular Golgi to plasma membrane carriers (GPC) is intimately linked with microtubules (Polishchuk et al., 2003). Firstly, the GPC precursors are always aligned along microtubules as they emerge from the TGN and the microtubule-associated motor kinesin is found at the tips of these structures. Secondly, the rate of the emergence of the GPC precursors from the TGN, at 0.2–1.5 μm/s, is similar to the rate of movement of GPC along microtubules in the periphery of the cell. The long-range movement of WPB in the cell is also dependent on microtubules and kinesin, but a requirement for microtubules at the earliest stage has not yet been demonstrated (Manneville et al., 2003).

The presence of multiple actin-associated proteins in the Golgi indicates that actin probably has an important role to play in TGN exit. This includes the involvement of the spectrin family proteins in transport from the ER-Golgi as well as the retrograde route. Actin-associated proteins specific to the TGN include p230, which is involved in the trafficking of GPI anchored proteins (Kakinuma et al., 2004); neurabin, which interacts directly with the TGN resident protein TGN38 (Stephens and Banting, 1999); and Spir 1, which localises to the TGN, as well as post-Golgi vesicles and the recycling

endosome and is required for the constitutive transport route from the TGN to the plasma membrane (Kerkhoff et al., 2001). Perhaps most interesting in the context of the WPB biogenesis is the presence of Hip1R at the TGN, as well as at the plasma membrane, where it interacts with both actin and clathrin (Carreno et al., 2004). Carreno and co-workers demonstrate that depletion of Hip1R using siRNA resulted in a 40% reduction in processing of the lysosomal hydrolase cathepsin D, due to a defect in trafficking from the TGN. Disruption of the actin cytoskeleton using actin toxins also leads to a 40% reduction in processing of cathepsin D.

Of course, as well as scaffolding proteins, actin-based motors are also present at the TGN. The Golgi associated motors include Myosin I, II (non-muscle), V and the atypical myosin motor Myosin VI, but whether they play a role in the initial formation of vesicles is unclear. Firstly, Myosin I is associated with Golgi stacks as well as Golgi-derived vesicles, but whether the motor is active at the Golgi is unclear. Fath et al. (1994) speculate that, in intestinal crypt cells, microtubules are required for the transport to the submicrovillar region, whereupon the vesicle, which incorporated Myosin I at the Golgi, switch to movement on actin filaments using this motor (Fath et al., 1994). They do not consider whether Myosin I also plays a role in the initial formation of the vesicle.

The role of Myosin II at the Golgi is more controversial. Whilst Musch and co-workers demonstrate a role for myosin II (p200) in the formation of TGN-derived vesicle destined for fusion with the bastolateral membrane, Simon et al. (1998) dispute this, suggesting instead that coatomer, and not myosin II is required for vesicle formation (Musch et al., 1997; Simon et al., 1998).

Although there is some evidence that myosin V is localised to the Golgi, most evidence points to it playing a role in the movement of secretory granules and lysosomes. Indeed the naturally occurring coat colour mutant mouse, dilute, fails to pass melanosomes from melanocytes to keratinocytes due to a defect in the MyoV gene (Wu et al., 1997). As well as the coat colour defects, these mice also have neurological defects, which may be explained by the role MyoV plays in transport from the ER in neurons (Tabb et al.,

1998). However, Myosin V is expressed in endothelial cells (Matthew Hannah, unpublished) and even in other cell types any role at the Golgi has yet to be described.

Like myosin V, the mouse mutant of myosin VI, the Snell's waltzer mouse, also shows defects in secretion, in this case of alkaline phosphatase (Warner et al., 2003). However in this case the association of myosin VI with the Golgi is more compelling. The TGN localisation of Myosin VI, which unlike other Myosins moves towards the minus rather than the plus end of actin, is dependent on the expression of optineurin since after siRNA mediated depletion of optineurin, Myosin VI is no longer localised to the TGN (Sahlender et al., 2005). Furthermore, knocking down optineurin results in a decrease in exocytosis of the vesicular stomatitis virus G-protein (VSVG), also suggestive of a role for Myosin VI in Golgi exit. Interestingly, optineurin also binds Rab8, another protein that is localised in the Golgi and plays a role in membrane trafficking. Together these proteins appear to play a role in basolateral trafficking via the AP-1 adaptor protein (Au et al., 2007; Spudich et al., 2007). Like both Myosin I and V, Myosin VI could also be required in the periphery of the cell; the ability of this protein to interact with clathrin is suggestive of a role in the earliest stages of budding, both from the plasma membrane or the TGN. Whether any of these proteins play a role in the biogenesis of WPB is unclear but will be considered in this thesis.

1.2.3 Scission from the Golgi

The last step before the WPB becomes an independent organelle is of course scission from the TGN. This is a step that is analogous to the scission following endocytosis at the plasma membrane and thus may involve some of the same machinery. This includes dynamin-dependent scission, protein kinase D (PKD)-dependent scission and brefeldin A (BFA)-dependent ADP-ribosylation substrate (BARS)-dependent scission. The best studied of these mechanisms is dynamin-dependent scission at the plasma membrane.

The GTPase dynamin was first identified in the *Drosophila melanogaster* temperature sensitive mutant *shibire*, which is unable to recycle synaptic vesicles (Kosaka and Ikeda,

1983a; Kosaka and Ikeda, 1983b; van der Bliek and Meyerowitz, 1991). Initially thought to be a neuronal specific protein, it has been extensively demonstrated that dynamin plays a role in multiple endocytic events. There are three mammalian family members, dynamin 1 that is indeed neuronal specific; dynamin 2, which is ubiquitously expressed and dynamin 3, which is expressed in the brain, testis and lungs (Cook et al., 1994; Nakata et al., 1993; Sontag et al., 1994). The action of dynamin may either be as a mechanoenzyme where upon hydrolysis of GTP it undergoes a conformational change, which allows it to sever membranes or in a mechanochemical fashion, whereby a helix of dynamin forms at the neck and there is a lengthwise extension of the helix causing scission (Hinshaw and Schmid, 1995; Stowell et al., 1999; Takei et al., 1995). As well as playing a role at the plasma membrane, dynamin 2 is also involved in scission at the TGN, although some of this evidence is controversial. McNiven and co-workers show that both dynamin 2-GFP fusion proteins (Jones et al., 1998) and endogenous dynamin-2 (Cao et al., 2000) are found at the TGN and colocalise with clathrin. They show that immunodepletion of dynamin 2 in a cell free system blocks vesicle formation, and that expression of a point mutant of dynamin, which is unable to bind GTP, results in retention of VSVG in the TGN. However, Schmid and co-workers find that expression of the same dominant negative constructs have no effect on budding from the TGN in HeLa and MDCK cells, whilst having a potent effect on endocytosis (Altschuler et al., 1998). The involvement of dynamin in clathrin dependent endocytosis has been well described and thus, given the requirement for clathrin in the formation of WPB, dynamin is a good candidate for scission of this organelle from the TGN.

Another type of scission from the TGN is PKD-dependent scission, which is limited to the TGN. Less is known about the precise molecular mechanism of PKD, although compared with dynamin, its role at the TGN is not disputed. Expression of a kinase-inactive form of PKD (K618N) in HeLa cells results in tubulation of the TGN. Cargo that is destined for the plasma membrane is found within the resulting tubules but is unable to exit the TGN, thus is highly suggestive of a requirement for the kinase activity of PKD in vesicle scission (Liljedahl et al., 2001). More specifically it has been demonstrated that PKD is required only for delivery to the basolateral membrane in

MDCK cells and is cargo-specific (Yeaman et al., 2004). Whilst it is known that the recruitment of PKD is dependent on diacylglycerol, and the kinase is activated by trimeric G-protein subunits beta gamma, the downstream effectors are less well understood. One effector that has been identified is phosphatidylinositol-4 kinase III beta, which is phosphorylated by PKD and is responsible for generating phosphoionsitol (4) phosphate at the TGN. However, whilst mutation of the serine residue 294 of PI4KIIIbeta, which is phosphorylated by PKD, results in decrease lipid-kinase activity, it has no effect on the VSVG transport (Hausser et al., 2005). This might be due to the presence of multiple PI4-kinases at the TGN and/or that there are multiple effectors of PKD that have not yet been identified.

The final set of scission machinery described to function at the TGN, is BARS (CtBP3) dependent. BARS (brefeldin A (BFA)-dependent ADP-ribosylation substrate) was originally identified as being involved in maintenance of Golgi homeostasis, however it has subsequently been shown to have a role in Golgi membrane fission. BARS is required for scission of GPC. An acute increase of BARS, brought about by injecting the protein into VSVG infected COS7 cells, caused an increase in the number of VSVG-positive GPC. Conversely injection of anti-BARS antibody results in a reduction in the number of GPC and delivery of VSVG to the plasma membrane. Injection of recombinant mutant proteins or mutant constructs, either containing only the nucleotide binding domain or with a point mutation in the region predicted to be required for fission also inhibit the formation of GPC and the arrival of VSVG at the plasma membrane (Bonazzi et al., 2005). BARS causes fission by lipid modification of the TGN membrane. Weigert and co-workers, demonstrated using Golgi derived membranes that it is acylation of lysophophatidic acid by BARS that leads to membrane fission (Weigert et al., 1999).

1.3 Recruitment of proteins to WPB

1.3.1 Recruitment of P-selectin

The recruitment of P-selectin, the protein responsible for the role of WPB in

inflammation, also occurs at the TGN. However, unlike VWF, P-selectin is not required for the formation of WPB, since expression of P-selectin in the non-endothelial model systems is not necessary or sufficient to make pseudo-WPB (Blagoveshchenskaya et al., 2002; Michaux et al., 2003; Wagner et al., 1991). P-selectin is a type I transmembrane protein that has a large extracellular domain and a short cytoplasmic tail. At the cell surface, P-selectin plays an essential step in the initiation of the leukocyte cascade (Lorant et al., 1993), following tissue injury the leukocytes are recruited from the fast flowing blood stream and transmigrate across the endothelium, direct to the sites of injury. P-Selectin is required for the initial rolling of leukocytes on the endothelium as the initial step in the leukocyte cascade. Using intravitial microscopy, this phenomenon of P-selectin dependent leukocyte rolling can be visualised (Thorlacius et al., 1997). However, when P-selectin antibodies are injected into mice no leukocyte rolling occurs. Whilst the extracellular domain is crucial for the interaction with leukocytes, the short cytoplasmic tail is important for its trafficking. Trafficking motifs in the cytoplasmic tail are important in the recycling of P-selectin back to the TGN where it can be incorporated into newly forming WPB. The residues KCPL are essential in the trafficking from the early to late endosomes, then the YGVF motif is important in the route from the endosome to the TGN (Harrison-Lavoie et al., 2006). Once in the TGN, the recruitment of newly formed or recycling P-selectin to the forming WPB is thought to be via a direct interaction with VWF. In HEK293 cells it has been demonstrated that P-selectin lumenal domain interacts with the D'-D3 domains of VWF (Michaux et al., 2006b). Indeed expression of just the lumenal domain is sufficient, although not necessary, for the recruitment of P-selectin to WPB. The absence of the lumenal domain does, however, slow delivery to WPB, suggesting another, indirect route of incorporation.

1.3.2 Recruitment of other proteins at the TGN

P-Selectin and VWF are not the only proteins that are incorporated into WPB at the earliest stage of biogenesis, although they are the best characterised. Other proteins that have been described to co-localise with VWF within WPB include endothelin-1 and its

converting enzyme which induce vasoconstriction; interleukin-8 (IL-8), angiopoietin-2 (Ang-2), alpha-1,3-fucosyltransferase VI, osteoprotegerin (OPG) and eotaxin-3, (Fiedler et al., 2004; Oynebraten et al., 2004; Schnyder-Candrian et al., 2000; Wolff et al., 1998; Zannettino et al., 2005) which along with P-selectin and CD63 may have roles in the inflammatory response; and controversially tissue-type plasminogen activator (tPA), which is responsible for the removal of clots (direct fibrinolysis) (Datta et al., 1999; Huber et al., 2002). However the co-storage of a clotting factor together with a factor involved in breaking down clots seems counter intuitive and further work has indicated that tPA is stored within a separate organelle (Emeis et al., 1997; Manneville et al., 2003). Unlike VWF, these factors are not always incorporated into WPB. For example, IL-8 is only present in newly forming WPB where its synthesis has been induced by IL-1beta (Wolff et al., 1998). Likewise eotaxin-3 is only found in WPB in the presence of IL-4 (Oynebraten et al., 2004). In the cases of the other proteins, when found, they are usually only in a subset of the VWF-positive WPB and interestingly, the presence of Ang-2 and P-selectin in WPB seems to be mutually exclusive (Fiedler et al., 2004).

1.3.3 Delivery of proteins post-TGN

The tetraspanin CD63 is recruited to WPB as they mature; suggested by its presence on WPB found in the periphery of the cell, but not the cluster of perinuclear WPB (Vischer and Wagner, 1993). CD63 is also found on late endosomes and lysosomes. The recruitment of CD63 to WPB is dependent on AP-3, the heterotetrameric complex in the same family as AP-1 (Harrison-Lavoie et al., 2006). Unlike AP-1, AP-3 is characteristically associated with endosomes, which places it in an appropriate context to perform this role. Furthermore the depletion of AP-3 in HUVEC using siRNA dramatically reduces the delivery of CD63 (and possibly other unknown components) to the WPB. The function for CD63 either in the WPB, or on the plasma membrane is unknown, although a role in the recruitment of integrins, which has previously been described to interact with tetraspanins (Hemler, 2005) and which operate downstream of P-selectin in the leukocyte cascade, seems plausible. Indeed in the AP-3 beta knockout mouse there is no firm adhesion of leukocytes to the wall of the endothelium

(unpublished data).

Two further proteins that are recruited in a maturation dependent fashion are the small GTPases, Rab27A and Rab3D (Hannah et al., 2003; Knop et al., 2004). Rab proteins are important for specifying identity of compartments (Ali and Seabra, 2005; Jordens et al., 2005). Rab27A is no exception, and is found on LRO such as melanosomes, platelet dense granules and lytic granules, as well as WPB (Hume et al., 2001; Stinchcombe et al., 2001; Wilson et al., 2000). The membrane association of Rab27A, as for all Rabs, is via prenylation (Leung et al., 2006). However, it has been shown that the recruitment of Rab27A is content dependent, rather than cell type dependent, since Rab27A can be recruited to the pseudo-WPB in HEK293 cells (Hannah et al., 2003), the recruiting component and mechanism leading to prenylation are unclear. The movement and more especially the exocytosis of other LRO is dependent on Rab27A. This is demonstrated in the naturally occurring mouse model, the ashen mouse, which is hypopigmented because the melanosomes fail to exit the melanocytes, reducing incorporation into the keratinocytes (Hume et al., 2001; Wu et al., 2001). The ashen mouse also suffers from immunological defects, due to a defect in the exocytosis of lytic granules from cytotoxic T-cells (Stinchcombe et al., 2001). However, the role for Rab27A in endothelial cells seems to be reversed and the protein may act as a negative regulator of stimulated exocytosis, demonstrated by an increase in the amount of VWF released upon agonist treatment in cells depleted of Rab27A (T Nightingale, personal communication). In addition, overexpression of Rab3D, as well as the constitutively active mutant variant results in reduced antibody uptake following stimulation, thus indicating a reduction in exocytosis (Knop et al., 2004). This finding indicates Rab3D is, likewise, a negative regulator of WPB exocytosis, in agreement with the observation that depletion of Rab3D using siRNA results in a similar phenotype to that observed after Rab27A depletion (T Nightingale, personal communication). The localisation of the Rab3D is slightly more controversial with published data from Knop and co-workers indicating that it is present on all WPB, whilst data from the Cutler lab indicates that, like Rab27A, it is recruited in a maturation dependent fashion. Another member of the Ras superfamily of small GTPases that is present in the same subcellular fraction as WPB is Ral (de Leeuw et al.,

1999). The role of Ral in exocytosis of WPB is discussed below. A diagram of the biogenesis of WPB, highlighting the recruited of the well-known proteins is shown below (Figure 1.2).

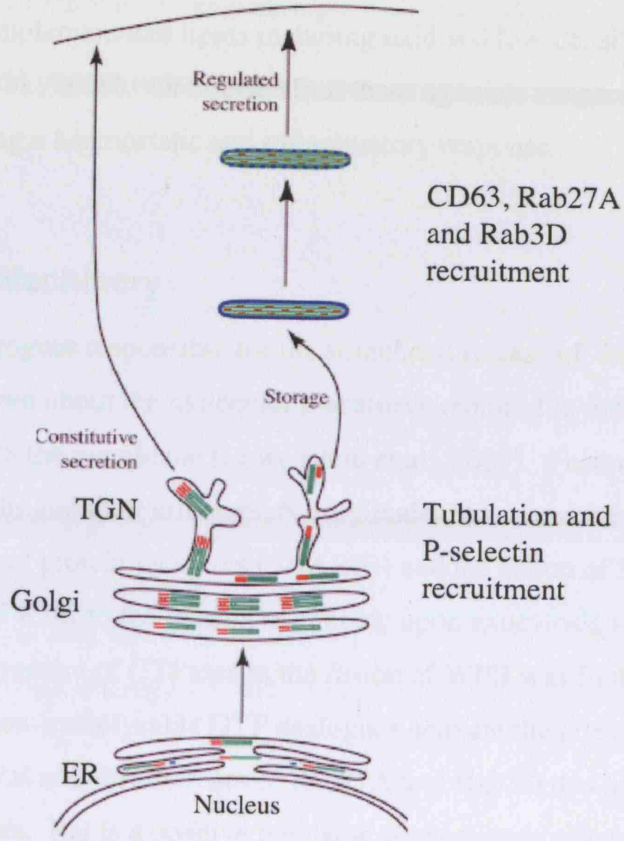

Figure 1.2 ***The biogenesis of WPB.***

Dimerisation of WPB occurs in the ER. VWF is then transport to the Golgi, once in the TGN multimerisation and tubulation occur contributing to the formation of the organelle. P-selectin is recruited at the TGN, whilst CD63, Rab27A and Rab3D are recruited to more mature WPB. The mature WPB are competent to undergo regulated exocytosis. Low molecular weight VWF is release constitutively, directly from the TGN. Figure adapted from Michaux and Cutler, 2004.

1.4 Exocytosis of WPB

1.4.1 Activators of exocytosis

WPB undergo exocytosis upon receiving a stimulus. The secretatogues that lead to exocytosis usually cause an increase the intracellular calcium level, or stimulate

production of cyclic AMP. For example, thrombin and histamine affect Ca^{2+} levels, whereas adrenaline stimulates cAMP production (Rondaij et al., 2004). The list of agonists is, however, extensive and also includes physical insults such as trauma, shear stress and hypoxia; chemicals such as ATP, leukotrienes and serotonin; proteins such as VEGF, fibrin and complement and lipids including oxidised low-density lipoprotein and ceramide (Rondaij et al., 2006). Of course all of these agonists are produced upon tissue damage, thus requiring a haemostatic and inflammatory response.

1.4.2 Molecular Machinery

Whilst many secretagogues responsible for the stimulated release of WPB have been identified, less is known about the molecular machinery required to make the WPB competent to fuse with the membrane (Lowenstein et al., 2005). Fusion of membranes generally requires Rabs and their effectors, N-ethylmaleimide-sensitive factor (NSF), soluble NSF attachment protein receptors (SNAREs) and the action of Sec1/Munc 18 family. The fusion of WPB to the plasma membrane upon exocytosis seems to be no exception. The involvement of GTPases in the fusion of WPB was first confirmed by the observation that non-hydrolysable GTP analogues activate the release of VWF, presumably because Ral acts downstream of Rab27A and Rab3D that are negative regulators of exocytosis. Ral is a positive regulator of exocytosis, since expression of active RalG23V resulted in a disappearance of WPB from endothelial cells and Ral activation correlates with agonist induced secretion of VWF (de Leeuw et al., 1999; Rondaij et al., 2004). Ral interacts with a number of proteins involved in exocytic events. Upstream, it interacts with calmodulin in a calcium dependent manner, which in turn enhances GTP binding to Ral, thus stimulating Ral-dependent exocytosis (Park, 2001; Wang et al., 1997). Downstream of Ral is RLIP76, which possess GTPase activity for Cdc42 and Rac, providing a link between Ral and the actin remodelling required for exocytosis (Jullien-Flores et al., 1995). Finally, Ral interacts with Sec5, a component of the exocyst complex (Moskalenko et al., 2002). The exocyst complex is composed of Sec3, Sec5, Sec6, Sec8, Sec10, Sec15, Exo70 and Exo84; it is implicated in the targeting and tethering of secretory vesicle to the plasma membrane (Lipschutz

and Mostov, 2002). Whether Ral interacts with Sec5 in endothelial cells is not known but would provide a molecular mechanism for the role of Ral in exocytosis of WPB.

Whilst no SNARE proteins have been formally localised to WPB, it is apparent that they do play a role in exocytosis. Incubation of permeablised endothelial cells with antibodies to either syntaxin 4 or VAMP3 (antibody reactive to VAMP1, 2 and 3 but only 3 is expressed in endothelial cells) prior to stimulation results in a 75% reduction in the exocytosis of WPB in the case of syntaxin 4 and 25% for VAMP, measured by the appearance of P-selectin on the cell surface (Matsushita et al., 2003). Likewise, depletion of syntaxin 4 using siRNA also causes a significant reduction in thrombin induced plasma membrane expression of P-selectin (Fu et al., 2005). The final SNARE making up the active SNARE complex required for exocytosis is likely to be SNAP23, which is indeed expressed in endothelial cells. Unsurprisingly, given the involvement of SNAREs in fusion, NSF is also involved in exocytosis of WPB. NSF function has been blocked by incubation of permeabilised cells with anti-NSF and by treatment of cells using a peptide inhibitor; this results in a reduction exocytosis, measured as above. NSF can also be inhibited by indirect means such as the addition of nitric oxide, which S-nitrosylates NSF thus blocking NSF dependent disassembly of SNARE complexes. Indeed it has long been known that nitric oxide inhibits vascular inflammation (Matsushita et al., 2003; Matsushita et al., 2005).

1.5 LRO and disease

Storage of cell type specific content and subsequent exocytosis is characteristic of LRO of which WPB are members. Further shared features between LRO and lysosomes, such as the low intraorganellar pH and recruitment of lysosomal proteins strongly indicate common mechanisms in the biogenesis of these organelles (Cutler, 2002; Dell'Angelica et al., 2000). However, perhaps even more suggestive of a common mechanism, is the fact that there are human diseases, which are characterised by defects in multiple LRO (Huizing et al., 2000; Starcevic et al., 2002). The proteins defective in these diseases are potential targets for a candidate-based screen. Indeed some of the disease causing

proteins have already been discussed, but will be considered again below in the context of disease and other LRO.

1.5.1 Hermansky-Pudlak syndrome

Hermansky-Pudlak syndrome (HPS), as well as the related diseases, Griscelli's syndrome and Chediak-Higashi Syndrome are diseases of LRO. The clinical manifestations of HPS include oculocutaneous albinism, bleeding defects and, in some patients, pulmonary fibrosis and granulomatous colitis (Oh et al., 1998). These symptoms are hypothesised to be due to defects in melanosomes, platelet dense granules and lysosomes respectively (Di Pietro and Dell'Angelica, 2005; Starcevic et al., 2002; Wei, 2006). Indeed at a cellular level, diagnosis of HPS is based on the absence of platelet dense granules. So far mutations in eight different genes in humans have been shown to give rise to HPS. In addition, there are mutations in at least 16 mouse gene loci, including homologues of the human disease genes, which result in phenotypes that resemble HPS (see table below) (Li et al., 2004). These genes encode components of the molecular machinery required for the biogenesis of these organelles.

Table 1.1 ***Proteins and complexes associated with Hermansky-Pudlak syndrome.***

Complex name	Subunit name	Human Disease	Mouse mutation
BLOC-1	Pallidin	?	pallid
	Muted	?	muted
	Cappuccino	?	cappuccino
	Dysbindin	HPS7	sandy
	BLOS1	?	?
	BLOS2	?	?
	BLOS3	HPS8	reduced pigmentation
	Snapin	?	?
BLOC-2	HPS3	HPS3	cocoa
	HPS5	HPS5	ruby eye-2
	HPS6	HPS6	ruby eye
BLOC-3	HPS1	HPS1	pale ear
	HPS4	HPS4	light ear
AP-3	β3A	HPS2	pearl
	δ3	?	mocha

The functions of some of the disease genes have been well characterised. HPS2 (pearl) encodes the β3A subunit of the AP-3 adaptor complex (Feng et al., 1999). This adaptor protein has been implicated in transport from both the trans Golgi network (TGN) and endosome to LRO and lysosomes of proteins with di-leucine motifs (Knuehl and Brodsky, 2003). As discussed earlier the recruitment of CD63 to WPB is dependent on AP-3 (Harrison-Lavoie et al., 2006). In addition, knockdown in AP-3 results in a 50% reduction in release of WPB upon stimulation, indicating that AP-3 is responsible for delivering more than just CD63 to WPB (unpublished data, T Nightingale and W Lui-Roberts). Likewise, the hypopigmentation phenotype of the pearl and mocha mice results mainly from a failure to deliver a protein from the endosome to LRO, in this case the delivery of the melanosomal specific protein tyrosinase to the forming melanosomes (Yang et al., 2000).

Another well-characterised protein, which has already been discussed, is Rab27A, the gene mutated in Griscelli's syndrome and the ashen mouse. Rab27A is best known for involvement in intracellular movements, often linked to exocytosis of lytic granules and melanosomes as well as other secretory organelles, although it has different effectors in these cell types (Neeft et al., 2005; Wu et al., 2001)

1.5.2 BLOC proteins

The other HPS proteins form three distinct complexes called biogenesis of lysosome-related organelles complex (BLOC) 1-3 (table 1) (Di Pietro et al., 2004; Falcon-Perez et al., 2002; Gautam et al., 2004; Martina et al., 2003; Nazarian et al., 2003; Zhang et al., 2003). The proteins comprising these complexes show no significant homology to functional domains previously described, although they are predicted to contain coiled-coil domains that may be important for protein-protein interaction (Burkhard et al., 2001; Dell'Angelica, 2004; Starcevic and Dell'Angelica, 2004).

Whilst biochemical studies have been utilised to identity and confirm the interaction within the complexes, morphological studies, using the mouse mutants, have

concentrated on the formation of melanosomes. These organelles are amenable to study as their high electron density means that they can be observed using light microscopy and transmission electron microscopy. Unlike the platelet dense granules, the melanosomes form but fail to mature in HPS-disease cells (Marks and Seabra, 2001). There are four discrete stages in the maturation of the melanosomes designated stage I - IV. At stage I the premelanosomes are morphologically similar to vacuolar early endosome. P-mel17 is recruited to the premelanosome it begins to assemble into fibrils. Stage II melanosomes have striated contents as the P-mel17/gp100 fibrils have been formed and tyrosinase, the enzyme that initiates melanin synthesis is recruited. The melanosomes are now elliptical. By stage III the melanosome is becoming increasingly pigmented and tyrosinase-related protein 1 (Tyrp1), which may have catalytic activity or modulate activity of tyrosinase and DOPAchrome tautomerase, which catalyses a late step in eumelanin formation are found in abundance. The stage IV melanosomes are fully pigmented (Marks and Seabra, 2001; Raposo and Marks, 2007).

The accumulation of melanosomes at any stage is indicative of a trafficking problem, or a defect in exocytosis and whilst many other proteins are required to form a fully pigmented melanosome the proteins mentioned above are mis-localised in the mouse colour mutants. An example of a defect in exocytosis is the accumulation of type IV melanosomes in the gunmetal and ashen mice because of either inefficient transport or secretion. However in the case of the other mutants, melanosomes accumulate before they are fully mature (Nguyen et al., 2002; Nguyen and Wei, 2004).

Localisation studies have been hindered by the relatively low expression of the HPS proteins and has relied on indirect methods such as subcellular fractionation combined with immunoblotting or immunofluorescence analysis using epitope tagged constructs. Using these techniques, all HPS proteins are found in both the cytosol and peripherally associated with membranes (Falcon-Perez et al., 2002; Gautam et al., 2004; Martina et al., 2003; Moriyama and Bonifacino, 2002; Salazar et al., 2006). More recently, using immunoelectron microscopy, both BLOC-1 and BLOC-2 have been localised to the tubules of EEA1 and transferring positive endosome (Di Pietro et al., 2006). However,

neither is found on the melanosomes themselves. BLOC-3 has been localised to tubulovesicular and vesicular structures near the Golgi complex and the membranes of maturing melanosomes (Oh et al., 2000). This evidence is consistent with a role for these proteins in the biogenesis of LRO, particular endosomal to LRO trafficking routes.

1.5.3 BLOC1

Mice defective in the BLOC-1 components have the most severe phenotypes. Indeed before the identification of HPS7/dysbindin (sandy) (Li et al., 2003) it was thought that defects in BLOC-1 must be embryonic lethal in humans. More recently HPS8, which is caused by a mutation in another BLOC-1 component BLOS-3 (reduced pigmentation), has been identified, although the pigmentation defect in this mouse is less harsh than the other BLOC-1 components. Biochemical studies have identified eight components of BLOC-1 so far (Moriyama and Bonifacino, 2002). One of these proteins, Snapin, is a coiled coil protein that is a binding partner of synaptosomal-associated proteins (SNAP) 25 and 23. Snapin has been implicated in the regulation of membrane fusion events (Starcevic and Dell'Angelica, 2004). Pallidin, another BLOC-1 component interacts with syntaxin 13, a t-SNARE involved in vesicle docking and fusion (Huang et al., 1999). HPS7 or dysbindin was first characterised as an interactor of dystrobrevin but any role for this interaction remains obscure. Finally, proteomics analysis of clathrin-coated vesicles identified the presence of seven of the eight BLOC-1 components and further biochemistry indicates that the eighth component, pallid, does indeed behave like a bona fide component of CCVs (Borner et al., 2006). The level of enrichment of BLOC-1 within CCV is similar to that of AP-3 and as will be discussed the association of BLOC-1 may be dependent on AP-3.

Morphological studies of the melanocytes of BLOC-1 mutants pallid and cappuccino, indicate that the biogenesis of melanosomes is perturbed at the earliest stage (Nguyen et al., 2002). The melanosomes remain in a multivesicular form, which presumably reflect this organelles endosomal origin. The lack of striation is due to aberrant trafficking or failure to cleave P-mel17/gp100. More recently BLOC-1 has been shown to be involved

in the delivery of tyrosinase-related protein 1 (TYRP1), but not tyrosinase to the forming melanosomes (Di Pietro et al., 2006; Setty et al., 2007). In cells from the mutant mice, TYRP1 is localised to syntaxin 13-positive early endosomes. This was initially thought to be an independent pathway to the AP-3-dependent pathway known to deliver tyrosinase from the endosome to the forming melanosomes. However, two groups have since shown that AP-3 interacts physically and functionally with BLOC-1 to deliver TYRP1 to the melanosomes (Di Pietro et al., 2006; Salazar et al., 2006). The operation of BLOC-1 and AP-3 in combination is not confined a melanosome specific pathway, as indicated by the increase in the surface expression of LAMP-1 in both BLOC-1 and AP-3 mutant cells. Finally, Salazar et al. show that levels of the SNARE VAMP7-TI, which is involved in transport to late endosomes and lysosomes and present on AP-3 generated vesicles, are reduced in both AP-3 and BLOC-1 deficient cells. Surprisingly, whilst the cognate SNARE pair of VAMP7-TI, syntaxins 7 and 8 are correctly localised in AP-3 deficient cells, there is a marked reduction in the co-localisation between the syntaxins in the BLOC-1 deficient cells, indicating that whilst the pathways overlap there are still some differential effects. Although many of the BLOC-1 deficiencies seemed to be caused by defects in the AP-3 dependent pathway, BLOC-1 is not required for the recruitment of AP-3 to the membrane, but perhaps may be involved in the recruitment or stabilisation of AP-3 specific cargo (Di Pietro et al., 2006).

1.5.4 BLOC-2

BLOC-2 consists of three proteins, HPS3 (cocoa), HPS5 (ruby-eye-2) and HPS6 (ruby-eye). Melanosomes from the BLOC-2 mutants, cocoa (HPS3), ruby eye (HPS6) and ruby eye-2 (HPS5) have normal striation patterns but fail to mature from a spherical to elliptical form (Nguyen et al., 2002). As the mice names suggest, the pigmentation defect in HPS5 and 6 is mostly confined to the eyes. Indeed hypopigmentation of the eyes is more common than the skin, presumably because any is defect is magnified since in the eye, melanosomes are synthesised in a burst during development, whereas skin melanosomes are constantly being made. This has recently been described with reference to the Rab38 (chocolate) mouse (Lopes et al., 2007). This may suggest that,

likewise, deletion of HPS5 and HPS6 do not cause a complete block in melanosome maturation. In the cocoa mouse the HPS5 and 6 proteins are absent, as well as HPS3, probably due to the increase degradation as the complex is destabilised by the loss of HPS3 (Gautam et al., 2004). This may contribute to the more severe hypopigmentation of the HPS3 mouse, compared with the HPS5 and 6 mice where only the mutated protein is absent. Of course all subunits may have functions in addition to their roles in the complex, which would also contribute to differences in the phenotypes of the mice.

Interactors for components of BLOC-2 have not been well defined. HPS5 has been shown to interact with the cytoplasmic tail of α3A integrin when it was used as bait in a yeast two-hybrid screen (Wixler et al., 1999). However this interaction could not be confirmed by another group and remains controversial (Zhang et al., 2003). HPS3 has a putative clathrin-binding domain (NCBI prediction) and has lately been shown to interact with clathrin in melanocytes, by immunopreciptation and co-localisation through the predicted domain. HPS3 and clathrin colocalise on small acidic vesicles in the perinuclear region, juxta-Golgi, although not with vesicle budding from the TGN, or with mature melanosomes (Helip-Wooley et al., 2005). However, unlike BLOC-1, no BLOC-2 components are enriched in CCVs, although none were directly tested for.

Boissy and colleagues (2005) claim that localisation of multiple melanosomal, as well as LRO specific, proteins is altered in HPS3 mutant cells. They claim that the distribution of tyrosinase, TYRP-1, dopachrome tautomerase, as well as LAMP-1 and LAMP-3 is more fine and floccular, compared to the coarse, granular appearance in normal melanocytes (Boissy et al., 2005). This redistribution is not common to all melanosomal proteins, with Pmel17, Melan-A, as well as CD63 and Rab27 being normally localised in HPS3 mutant cells. Likewise in HPS5 deficient cells there is both a reduction and redistribution of TYRP-1 away from dendrites to the perinuclear area only (Helip-Wooley et al., 2007). Further work has shown that BLOC-2 is involved in the delivery of TYRP-1 to melanosomes, in concert with BLOC-1, but independently of AP-3 (Di Pietro et al., 2006). The roles of AP-3 and BLOC-2 in independent pathways is further confirmed by the fact that the double mutant mouse is more severe than either single

mutant and indeed phenocopies BLOC-1 mutants (Gautam et al., 2006).

1.5.5 BLOC-3

Unlike, the BLOC-1 and BLOC-2 mutants, the population of melanosomes in the pale ear and light ear mice (BLOC-3) is virtually indistinguishable from the corresponding background strain, C57BL/6 apart from the ears and tail. Whilst some groups report the presence of enlarged melanosomes (Sarangarajan et al., 2001), careful analysis highlights a slight increase in the number of immature forms, which is indicative of a rate limiting step rather than a block (Nguyen et al., 2002). This would explain the modest hypopigmentation defect observed in these mice, although some BLOC3 patients can suffer from severe hypopigmentation defects.

No interactors have yet been identified for BLOC-3 and perhaps because of the limited effect on pigmentation no proteins been reported to be mislocalised in melanocytes. However, the effects of BLOC-3 deletion have been considered in fibroblasts. Firstly, the distribution of LAMP-1 is disrupted, with LAMP-1 positive structures confined to the perinuclear area and not in the cell periphery. Internalised dextran in these LAMP-1 positive structure indicate these structures are true lysosomes and not as a result of mis-localisation of LAMP-1 (Nazarian et al., 2003). An obvious explanation for the localisation is a failure to connect effectively with the microtubule cytoskeleton, which is responsible for the long-range movement around the cell. Timelapse studies demonstrate that although the lysosomes are able to move, they do so at a lower frequency than the movement of lysosomes in wild type cells, suggesting that BLOC-3 may contribute to the link between the organelle and cytoskeleton (Falcon-Perez et al., 2005). In addition to the defect in the movement of lysosome there is a decrease in secretion of lysosomal enzymes in pale ear (HPS1) mice (Brown et al., 1985). Finally, levels of the SNARE vti1b are reduced in BLOC-3 deficient cells, but this has not been investigated further (Salazar et al., 2006).

1.5.6 Double and triple mutants

More recently a major study of mice doubly or triply deficient in the subunits of BLOC and AP-3 has been performed, to assess whether the complexes genetically interact in vivo, although interactions between BLOC-1, BLOC-2 and AP-3 have been discussed earlier (Gautam et al., 2006). In terms of coat colour Gautam and coworkers find that double and triple mutants of BLOC-1 and BLOC-2 and or BLOC-3 and AP-3 phenocopy the BLOC-1 single mutant, thus indicating that the complexes are found on the same pathway, with BLOC-1 operating furthest upstream. However, the finding that the BLOC-2 and BLOC-3 double mutant is less pigmented than the single mutants suggests they also interact in an additional pathway.

In the knockout mice Gautam et al. (2006) also considered defects in another LRO and the lysosome. Firstly, defects in the lamellar body, an LRO found in lung type II cells, were considered by measuring the accumulation of lung phospholipids (p-lipids). An increase in the accumulation of p-lipids reflects surfactant accumulation in lamellar bodies, which are subsequently larger (Lyerla et al., 2003). There is no increase in p-lipid in any of the single mutants, however, there is an accumulation in both BLOC-2 and BLOC-3 mutants in combination with knockout of AP-3 and also the BLOC-1 and BLOC-3 double mutant, as well as the BLOC triple mutant (Gautam et al., 2006). Immunohistochemistry was used to confirm that these double and triple knockouts did indeed contain enlarged lung lamellar bodies. Finally, to test for defects in the lysosome, the secretion of lysosomal enzymes was measured. As discussed earlier, mutation in HPS1 causes a reduction in enzyme secretion. This study shows that all of the double mutants of the BLOC complexes, as well as the double mutants of BLOC-2 and BLOC-3 with AP-3, also have reduced enzyme secretion. The level of secretion is particularly low in the BLOC-2 and BLOC-3 double knockdown, which confirms the pigmentation finding that they operate on an additional pathway to BLOC-1.

1.5.7 BLOCs are not required for all LRO biogenesis

Whilst the formation of melanosomes and indeed platelet dense granules, which are

absent in all forms of HPS, are intimately linked with the BLOC proteins not all LRO require a complete set of functional HPS proteins. Firstly, the function of lytic granules, the secretory lysosomes of cytotoxic T-cells (CTL) is not dependent of BLOC function (Bossi et al., 2005). AP-3 and Rab27A, two proteins also required for the function of WPB, are required for effective release of perforin upon stimulation (Clark et al., 2003; Stinchcombe et al., 2001), but none of the BLOC proteins tested had any effect on release. The absence of severe immunological disorders in either the patients or the mouse mutants would seem to confirm this finding. Secondly, and perhaps even more surprisingly, the other LRO in platelet, alpha granules, do not require functional BLOC-2 or BLOC-3. Ultrastructural examination of the platelets from HPS patients comprising BLOC-2 and BLOC-3 indicates that distribution, size and quantity of alpha granules are unaffected (Huizing et al., 2007). Whether or not BLOC-1 is required for the formation of alpha granules has been yet been reported.

1.6 Objectives

The major aim of this study is to provide further insight into the biogenesis of WPB, the lysosome related organelle present in endothelial cells. More specifically, a survey of ultrastructure of the WPB in HUVEC was undertaken to investigate the relationship between the VWF tubules and the membrane during formation of the organelles (Chapter 3). Whilst the requirement for tubulation has been well-described, this study also aims to investigate if the cytoskeleton and various scission machinery play an additional role in formation from the TGN (Chapter 4). Finally, the HPS proteins are good candidates to play a role in the biogenesis of WPB and this study will consider whether the proteins forming BLOC-2 and BLOC-3 are required (Chapter 5).

2 Materials and methods

2.1 Cell culture

2.1.1 Cell lines and maintenance

All cells were grown in Nunc tissue culture plastic dishes from Gibco/Invitrogen at 37 °C and 5% CO_2.

Human umbilical vein endothelial cells (HUVEC) were purchased from TCS Cellworks. The cells were grown in M199 medium (GIBCO-BRL) supplemented with 20% fetal calf serum (BioWest), 10U/ml heparin (Sigma) and 30μg/ml endothelial cell growth supplement (Sigma). HUVEC were used only for a maximum of five passages, after which the cells lose some of their endothelial characteristics.

HEK293 cells were grown in MEM-alpha (GIBCO-BRL), supplemented with 10% fetal calf serum (BioWest).

2.1.2 Freezing and thawing cultured cells

Aliquots of $1x10^7$ cells were suspended in 1 ml of FCS supplemented with 10% DMSO. These were frozen overnight at -80°C. The aliquots were moved to liquid nitrogen and stored permanently under liquid nitrogen. Individual aliquots were thawed rapidly at 37°C and placed in a 15cm dish with 30 ml pre-warmed medium. Cells were then grown in fresh medium, and initially passaged two to three days post-thawing.

2.1.3 Transient transfections

For transient transfection experiments, cells were grown to 80% confluency and transfected by nucleofection with the appropriate DNA or siRNA construct using a nucleofector device from Amaxa Biosystems.

Cell number, nucleofection program and DNA or siRNA concentration were used according to the nucleofection machine manufacturer's instructions. For HUVEC, the 'old' nucleofection program U-01 was used to transfect either 5μg of a DNA construct or 10μM siRNA. The same concentration of DNA and siRNA were also nucleofected into HEK293 cells using program A-23.

The constructs used in this study are listed in table 2.1, whilst the siRNA oligos are listed in table 2.2, all siRNA were purchased from Qiagen, with the exception of HPS1 siRNA, which was purchased from Invitrogen.

2.1.4 Microinjection

For microinjection, HUVEC were grown on coverslips that had previously been marked using a diamond scorer. At 70-80% confluency, the tissue culture dishes were placed on the upright microscope connected to the microinjector, in a chamber at 37°C and 5% CO_2. Thin glass capillaries were pulled to form needles (heat 447, pull 35, velocity 55), which were filled with 3μl of the DNA construct at 0.1μg/μl and attached to the pump. Each dish remains in the chamber for only 20 minutes, in which time approximately 200 cells were injected.

Table 2.1 ***Details of constructs used in this study.***

Construct	Source
wtVWF	Cutler laboratory
VWF-GFP	Jan Voorberg, Sanquin Research Laboratory
Myosin VI-GFP	Folma Buss, University of Cambridge
Myosin VI tail only-GFP	"
Rab8-GFP	"
Rab8Q67L-GFP	"
FAPP-PH-YFP	John Lucocq, Dundee University
wtPKD-GFP	Vivek Malhotra, UCSD
PKD-kinase dead-GFP	"

Dynamin 2	Harvey McMahon, University of Cambridge
Dynamin 2 K44A	"
HPS3-GFP	detailed in this thesis
HPS3-CBD-GFP	Marian Huizing, NIH, Bethesda

Table 2.2 ***Details of siRNA oligos used in this study.***

Target/siRNA	**DNA target sequence**
Hip1R	AAGGATCCTTGGTTGCTGTAC
HPS1	GCAACTTCCTGTATGTCCTTCACCT
HPS2	AATGGCTTGGTCTGTCTGCTG
HPS3-1	AAGACGGACAGAAGAAGGCAT
HPS3-2	CTCAATCAATTTAATTGTCTA
HPS3-4	CTCGTTGGCTGCACAAATAAA
HPS4	AACGGATGCTTGTCTGGCCAT
HPS5	CTGGCTGAATTGACAACATTA
HPS6	AAGCCCATATGAGGACATCCT
Scrambled/control	AATTCTCCGAACGTGTCACGT

2.1.5 Inhibitor studies

Inhibitors were resuspended according to the manufacturers recommendations and added directly to pre-warmed tissue culture media, with the exception of protease inhibitors which were added to cell lysates. A list of the inhibitors used is listed in the table below (Table 2.3).

Table 2.3 ***List of inhibitors used in this study and their working concentration.***

Inhibitor	Source	Working concentration
Monensin	Sigma	10μM
DTT	Sigma	20μM
Nocodazole	Sigma	10μg/ml
Aurintricarboxylic acid	Sigma	100μM
Jasplakinolide	Sigma	0.5μM
Cytochalasin D	Sigma	200nM
Blebbistatin	Sigma	10μM
Protease inhibitor cocktail	Sigma	1:1000

2.1.6 Immunofluorescence microscopy

Cells were grown in 30mm diameter glass coverslips (VWR International) for immunofluorescence studies. Cells were fixed with 3% ultra pure paraformaldehyde (Polysciences Inc.) in PBS for 10 minutes at room temperature followed by permeabilization with 0.2% saponin and free aldehyde groups were quenched with 50mM ammonium chloride in PBS for 15 minutes and then blocked for at least 5 minutes with 0.2% gelatin, 0.02% saponin and 0.02% sodium azide in PBS (PGAS). Cells were then incubated in primary antibody in PGAS blocking buffer for 30-45 minutes at room temperature. After extensive washing, the cells were incubated with secondary antibody in PGAS for 30 minutes. Finally, the cells were washed again 3 times in PGAS, then PBS and once in distilled water and mounted with Prolong Antifade mountant (Molecular Probes). Cells were imaged using a scanning confocal microscope, either the Biorad MRC1024 or Leica SPE. The primary and secondary antibodies used in this thesis are listed in the tables below.

Table 2.4 *List of primary antibodies used for immunofluorescence in this study.*

Antibody	Raised in	Source	Dilution for IF
VWF	rabbit	VWR	1:10,000
Tubulin	mouse	Sigma	1:200
GFP	sheep	Biogenesis	1:100
TGN46	sheep	Serotec	1:300
GM130	mouse	BD transduction	1:200
P-selectin (AK6)	mouse	Serotec	1:200
CD63	mouse	Abcam	1:300
LAMP-1 (H4A3)	mouse	DSHB	1:100

Table 2.5 *List of secondary antibodies used for immunofluorescence in this study.*

Antibody	Raised in	Source	Dilution for IF
rabbit-texas red	donkey	Jackson	1:1000
mouse-texas red	donkey	Jackson	1:1000
sheep-texas red	donkey	Jackson	1:1000
rabbit-FITC	donkey	Jackson	1:1000
mouse-FITC	donkey	Jackson	1:1000
sheep-FITC	donkey	Jackson	1:1000
rabbit-Cy5	donkey	Jackson	1:1000
mouse-Cy5	donkey	Jackson	1:1000
sheep-Cy5	donkey	Jackson	1:1000

2.1.7 Timelapse microscopy

For timelapse microscopy, after nucleofection with VWF-GFP, the cells were plated on tissue culture dishes with a glass coverslip embedded in them. Timelapse microscopy was performed using a Zeiss Axiovert Openlab fluorescence timelapse system enclosed

at 37°C. Images were taken every 5 seconds for 5 minutes.

2.2 Electron microscopy

2.2.1 High pressure freezing

Cells were grown on carbon and gelatin -coated, 1.4 mm diameter sapphire coverslips (Leica Microsystems UK). The coverslips were placed cell-side up into 1.5 mm diameter flat specimen holders under tissue culture medium and transferred to the EMPACT high pressure freezer (Leica Microsystems UK) as quickly as possible and frozen in liquid nitrogen at 2000bars. The specimens were stored under liquid nitrogen until freeze substitution was carried out.

2.2.2 Freeze substitution

The Leica AFS freeze substitution unit was pre-cooled to -90°C (FS-A) or -80°C (FS-B) and samples were transferred into the chamber under liquid nitrogen into pre-cooled fine mesh-based plastic capsules in universal containers (Leica Microsystems UK). For freeze substitution A (FS-A), samples were freeze substituted for 22 hours in 0.5% osmium tetroxide (TAAB) in extra dry acetone (Fisher Scientific). The osmium tetroxide was removed and, after a 2 hour acetone wash, replaced with 0.1% tannic acid (TAAB) in acetone for 8 hours. The AFS unit was then warmed at 5°C per hour to -60°C, held at -60°C for 8 hours, followed by a warm up to -30°C. The samples were held at -30°C for 8 hours after which the tannic acid/ acetone was exchanged for acetone. The samples were then warmed to 0°C at 5°C per hour, held for one hour and quickly warmed to 20°C in one hour to prevent evaporation of the acetone. For FS-B, the samples were placed in plastic containers holding up to 10 holders in the AFS unit. The samples were incubated with 0.1% tannic acid and 0.5% glutaldehyde, or tannic acid alone in acetone for 72 hours at -80°C. The tannic acid was then replaced with 2% osmium tetraoxide and held at -80°C for a further 3 hours. The temperature was then raised by 4°C per hour until -20°C was reached, and then 6°C per hour until the samples

were at 4°C, when the sample were washed with acetone. For both FS-A and FS-B samples were washed at room temperature in propylene oxide, twice for 10 minutes each, after which samples were infiltrated with propylene oxide:epon (1:1) for 1 hour followed by two changes of epon for two hours each (the composition of the epon is outline in table 2.6). The sapphire coverslips, still in the flat specimen holders from FS-A, were placed into flow-through capsules inside gelatin capsules (Leica Microsystems UK), topped up with epon and baked at 60°C overnight. In contrast, the sample holder used in FS-B could be filled with epon and baked overnight.

Table 2.6 ***Composition of epon used for embedding.***

Chemical	Volume (g)
TAAB 812	19.2
DDSA	7.6
MNA	13.2
DMP-30	0.8

2.2.3 Electron microscopy

Following polymerisation, the epon blocks were cut out of the plastic/ gelatin capsules with a razor blade. The specimen holders and sapphire coverslips were snapped off the epon stubs by plunging into liquid nitrogen and then 'flicking off' with a razor blade. Ultrathin sections were cut on an Ultracut UCT ultramicrotome (Leica Microsystems UK), post-stained with lead citrate and observed using a Tecnai G2 Spirit transmission electron microscope (FEI, Eindhoven, Netherlands). Images were collected using a Morada CCD camera (Olympus Soft Imaging Systems).

2.3 Molecular biology

2.3.1 Polymerase chain reaction

DNA was amplified in a thermocycler (PTC-200, MJ Research). PCR reactions used a final volume of 20 µl containing 10 ng template DNA, 50µM dNTPs (Promega), 0.25 µl Taq polymerase (Promega) was used when testing for HUVEC specific expression, whilst 0.25µl Pfu (Promega) was used for cloning, 20µM of each oligonucleotide primer (Invitrogen) and 2µl of the respective polymerase 10x buffer. DNA was amplified using reaction specific programmes within the following parameters: 1x at 95°C for 5 min, 30-35x [95°C for 1 min, 55-65°C for 1 min, 72°C for 1 to 3 min, depending on the length of product] and 1x 72°C for 10 min. PCR products were purified for cloning using the QIAquick® PCR Purification Kit (Qiagen) according to the manufacturers instructions.

2.3.2 Restriction digests

Plasmid DNA and PCR products to be digested (2-5 µg DNA per reaction) were added to 2 µl appropriate restriction enzyme buffer (NEB), 2 µl of 10x Bovine Serum Albumin (BSA, NEB), and 0.6 µl (approximately 10 units) of each restriction enzyme (NEB). Reactions were made up to a final volume of 20 µl using distilled H_2O (dH_2O) and were incubated for 1 hr at either 25°C or 37°C as appropriate. Cut vectors were then further treated with Calf Intestine Phosphatase (CIP, NEB). 160 µl H_2O, 20µl CIP Buffer (NEB), and 4 µl CIP were added to the vector restriction digest mixture, and incubated at 37°C for 1 h. 1 µl of 0.5 M EDTA was then added to the mixture and the reaction was brought to 75°C for 10 min.

2.3.3 Agarose gel electrophoresis

DNA was separated by agarose gel electrophoresis at 120 mA for 30 minutes to 1 hour on 1% TAE (Tris-acetate 50x stock: 2 M Tris Acetate 100 mM Na_2EDTA, diluted with dH_2O) agarose gels. Ethidium bromide (Sigma) was added to the gel to a final concentration of 0.5 µg/ml to allow visualisation of DNA under UV light. This enabled

the integrity and purity of the DNA to be assessed. Samples for electrophoresis were added to an appropriate volume of DNA loading buffer (6x stock: 0.25% Xylene cyanole (w/v), 0.25% Bromophenol blue (w/v), 40% sucrose (w/v) made up in dH_2O). DNA fragment sizes were estimated by comparison with a 1Kb DNA ladder (Invitrogen) or 100bp ladder (Promega).

2.3.4 Extraction of DNA from agarose gels

DNA was purified from agarose gels using the QIAquick® Gel Extraction Kit (Qiagen) according to the manufacturers instructions.

2.3.5 Ligations

Ligation reactions were carried out using a molar ratio of vector:insert of 1:5. Reactions were carried out in a final volume of 20 µl containing 2 µl 10x DNA ligase buffer (Roche) and 1 µl T4 DNA ligase (5 U/µl, Roche). Ligations were incubated overnight at 16°C.

2.3.6 Transformation of E.coli by 'heat shock'

Competent cells (DH5α strain) were thawed quickly at room temperature and placed on ice. DNA constructs (1 µl of plasmids for amplification) to be transformed were placed in 1.5 ml microfuge tubes and mixed with 50 µl competent cell suspension. Tubes were tapped and placed on ice for 5 min. Cells were heat-shocked by incubation at 42°C for 45 sec and were then immediately returned to ice for 5 min. Pre-warmed LB-Broth (500 µl per transformation) was added and the cells were incubated with moderate agitation for 10 min. 200 µl of transformed bacteria were plated onto selective LB agar plates containing either ampicillin (50 µg/ml) or kanamycin (30 µg/ml) as required. Plates were incubated overnight at 37°C.

2.3.7 Bacterial DNA preps

Mini preps were performed using the QIAprep spin miniprep kit according to manufacturers instructions (Qiagen).

Qiagen plasmid maxi kit was used for all DNA maxi preps, and manufacturers instructions were followed.

2.3.8 HPS3 construct

HPS3 was PCR from IMAGE clone 4385940 using the primers listed below. The PCR produce was subsequently cloned into pEGFP-C1 vector (Clontech) using the BamHI and XbaI restriction sites.

Table 2.7 ***Primers used to make HPS3-GFP.***

Primer	Sequence
HPS3 forward	CCGGACGTCGGGATGGTG
HPS3 reverse	TCCTTGGAATAAAAGTCAATCCCA

2.3.9 RNA extraction

Cell were lysed in lysis buffer, plus β mercaptoethanol, included in the Qiagen RNeasy mini kit. The lysates were homogenised using the Qiashredder and then processed according to manufacturers instruction in the Qiagen RNeasy mini kit. RNA was eluted in 30μl of RNase free water.

2.3.10 Reverse transcription

RNA was reverse transcribed using the SuperScript™ III First-Strand Synthesis System for RT-PCR (Invitrogen). 10μl of RNA was used for each reaction and random hexamers are used as primers in this reaction to ensure total DNA amplification. Incubation times were according to manufacturers instruction.

2.3.11 DNA quantitation

The concentration and purity of DNA preparations were examined by optical density ($Abs_{260/280}$).

2.3.12 Real time PCR

DyNAmo™ SYBR® Green qPCR Kit was used to quantify the relative amount of DNA in the various samples. This kit is composed of a master mix containing modified Thermus brockianus DNA Polymerase, SYBR Green I dye, optimized PCR buffer, 5mM $MgCl_2$, dNTP mix including dUTP. Added to this were the gene specific primers either at 1.2μM or 1X final concentration for the quantitect primers and the DNA samples, which are diluted to 150ng/μl. The sequences of the primers are set out in table 2.8 and the cycling conditions in table 2.9. All primers were designed to produce a product that encompasses two exons to ensure that no genomic DNA contaminated the cDNA preparations and the amplicons were 100-200 base pairs.

Table 2.8 ***Primers used in the real time PCR.***

Target	Sequence
Hip1R	Quantitect primer from Qiagen
HPS1	Quantitect primer from Qiagen
HPS2	**forward:** GTCATCAGTGTCAGTACTCCTGCA
	reverse: AAAAATGCAAGGCTGTCTTGG
HPS3	**forward:** TTGGGAAGCTCAGCTAGTGG
	reverse: ATCAGATCCTCCGATGTTCG
HPS4	Quantitect primer from Qiagen
HPS5	Quantitect primer from Qiagen
HPS6	Quantitect primer from Qiagen
Actin	**forward:** GCGAGAAGATGACCCAGAT
	reverse: TGGTGGTGAAGCTGTAGCC

Table 2.9 *Cycling conditions used for real time PCR*

Step #	Purpose	Temperature	Time
1	Initial denaturation	95°C	10 mins
2	Denaturation	94°C	10 secs
3	Annealing	55°C	15 secs
4	Extension	72°C	20 secs
5	Fluorescence measurement	72°C and 77°C	1 sec each
Steps number 2-5 are repeat 39 times			
6	Final extension	72°C	8 mins
7	Melting curve	72°C -95°C	approx. 20 mins
8	Reannealing	72°C	8 mins

The melting curve was used to check the specificity of the amplified product. Primers that formed more than one product were discarded. The relative knockdown for each product was determined by comparing the cycle number at which the amount of PCR product exponentially increases (C(t)) between knockdown and mock transfected cDNA sample using the $2^{-\Delta\Delta C(t)}$ method (Livak and Schmittgen, 2001).

$\Delta C(t)$ gene specific = knockdown C(t) – mock C(t)

$\Delta C(t)$ housekeeping = knockdown C(t) – mock C(t)

$\Delta\Delta C(t) = \Delta C(t)$ gene specific - $\Delta C(t)$ housekeeping

2.4 Biochemistry

2.4.1 Secretion assay

HUVEC were plated on to either 6 well plates or 6cm dishes, usually 48 hours after the second round of nucleofection of siRNA. The cells were washed and then incubated in

release medium (M199 plus 10mM HEPES and 1.9mg/ml BSA) for 30-45 minutes at 37°C. This medium was collected and replaced with release medium containing 100 ng/ml PMA for 30-45 minutes also at 37°C. The remaining VWF was released by cell lysis at 4°C for 30 min in the lysis medium (release medium containing 0.5% vol/vol Triton X-100, 1 mM EDTA, and protease inhibitors). The amount of VWF in these samples was assessed using ELISA.

2.4.2 ELISA

VWF released in the secretion assay described above and cell lysates was measured by a solid-phase sandwich ELISA. Maxisorp 96-well plates (Nunc) were coated for 1 hour with 100 µl/well of rabbit polyclonal anti-VWF diluted in PBS (9.7 µg/ml) at room temperature with agitation. The antibody solution was removed and the plates were then incubated for 1 hour at room temperature to block nonspecific binding by using 250 µl/well of 1X TXEB (1% Triton X-100, 0.2% gelatin, 1 mM EDTA in PBS). The 1X TXEB was removed, each well was filled with 100 µl of 2X TXEB plus 100 µl of sample, and the plates were incubated, while shaking for 1 hour. The plates were washed three times with 250 µl of 1X TXEB and incubated (100 µl/well) with rabbit polyclonal anti-VWF conjugated with horseradish peroxidase (HRP) diluted in 1X TXEB to 1.3 µg/ml for 1 hour with agitation. After three washes with 250 µl/well of 1X TXEB and the HRP was detected using a kinetic assay, by adding 200µl o-phenylenediamine in citrate phosphate buffer with 0.1% Triton X-100. The reaction was followed over 30 minutes at 450nm using Softmax pro software and a Thermomax microplate reader (Molecular Devices).

2.4.3 SDS polyacrylamide gel electrophoresis

Polyacrylamide gels were prepared according to details in Table 2.10, using reagents from Sigma. N,N,N,N-tetramethyl-ethylenediamine (TEMED, National Diagnostics) and ammonium persulphate (APS, Bio-Rad) were used to induce polymerisation.

Table 2.10 ***Constituents of polyacrylamide resolving and stacking gels.***

Reagent	8% resolving gel (volume for 10ml)	5% stacking gel (volume for 3ml)
H_2O	4.6ml	2.1ml
30% Acrylamide	2.7ml	0.5ml
1.5M Tris-HCl pH8.8	2.5ml	0.38ml
10% SDS	100µl	30µl
10% APS	100µl	30µl
TEMED	10µl	3µl

Samples were mixed with protein sample buffer (10mM Tris-HCl – pH8.0, 1mM EDTA, 2% SDS, 8M Urea, plus Bromophenol blue) and heated to 95°C for 10 min prior to loading. Gels were run in Bio-Rad Mini Protean II™ tanks using SDS-PAGE running buffer (National Diagnostics). Gels were run at RT. Full range rainbow markers (Amersham) were loaded as molecular weight markers.

2.4.4 Western blotting

For Western blotting, proteins were transferred using a Bio-Rad Trans-blot SD, semi-dry transfer cell. Protran nitrocellulose transfer membrane was soaked in transfer buffer (25 mM Tris, 192 mM glycine and 10% methanol), along with six sheets Whatmann 3M filter paper. Three pieces of the filter paper were placed on the transfer and pressed down with a pipette to remove air bubbles. The nitrocellulose membrane was then added, followed by the gel, three more sheets of filter paper, pressing down after each sheet. The transfer cell was and the transfer was carried out at 10V for 30 minutes.

Membranes were blocked by shaking in 5% 'Marvel' milk powder-PBS-Tween® (Sigma) for 1 hr at room temperature. Primary antibodies were added for either 1 hr at room temperature or overnight at 4°C with agitation. Membranes were washed 5 times

for 10 min at room temperature in PBS-Tween® and reblocked in 3% milk-PBS for 30 min followed by addition of peroxidase conjugated secondary antibodies (Jackson Immunochemicals) for 1 hr at room temperature with agitation. Secondary antibodies were washed off using 3x 10 min washes in PBS-Tween®. Bands were then visualised using ECL western blotting detection reagents (Amersham) and high performance chemiluminescence film (Hyperfilm, Kodak) according to the manufacturers instructions. The list of antibodies is shown in table 2.11.

Table 2.11 ***List of antibodies used for Western blotting and immunoprecipitation.***

Antibody	Species	Source	Working dilution
Clathrin	mouse	BD transduction	1:1000
GFP	rabbit	Abcam	1:100
mouse-HRP	donkey	Jackson	1:5000

2.4.5 Co-immunoprecipitations

Paramagnetic anti-rabbit dynabeads (Dynal PROTECH) were prepared by removing supernatant, using the magnet provided to pellet the beads at each stage. The beads were first washed and then incubated for 1 hour in PBS with 0.1% BSA at 4°C.

The lysates were prepared by incubating the cells on ice and washing with ice cold PBS. The cells were then scrapped in 1X lysis buffer (20mM Tris-HCl pH7.4, 150mM NaCl, 1mM EDTA, 1% Triton X-100, 0.5% NP-40, 1mM Na_3VO_4, 1mMNaF and protease inhibitors). The lysates were subsequently passed through a 25g needle three times and spun down at 12,000g for 10 minute at 4°C.

The blocking buffer was removed from the beads, using the magnet to pellet the cells. The beads were then resuspended in the lysate and incubated for 1 hour on a rotating wheel in the cold room. The beads were then pelleted on the magnet and washed 5 times with lysis buffer. Finally, the beads were resuspended in reducing buffer and

boiled for 5 mins. The samples were then analysed by SDS-PAGE and Western blotting.

2.5 Computational Software

All image analysis was performed using Adobe Photoshop (Adobe Systems), version 8.0 and ImageJ (Wayne Rasband, NIH). Quantification of the amount of non-ER fluorescence after cytochalasin D was performed using a macro for ImageJ written by Miguel Branco (MRC-CSC, London). The macro is available in Appendix I. Quantitative data was depicted using Microsoft Excel. Sequence alignments were performed using Clustal W software.

3 High pressure freezing and WPB

3.1 Introduction

WPB were first observed and described using electron microscopy (EM) and like other LRO, EM is still used extensively to study their formation and content (Weibel and Palade, 1964). WPB in particular are instantly recognisable under the electron microscope due to the unique elongated 'cigar' shaped conformation of the organelle and the internal striations, which immunoEM has identified as VWF (Ewenstein et al., 1987). Indeed, these two phenomena are intimately linked with the tubulation of VWF causing the elongated shape (Michaux et al., 2006a). The functional importance of tubulation is that only when the VWF is stored in such a conformation can the VWF be released as long platelet-capturing strings upon exocytosis. Michaux et al. demonstrate that tubulation of VWF is dependent on an interaction between the propeptide and the mature form of VWF. This interaction is only stable at a relatively low pH and is disrupted upon exocytosis and exposure to the neutral pH of the blood. The release of VWF strings, but not the shape of the organelle, is also dependent on the disulfide bonds that form as the VWF multimerises (Michaux et al., 2006a). This exciting work has prompted a need to consider the relationship between the tubules and the formation of the organelle in more detail, and the perfect technique to do this is electron microscopy. However, use of conventional fixation is not sufficient for an in-depth study. The development of a new fixation technique of high pressure freezing (HPF) and the commercial production of the instruments required has allowed the improved fixation of endothelial cells to study the biogenesis of WPB and hopefully other LRO in the future.

The main advantage of HPF is, of course, the speed of fixation. The increase in pressure inside the machine to 2000 bars allows the sample to be frozen instantaneously in liquid nitrogen (Reipert et al., 2004; Studer et al., 2001). The speed of freezing also means that all components of the cell are fixed at the same moment. As with all EM samples, in order to allow for observation the sample must be dehydrated, and it is thought that it is freeze substitution after fixation that accounts for much of the improvement in the

quality of the EM sample after HPF. During freeze substitution the water in the cells is replaced with acetone, but importantly this is done at extremely low temperatures, usually starting between –80 to -90°C and samples are only warmed up to room temperature extremely slowly (Giddings, 2003). This is less harmful to the samples than the ethanol dehydration that is often used, which is thought to contribute to the artefactual curvature of the membrane that can sometimes be seen.

The use of HPF has allowed for the in-depth study of the relationship between the tubules and membrane in forming the uniquely shaped WPB. In addition, further details in the maturation of WPB have been identified, as well as raising many questions that should and can now be addressed.

Chemical fixation has been used to great effect to study the biogenesis of WPB. However, using this method the connections to the TGN in particular are not well preserved. Figure 3.1 is composed of electron micrographs prepared and processed by Lindsay Hewlett of the peri-Golgi area, indicating the difficultly in preserving that area well. Panel A shows the Golgi stack with two bulbous structures (arrows) protruding from the trans-most cisternae (all images in this thesis are included on a CD at the back of this thesis). The structures have an amorphous content but their size is suggestive of forming WPB. In panel B it is possible to identify structures with tubular content (arrows) and with the characteristic clathrin coating in close proximity to the Golgi stack (bottom of picture). However, none of these structures have preserved connections to the Golgi stack. Likewise, in panel C there are two more elongated structures close to the Golgi (bottom right), also containing tubules, but again with no connections maintain. Finally, in Figure 3.1D is the only example found in the vast collection of the Cutler lab in which the connection of the forming WPB is observed. It is possible to distinguish both tubular content and clathrin coating on this structure, confirming that it is indeed a WPB.

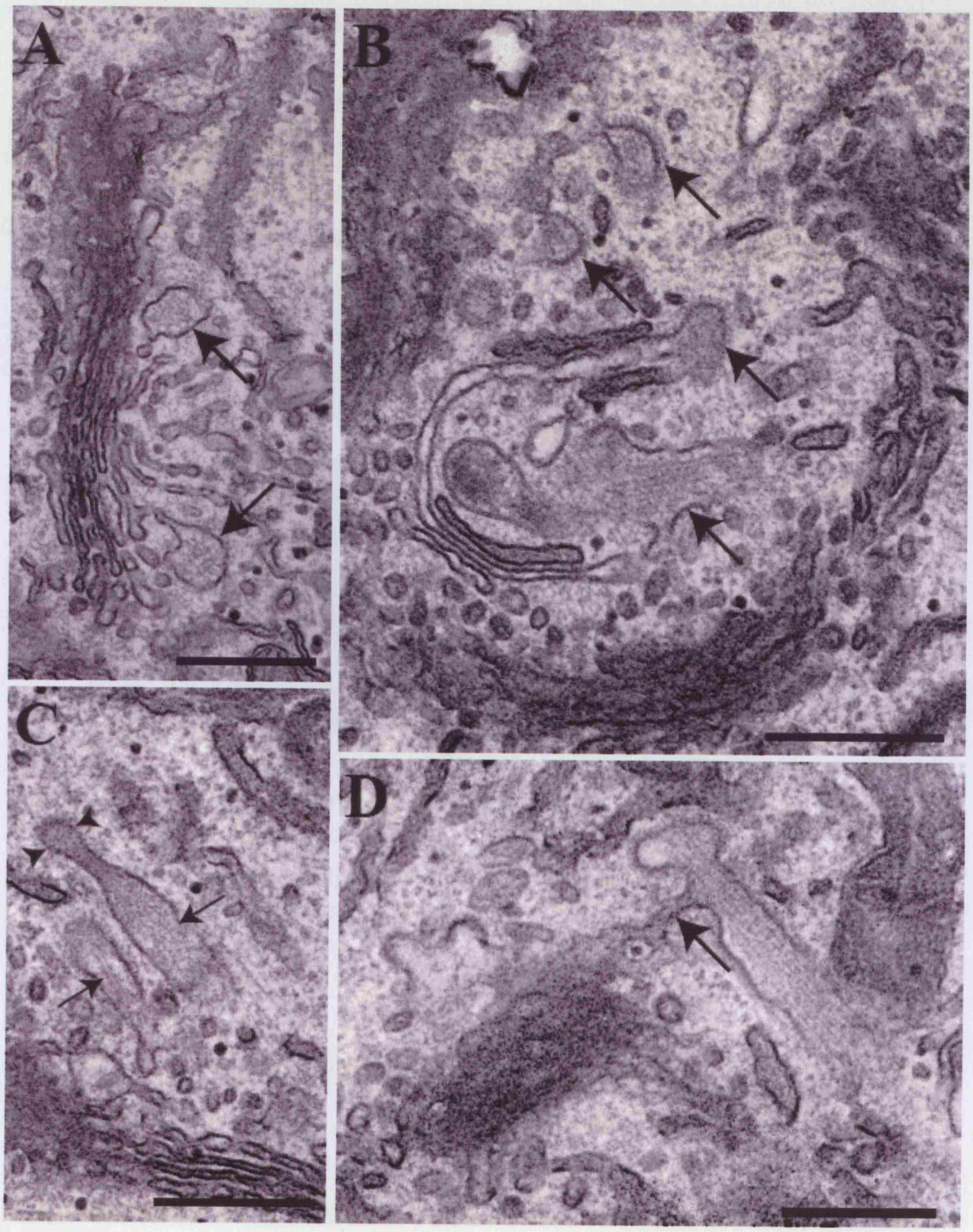

Figure 3.1 ***Cultures of HUVECs prepared for conventional transmission EM after chemical fixation give hints of the early biogenesis itinerary of WPB.***

HUVEC are grown on coverslips and fixed using conventional chemical fixation and processed for electron microscopy by Lindsay Hewlett. Arrows in panel **A** and **B** indicate potential WPB and in the case of panel **B** with clathrin coating. In panel **C** arrows refer to VWF tubules and in panel **D** the arrow indicates a connection to the

TGN. All scale bars represent 200nm.

WPB themselves are well preserved and the relationship between the tubules and the membrane is uncomplicated with the membrane wrapped directly around a bundle of tubules (Figure 3.2 from L. Hewlett). In addition the VWF tubules are all neatly aligned to one another and appear to run alone the whole length of the WPB, perhaps suggesting that the length of the organelle is directly determined by the length of the VWF tubules incorporated. However the distorted membrane suggests that the preservation of this sample is not optimal, possibly arising from the dehydration steps at room temperature.

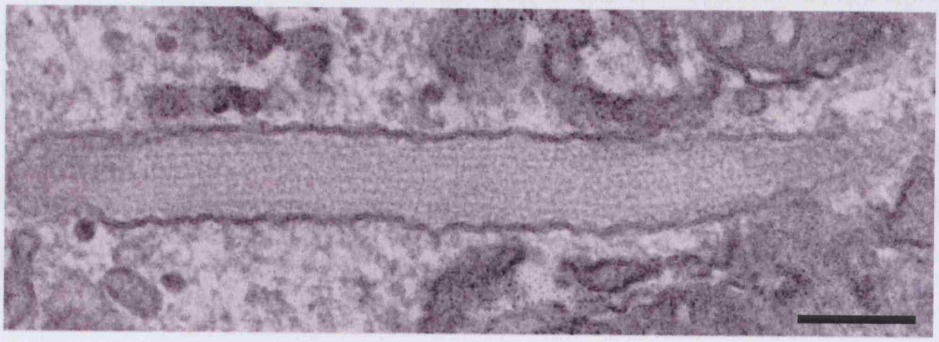

Figure 3.2 ***The membrane of the WPB is wrapped directly around VWF tubules in EM images after chemical fixation.***

HUVEC are grown on coverslips and fixed using conventional chemical fixation and processed for electron microscopy. Scale bar presents 200nm.

3.2 Results

The findings are somewhat different when using HPF-FS to prepare the sample. For HPF, the HUVEC are grown on 1.2mm diameter sapphire coverslips, which are coated with carbon and gelatin, for 40-48 hours prior to fixation. This protocol balances the need for the cells to remain attached to the coverslips during the freezing procedure yet not be so firmly attached that they remain on the coverslip instead of being embedded in the epon after the coverslip is removed. The coverslips are removed from the tissue culture dishes and placed in the high pressure freezer as quickly as possible. A small amount of media in the sample holder is sufficient to act as a cyroprotectant for the cells. After fixation the samples must remain under liquid nitrogen at all times until ready for

freeze substitution. The freeze substitution protocol used in this thesis, FS(A) and FS(B) are longer protocols taking four and five days respectively. In both cases, the cells are incubated in osmium tetraoxide and tannic acid, which contribute to the staining of the sample. Water is kept to a minimum during this process to avoid any ice damaging during the substitution process, as the sample are slowly warmed to room temperature. As discussed earlier, the samples are then embedded as normal in epon. Figure 3.3 is an electron micrograph produced using HPF-FS. The improvement in preservation is immediately obvious with less extracted cytoplasm, better-defined membranes with no artefactual membrane curvature and more distinct clathrin coats. The image is of the peri-nuclear area and is dominated by Golgi ribbons and TGN, as well as multiple vesicles, many with clathrin-coating. In addition, there are three WPB, identified by their tubule content and indicated by arrows. Interestingly, there is a clathrin-coated vesicle emerging from the WPB on the left hand side, indicating that sorting could be occurring at a very early stage in biogenesis; this will be discussed in more detail later in the chapter.

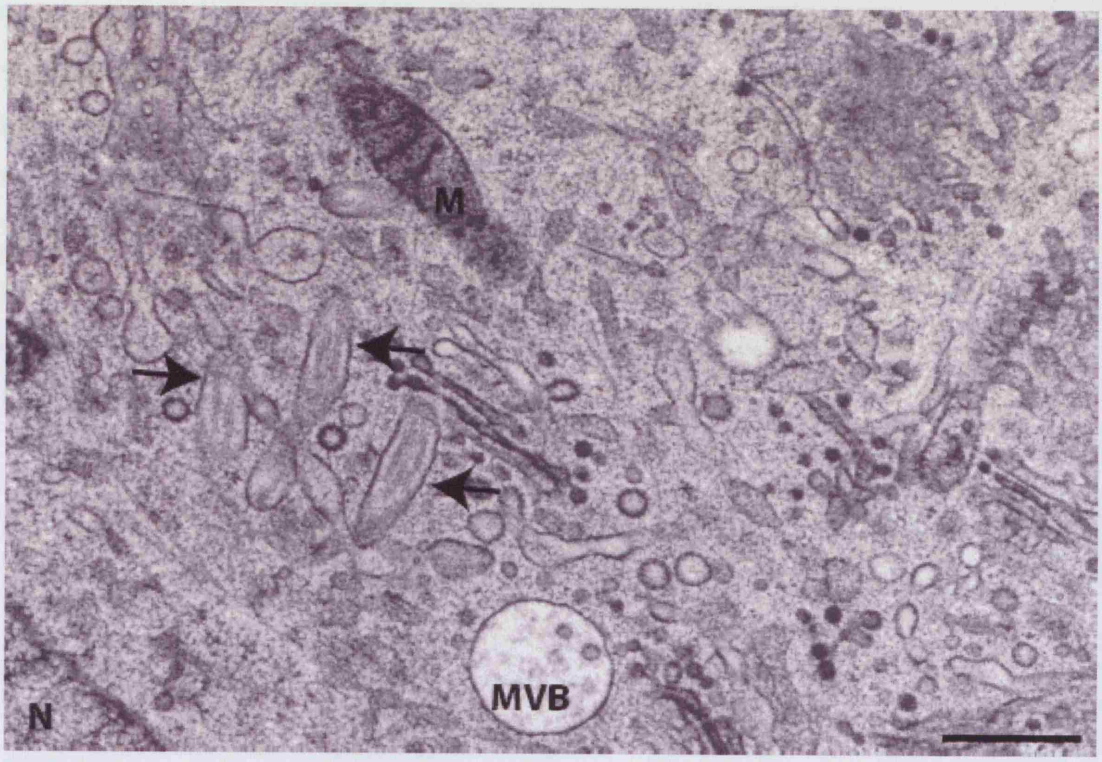

Figure 3.3 ***Use of HPF-FS results in better preservation of HUVEC.***
HUVEC were grown on sapphire coverslips and processed using HPF-FS. N – nucleus, M – mitochondria, MVB – multi-vesicular body. Scale bar represents 500nm

3.2.1 Tubulation in the TGN

It has long been suspected that the tubulation of VWF takes place within the TGN. It cannot occur at an earlier point in the secretory pathway since the protease furin, which is localised to the TGN, is responsible for cleavage of proVWF into the propeptide and mature form of VWF that subsequently interact allowing the formation of tubules (Mayadas and Wagner, 1989; Wagner et al., 1986; Wise et al., 1991; Wise et al., 1988). Low pH in the TGN is also required for the interaction and cell type differences in intra-Golgi pH may account for why some cells are able to form pseudo-WPB whilst others are not. Figure 3.4 taken by Lucy Collinson clearly demonstrates that tubulation does begin within the TGN and not confined to the post-Golgi WPB. The TGN is identified by its proximity to the Golgi stack, the fenestrations it contains and the numerous clathrin-coated buds. The protrusion contains a single tubule of 314nm, which perhaps

may be sufficient to support the extension of the membrane from the TGN, and represent the earliest stage of WPB formation. The presence of the clathrin coat on the protrusion indicates that clathrin is required at the very earliest stage of biogenesis; this supports the finding from Lui-Roberts et al. (2005); that clathrin is required for the formation of WPB. Whether clathrin is required for the formation of tubules or to support the growing organelle is unclear but Lui-Roberts and co workers do demonstrate that is not required for the maintenance of the tubules post-budding (Lui-Roberts et al., 2005). How this protrusion is formed will be discussed in the next chapter.

Figure 3.4 **Tubulation of VWF begins in the TGN.**
An electron micrograph of HUVEC fixed using HPF-FS(A) by Lucy Collinson. Arrowheads point to a VWF tubule. TGN – trans-Golgi network; G – Golgi. Scale bar represents 500nm

3.2.2 Stalk-like structures maintain the connection between the forming WPB and the TGN

As the WPB grow longer and become more filled with tubules, they remain attached to the TGN by 'stalk-like' structures that are significantly narrower at approximately 50nm than the width of the forming WPB (Figure 3.5). These pictures indicate that WPB are not simply swollen sections of cisternae that become filled with tubules as they are formed in the TGN, but rather there is a positive force that is driving the formation. Interestingly, as is apparent from panels A and B, the WPB are lined up in parallel to the TGN and Golgi stack perhaps suggesting a role for some tethering factor along the

length of WPB. However as panel C, by Lucy Collinson, shows this is not always the case, where the WPB is protruding away from the TGN. The membranous stalks themselves are devoid of tubules and whether these connections are an intermediate stage in fission of the WPB from the TGN, after they are sufficiently full of VWF, is a possibility. This is supported by the fact that the tubule-filled structures that remain attached are a similar length to the immature WPB, rather than shorter structures that still need to recruit more VWF. In panel D there is a single tubule within a clathrin-coated bud at the TGN, and although there is negative curvature at the neck of the bud it seems likely that the tubule will prevent scission from occurring. Thus the continued delivery of tubular VWF may be important in ensuring the WPB reaches its correct size by blocking the action of the scission machinery.

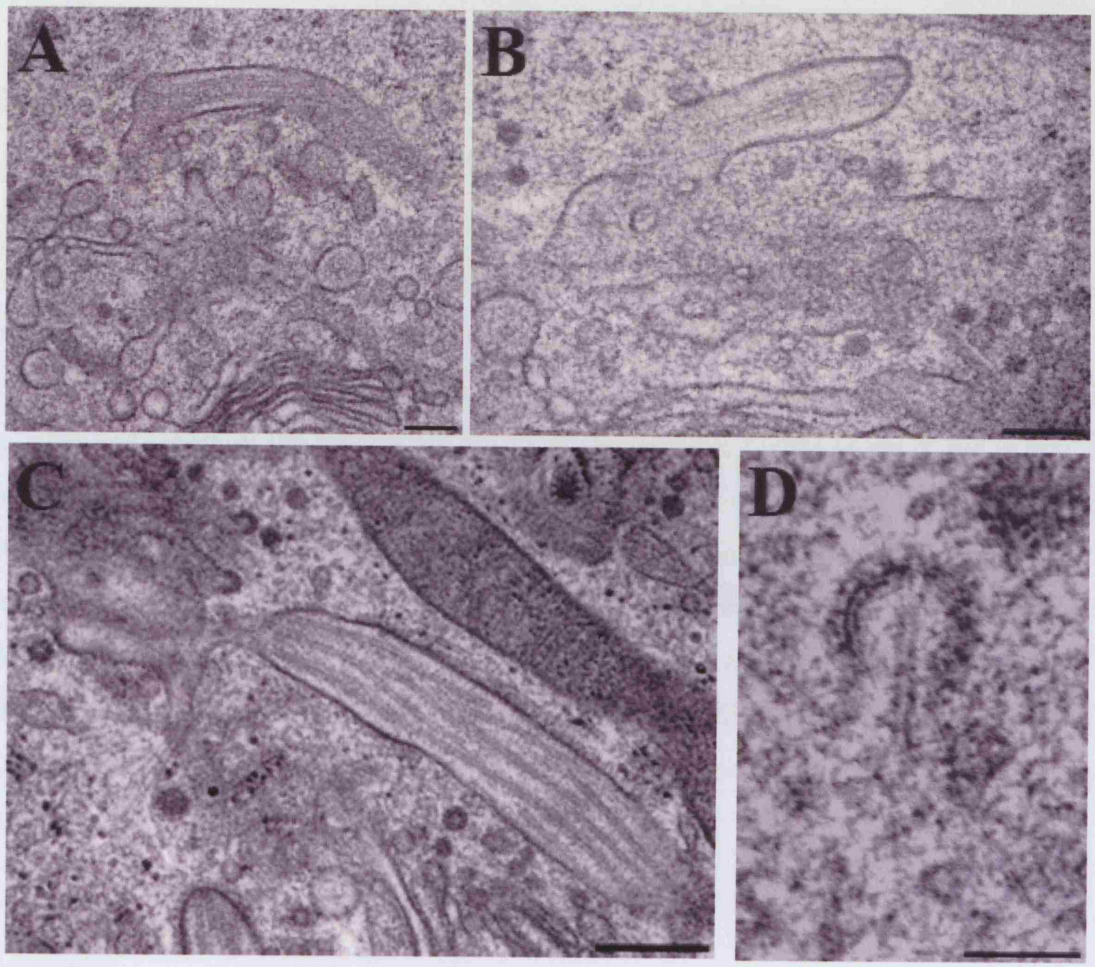

Figure 3.5 ***WPB remain attached to the TGN by membranous stalks and the tubules may be important in ensuring that premature scission doesn't take place.***

HUVEC are fixed using HPF and panels **A** and **B** are processed using FS(B) and panels **C** (by Lucy Collinson) and **D** using FS(A). These picture focus on the peri-Golgi area. Scales represent 200nm for **A-C** and 100nm for panel **D.**

The frequency at which this stalk-like connection is observed seems to suggest that it is a relatively stable conformation, further implying that budding is a two-step process with the generation of negative curvature to form the stalk, occurring prior to the action of the scission machinery. Of course there may be small multimers not yet formed into the characteristic tubules being delivered through this connection to the TGN and other secretory and membrane proteins may also be recruited at this point before full scission from the TGN occurs. The need to deliver cargo could of course contribute to the stability of the membranous stalk.

3.2.3 The relationship between the tubules and membrane in immature WPB is complex

In Figure 3.2 it would seem that the membrane of the WPB is simply wrapped around the tubules of VWF that it contains and thus the tubules are directly responsible for determining the size and shape of the organelles. Results from HPF (Figure 3.5 and Figure 3.6) indicate that the relationship is more complex, although it is likely that the number and length of the tubules are ultimately responsible for the shape of the organelle. Figure 3.6 consists of micrographs of a number of immature WPB, defined as such by their proximity to the nucleus and Golgi. They contain differing numbers of tubules, which may refer to their state of maturation, or simply indicate that WPB are a heterogeneous mix of sizes. In panels A-C, the WPB are *enface*, with panel A probably representing the most immature WPB, and panel C respecting the most mature. Panels D and E are cross-sections of WPB, with the circular content indicating that VWF forms true tubules.

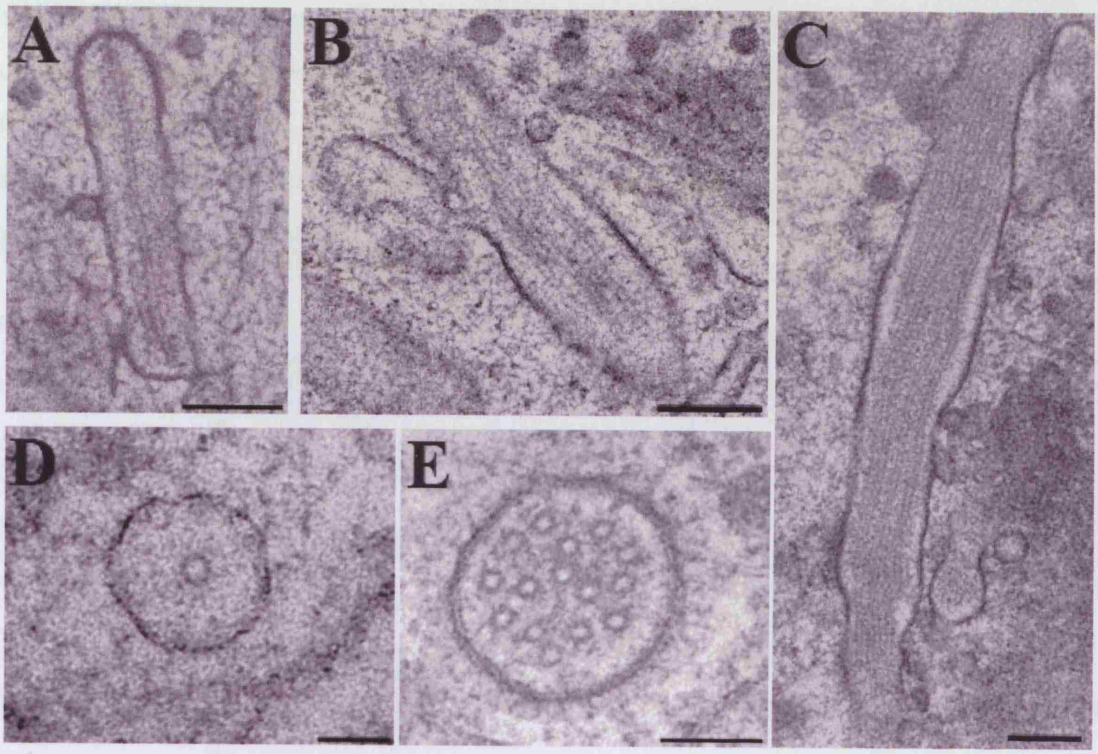

Figure 3.6 ***The tubules in immature WPB are disordered and are able to contact each other or the membrane along their long axis.***

HUVEC were grown on coverslips and processed using HPF-FS(B). Images were taken in the peri-Golgi area. Scale bars represent 200nm for **A-C**, 50nm for **D** and 100nm for **E**.

What holds true in all of these images is that the membrane is not directly wrapped around the tubules; rather the tubules and membrane never come into contact along their long edge, although they are able to abut the membrane at the tip. There is a great deal of disorganisation in these early WPB and by no means do all tubules run parallel to each other along the full length of the WPB. However, the tubules do seem to overlap such that in these elongated structures there are no areas that are completely devoid of tubules. Furthermore, the tubules, whilst relatively disorganised, also do not seem to contact each other, never lining up next to each other, although they can cross each other. The space between the tubules and indeed between the tubules and the membrane seems quite regular, and the graph in Figure 3.7 indicates that this may indeed be the case. This is also demonstrated quite clearly in the cross section of the immature WPB (indicated by the presence of the clathrin coat) in panel E, where although the spacing

between the tubular cross sections is not completely regular the spacing is certainly very similar. It is also apparent that the tubules are able to come into closer proximity with each other than with the membrane. The widths of the immature WPB were measured using the iTEM software, where each side of WPB remained within section, and the number of tubules within the WPB was recorded.

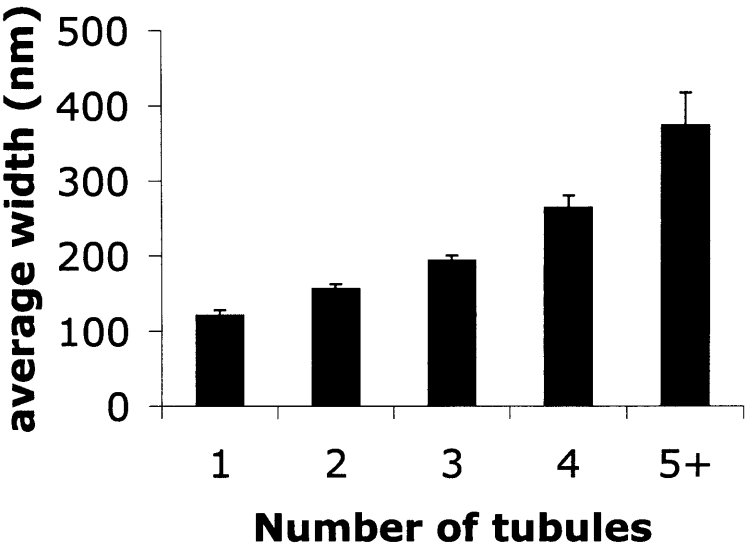

Figure 3.7 ***The width of the WPB is determined by the number of tubules incorporated.***

WPB were grouped using the number of tubules apparent in the section and the width was measured. n = 4-20 per bar; error bars represent standard error.

It is clear from the graph that the width of WPB is proportional to the number of tubules incorporated at the captured section of the organelle. The consistent spacing of the tubules suggests repulsion between the tubules. This could be explained by the fact that VWF is extensively decorated with sialic acid, a negatively charged carbohydrate moiety (Samor et al., 1982). The negatively charged membrane would also be unable to come into close proximity with the tubules. Indeed there are clinical VWF mutations affecting the glycosylation state of VWF and causing disease and likewise as mentioned in the introduction the only VWF modifier gene identified so far is a sialic acid transferase (Ellies et al., 2002). However, these defects could be due to a failure to bind components in the blood or reduce the half-life of the VWF, rather than affecting the

organisation of the VWF tubules. The minimum width of the tubule containing structures observed is 120nm, wider than would be expected from the 'repulsion hypothesis', but could be due to the presence of clathrin when the WPB is first forming.

3.2.4 Maturation: a second role for clathrin?

Clearly clathrin has an essential role in the formation of WPB, and as the micrographs above indicate, this is probably at the very earliest stage of formation. However, Figure 3.8 indicates clathrin also plays a continuing role in the global organisation of the WPB. In panel A, the immature WPB is coated at the left-hand tip is coated with clathrin, which is probably playing the supportive role shown earlier. However, there is also a clathrin-coated protrusion on the right hand side of the WPB. Whether this is involved in reorganisation of the tubules and membrane or a region budding off from the WPB is not clear. In panels B and C there are clearly clathrin-coated structures budding off the WPB. Indeed in panel B the vesicle, indicated by the arrow, is almost completely detached from the WPB. The presence of the coat on these structures indicates that material is being removed from the WPB as opposed to being delivered.

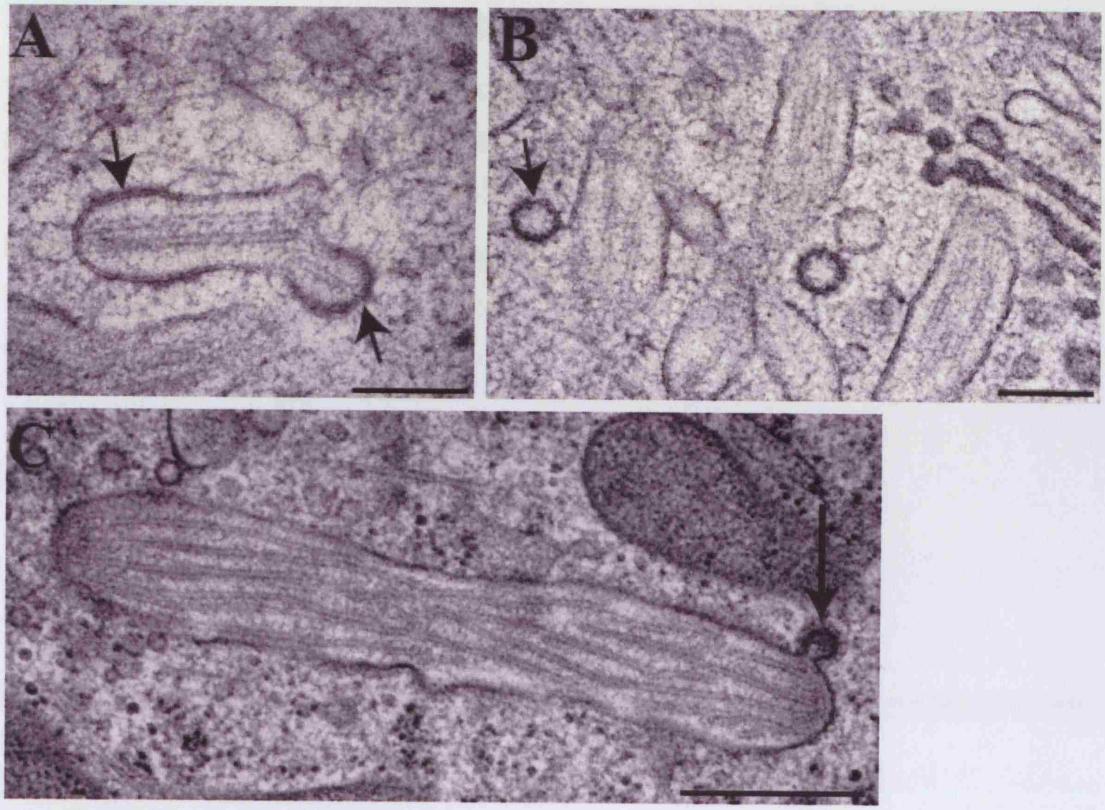

Figure 3.8 ***Clathrin has a dual role in the biogenesis of WPB***

HUVEC are fixed using HPF and processed using FS(B) for panels **A** and **B** and FS(A) for panel **C**. Arrows indicate clathrin-coated buds. Scale bar represent 200nm, 200nm and 500nm respectively.

Unlike the larger protrusion in panel A, there are no tubules apparent in the buds and it is likely that either material is being removed to be recycled back to the TGN, or that this is a form of constitutive-like secretion (Dittie et al., 1999; Klumperman et al., 1998; Kuliawat and Arvan, 1992) , whereby low molecular weight multimers are removed from the WPB and are secreted into the bloodstream. The adaptor protein complex responsible for the removal of material has not yet been identified. This maturation step may be analogous to the removal of TGN resident proteins from the secretory granules of neuroendocrine cells (Kakhlon et al., 2006). An obvious outcome of this removal is the concentration of cargo, which is an important step in the maturation of the granules; the use of HPF indicates that a similar process may occur for the WPB.

3.2.5 Cargo concentration in the mature WPB

Using light microscopy it is possible to distinguish between the newly formed or immature WPB and the mature WPB by the membrane proteins that are incorporated. As mentioned in the introduction, Rab27a and CD63 are recruited as the WPB mature, however, no such distinction can be made in chemically fixed samples. The case is somewhat different after HPF-FS. Figure 3.9 is made up of images of mature WPB, and it is obvious that there is a dramatic increase in the electron density of the organelle when compared with Figure 3.6.

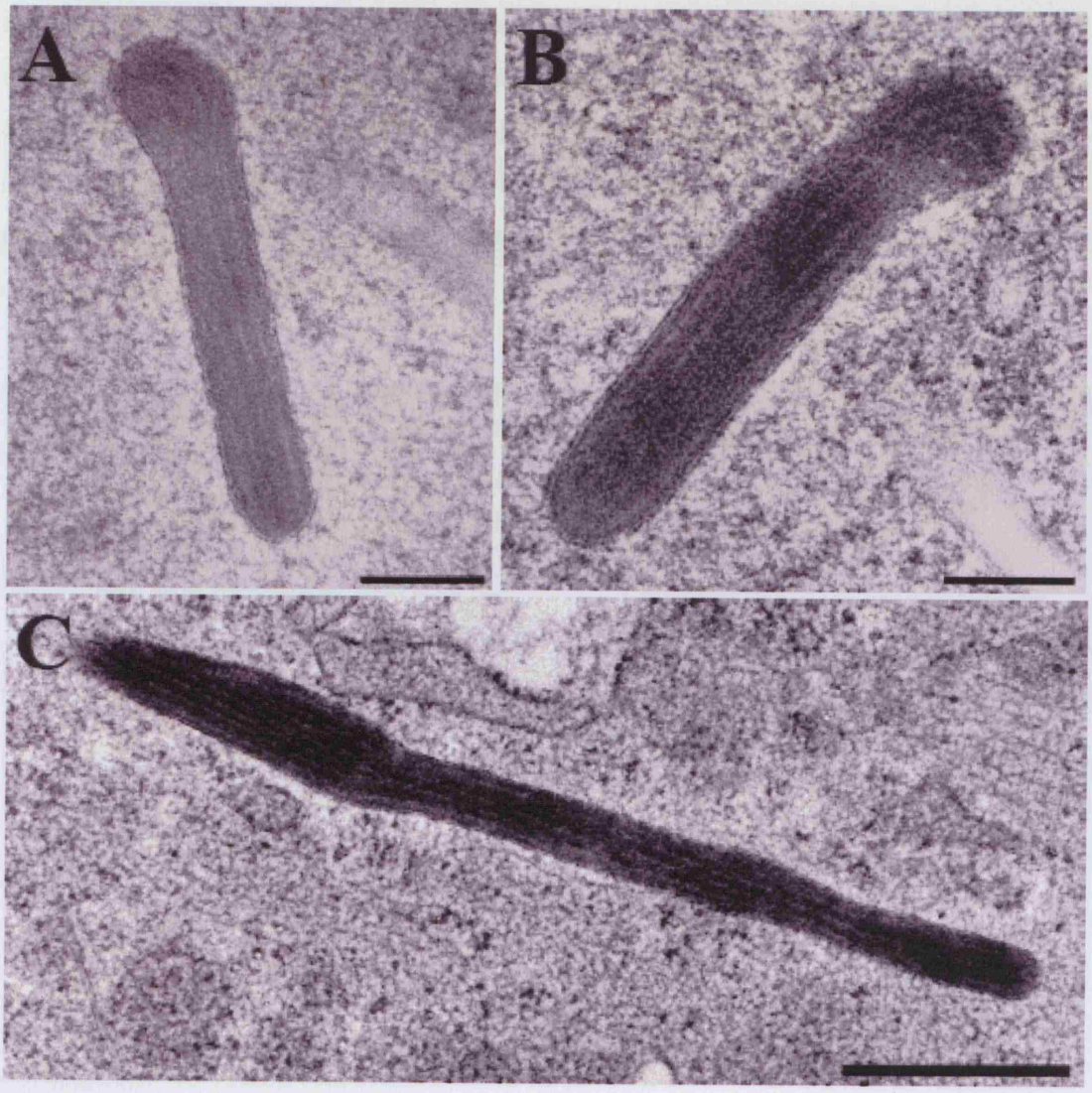

Figure 3.9 ***Mature WPB are more electron-dense than immature WPB and the relationship between the tubules and between the tubules and membrane is less complex.***

HUVEC were grown on coverslips and processed using HPF-FS(B). Scales bars represent 200nm for panels **A** and **B** and 500nm for panel **C**.

These WPB were first designated as mature by their position in the cell. The WPB positive for Rab27a and CD63 are found in the periphery of cells, whilst the ones in the peri-Golgi area are negative for these membrane proteins. This designation correlates well with the electron-lucent and electron dense organelles. Figure 3.10 is a low power image showing both an immature, electron-luent WPB (arrowhead) next to the Golgi, whilst the mature, electron-dense WPB (arrow) in the periphery. The presence of both

immature and mature WPB within the same images indicate that the increase in electron density is not due to differences in staining. Whether the increase in electron density exactly correlates with the recruitment of membrane proteins is not known. The increase in electron density could be attributed to the recruitment of additional, as yet not identified, proteins to the WPB. Alternatively it could be due to the accumulation of charge, since it is known that the mature WPB are lower in pH than the immature ones.

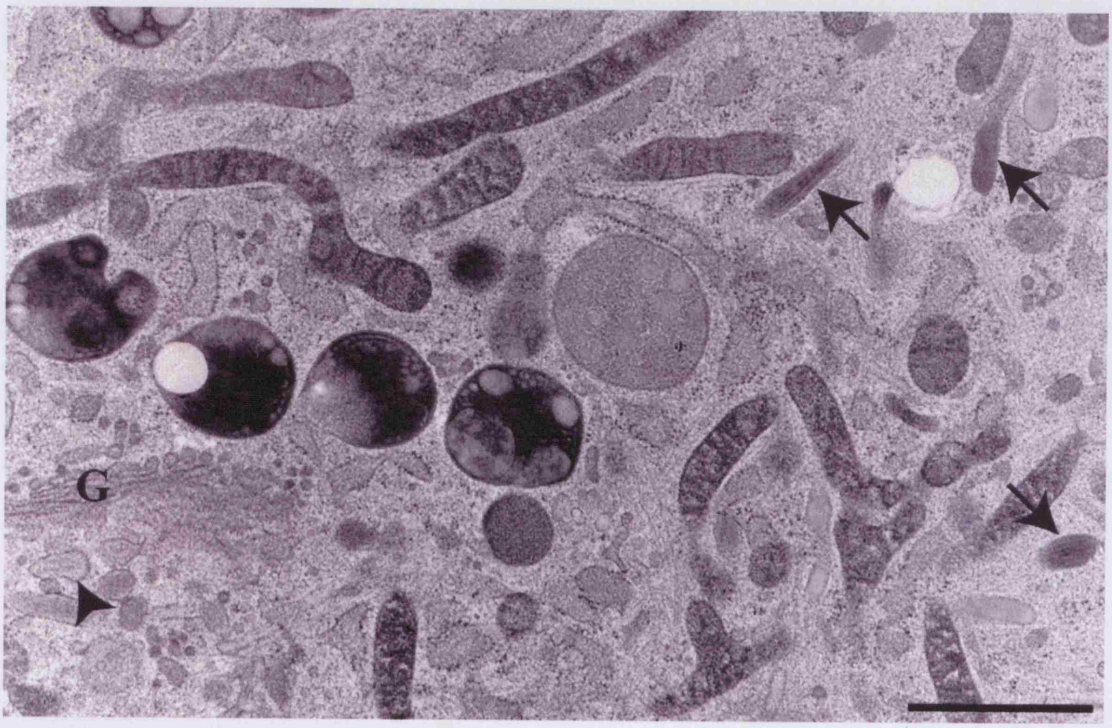

Figure 3.10 ***A low power view of an endothelial cell showing both immature and mature WPB.***

HUVEC were grown on coverslips and processed for EM using HPF-FS(B). The arrowhead indicates an immature WPB, whilst the arrows point to mature, electron dense immature WPB. G – Golgi. Scale bar represents 1μm.

The inter-tubule relationship as well as that between the tubules and the membrane also changes as the organelle matures, and this will contribute to the increase in electron density. The tubules within mature WPB are more ordered than those in immature WPB, arguably to ensure that the strings do not become entangled upon exocytosis. Furthermore, the tubules are now able to contact each other and the membrane along the long edge as well as at the tips. To continue the hypothesis that it is the negative charge

of VWF that is causing repulsion between the tubules the membrane, then the decrease in pH by the addition of hydrogen ions could be sufficient to overcome this repulsion. Further support of the hypothesis that there is no longer significant space between the tubules and the tubules and the membrane is the finding that the mature WPB are in fact narrower than the immature ones, despite the fact that they seem to have more tubules incorporated (Figure 3.11A). However, whilst there is a difference in the mean width of mature versus an immature WPB, there is significant overlap between the populations (Figure 3.11B). This is presumably a reflection of the fact that, ultimately, the width of the organelles is dependent on the number of tubules incorporated.

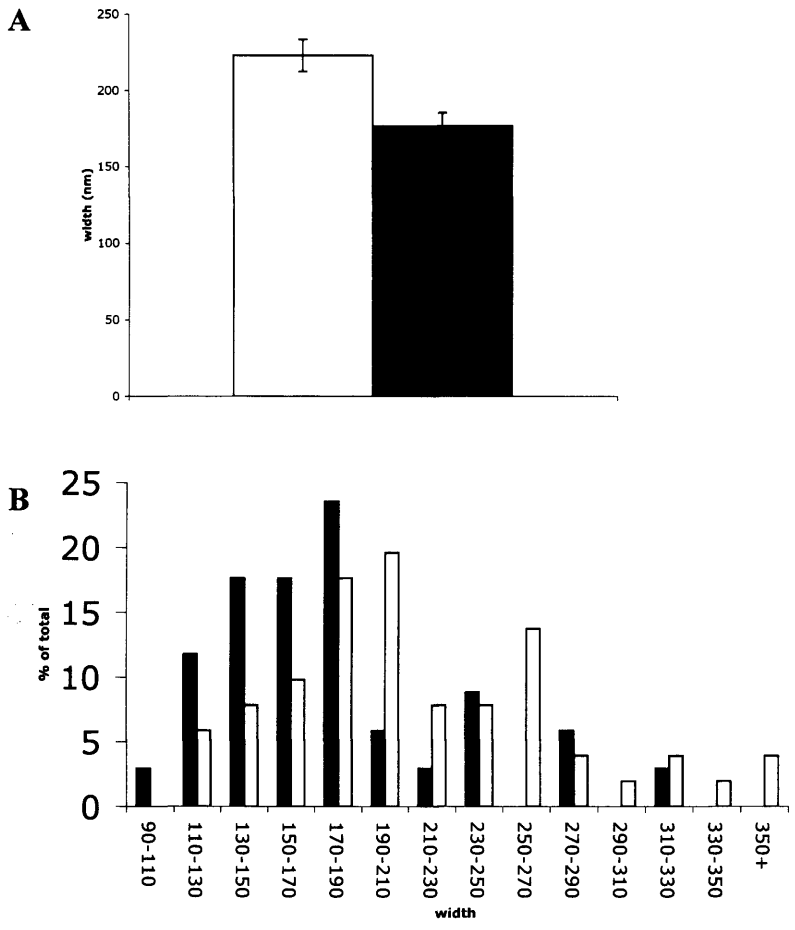

Figure 3.11 ***Mature WPB are, on average, narrower than immature WPB.***

WPB were defined as immature (white) or mature (black) on the basis of their electron density. The width of each organelle was measured and panel **A** is a graphical representation of the mean width. To generate the graph in panel **B** the WPB were

grouped into size bins to highlight the diversity in widths and number are expressed as the percentage of the total number of WPB. n=51 for white and n=34 for black. Error bars represent standard error.

3.2.6 An alternative organelle

In addition to the mature WPB that have been displayed thus far, there also seems to be an alternative form of mature WPB shown in Figure 3.12. These organelles are the same size as mature WPB, but they have no obvious tubular content. Like mature WPB they are found in the periphery of the cell, and as panel D shows they even cluster together. The electron density of these alternative WPB is somewhat less uniform than that observed in mature WPB. ImmunoEM will be required to confirm whether these structures truly are WPB. However, it would be surprising if they can maintain their elongated shape without tubular content, since Michaux et al. (2006) demonstrated that disrupting tubules using monensin cause the rounding of all WPB. Perhaps more likely is that these structures do contain tubules that are masked by other content proteins that are sometimes incorporated into WPB.

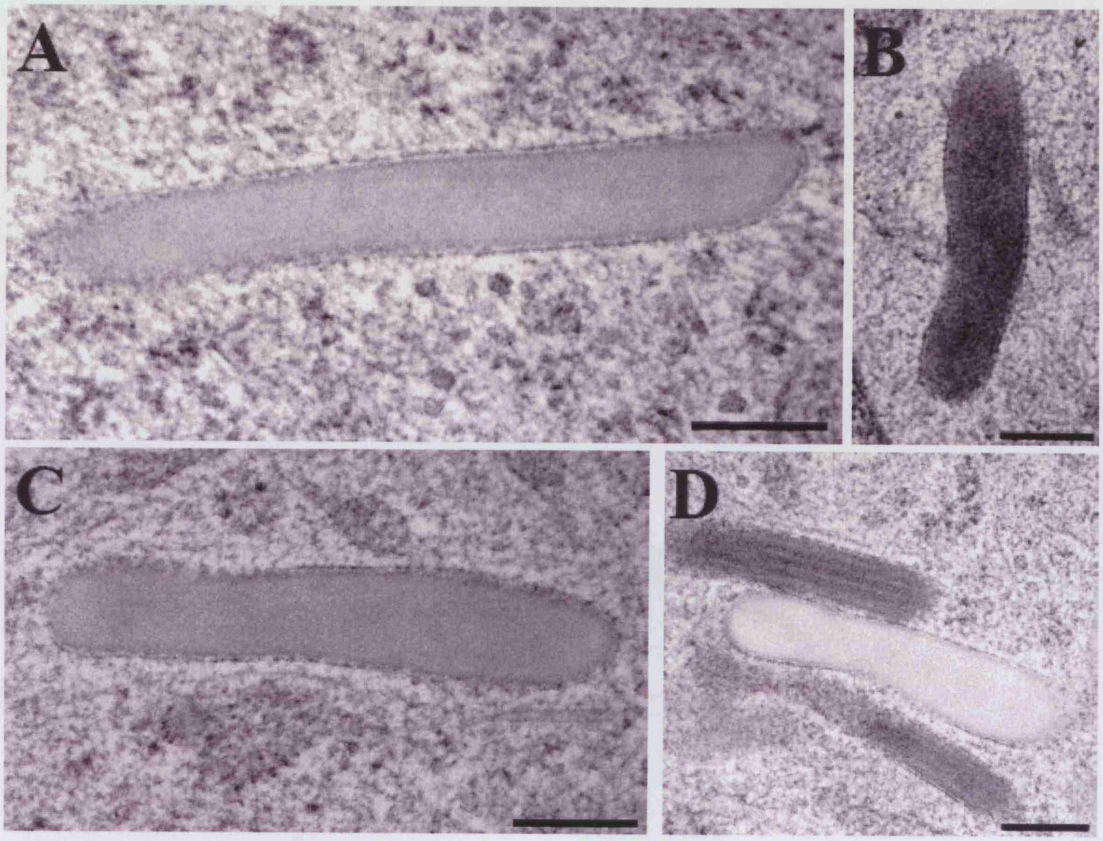

Figure 3.12 ***Elongated structures that have no obvious tubular structure are also found in HUVEC.***

HUVEC were grown on coverslips and processed using HPF-FS(B). Scale bars represent 200nm.

3.2.7 Fusion of WPB

Whilst the mature WPB are narrower on average than the immature WPB, it is immediately obvious that mature WPB are longer. However, it is not possible to measure length using the images generated by EM, since the length of the WPB greatly exceeds the section thickness (70nm). The length of both immature and mature WPB was measured using immunofluorescence images, with the recruitment of Rab27a used to designate the mature WPB. The measurement is likely to be an underestimate, since only straight WPB are measured as it is impossible to determine whether a "bent" WPB is, in fact, made up of multiple WPB. The EM images and timelapse movies previously published (Figure 3.16 and (Zenner et al., 2007)) show that the WPB can and do bend as

they move around the cell and are likely to be amongst the longest WPB in the cell. Despite the probable underestimate in the length of the mature WPB using this method, it is apparent that the mature WPB are indeed on average longer than the immature ones (Figure 3.13A). Using the average lengths calculated from the immunofluorescence images and the average widths calculated from the EM images, the surface area using the simplistic assumption that WPB are roughly cylindrical can be calculated (Figure 3.13B).

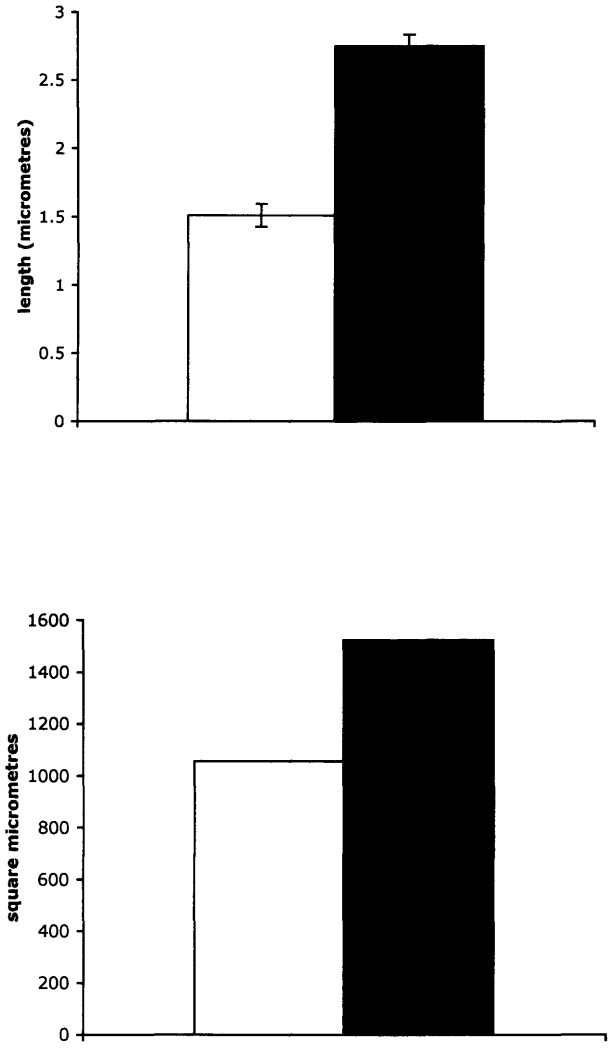

Figure 3.13 ***The mature WPB are longer and have a bigger surface area than immature WPB.***

In panel **A** the length of WPB was measured from immunofluorescence images and divided into immature (white) and mature (black) categories using Rab27a to designate mature WPB. n=76 for immature WPB and 142 for mature WPB, error bars represent standard error. The surface area represented in panel **B** is calculated from the mean width and length of the immature and mature WPB, assuming that the WPB are roughly cylindrical.

It is apparent that the surface area of the mature WPB is an additional 50% greater than that of the immature WPB, despite the removal of membrane by the clathrin-coated buds identified in Figure 3.8. This is indicative of fusion taking place; whether this is due to multiple small vesicles fusing with the WPB or WPB fusing with each other is not clear. Timelapse movies have been used to give an indication as to whether fusion of WPB is taking place. HUVEC were nucleofected with VWF-GFP and imaged both after 4 hours and one-day post transfection. The earlier timepoint was particularly useful because the presence of fewer fluorescent WPB, making it easier to distinguish if fusion was occurring. The WPB move quickly around the cell, thus images were taken every 5 seconds over a 5 minute period. Stills taken from the movies that represent possible fusion events are shown in Figure 3.14; the movie is available on the CD accompanying the thesis.

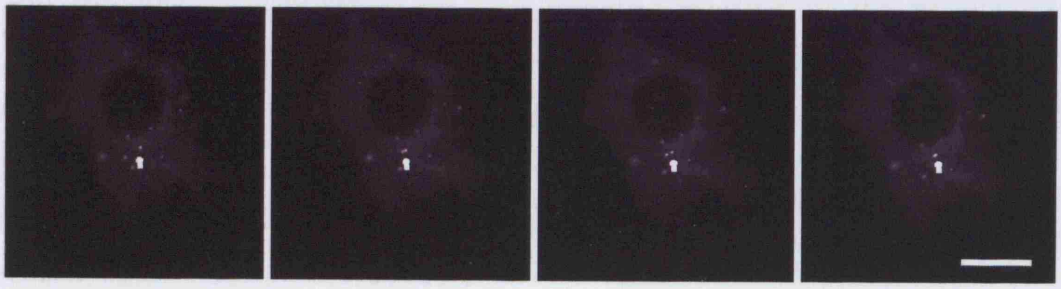

Figure 3.14 ***WPB appear to undergo homotypic fusion.***

HUVEC were nucleofected with VWF-GFP and after 4 hours were placed on the timelapse microscope. Images were taken every 5 seconds for 5 minutes. Scale bar represent 20μm.

Of course it is difficult to distinguish whether fusion is occurring or the WPB are simply aligned with one another, or indeed on top of one another. An indirect way to distinguish between these possibilities is to block fusion to determine if these suspected

fusion events still continue to occur. Within the cell, fusion of membranes is dependent on SNAREs, which in turn are dependent on NSF (Gotte and von Mollard, 1998). It is possible to block the activity of NSF using NEM, which can be added directly to culture media (Band et al., 2001). Thus further movies were made using the protocol discussed above, except with NEM added before filming began. However, it was quickly found that the effects of NEM were not specific enough for this study since movement of WPB is also blocked (see movie of NEM treatment on CD) and further reading indicates that NEM effects AAA-atpases, including motor proteins.

This result suggest that the fusion studies done using NEM without accompanying timelapse information should be revisited, since NEM treatment is able to block fusion indirectly by preventing movement. Treatment with DMSO alone has no such effect on the movement of WPB. Additionally, there are certainly EM images that are suggestive of fusion (Figure 3.15), but without correlation with live microscopy this cannot be proven. Figure 3.15 shows two potential fusion events, one between immature WPB and the other between two mature WPB. The fusion events in both cases are complete and of course could just represent the flexibility in WPB touched on earlier and discussed in more detail below. However, in panel A the presence of the branch point part way down the main shaft of the WPB does not seem a position that would offer the WPB any increase in flexibility. Likewise in panel B, the way the WPB is completely bent back on itself, but with no broken tubules apparent, seems more likely to a result of fusion of two WPB aligning alongside each other.

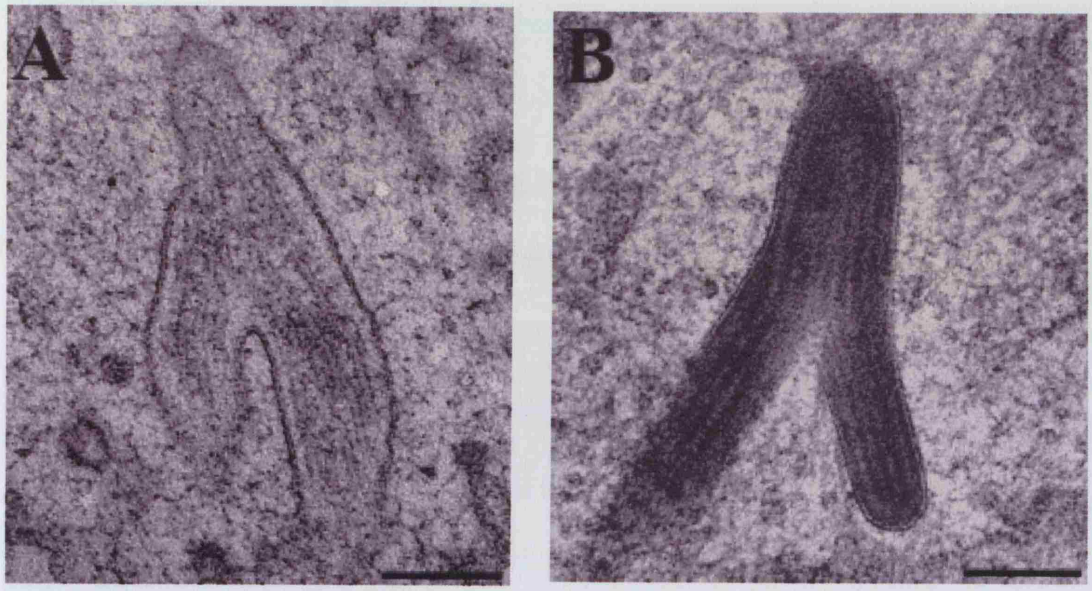

Figure 3.15 ***WPB may be able to undergo homotypic fusion.***
HUVEC are grown on coverslips and processed for EM using HPF-FS(B). Scale bars represent 200nm.

In a recent paper, Valentijn et al. (2007) have also claimed that they have demonstrated fusion from the 3D EM tomograms they have collected. They show WPB that are bent with discontinous tubules inside, and suggest that this is evidence of fusion (Valentijn et al., 2007). However, some of the images they have represented seem more like WPB that have bent in order to provide the organelle with the flexibility to move around the cells. Live cell imaging done in the Cutler lab (Zenner et al., 2007) shows that WPB do bend at sharp angles to move around the cell. Figure 3.16 shows EM pictures that seem to demonstrate this flexibility. In panels A and B it is possible to see broken tubules which could be indicative of a force that has been applied to allow for movement. Panel C shows that the 'alternate'mature WPB also bent at a sharp angle. However, it will not be possible to prove fusion is taking place without more complex live cell imaging and/or correlative live microscopy and EM.

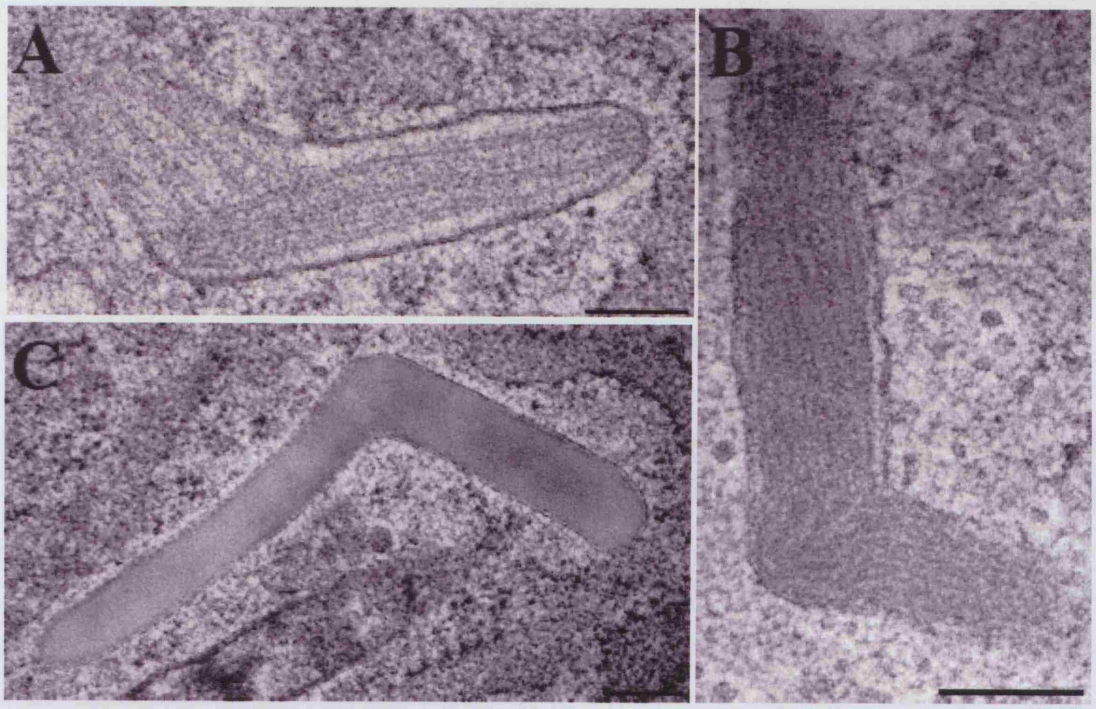

Figure 3.16 ***WPB are able to bend at sharp angles as tubules within the organelle break.***

HUVEC are grown on coverslips and processed for EM using HPF-FS(B). Scale bars represent 200nm.

3.2.8 Disruption of tubules

The tubules can also by disrupted chemically. In the paper by Michaux et al. (2006), considering the role of tubules in the formation of WPB, they used both monensin and DTT treatment. Monensin affects both tubulation and the formation of new disulfide bonds by disrupting the interaction between the propeptide and mature VWF, whilst DTT will affect all disulfide bonds. To look at the ultrastructure of the resulting structures, HUVEC were fixed using HPF followed by freeze substitution.

In Figure 3.17, the cells were treated with 10μM monensin for one hour at 37°C, after which the coverslips were transferred to the high pressure freezer as quickly as possible. It is immediately obvious that the monensin has had an effect, indicated by the vastly swollen Golgi. Although, as a comparison between panels A and B, both of which correspond to the Golgi, shows there is some variability in the strength of the effect. In

panel A, structures that are likely to be WPB are indicated by arrows. Of course they are now rounded and it is not possible to discern tubular content. Panels C and D show close up views of similar, rounded structures. They contain a relatively amorphous content, although it is possible to discern what appears to be the cross section of a VWF tubule in panel C (arrowhead). Finally, panel E show another structure that it found in the monensin treated HUVEC but has not been identified thus far in untreated cells. It also appears to have some internal content. Whether this is a WPB is unclear.

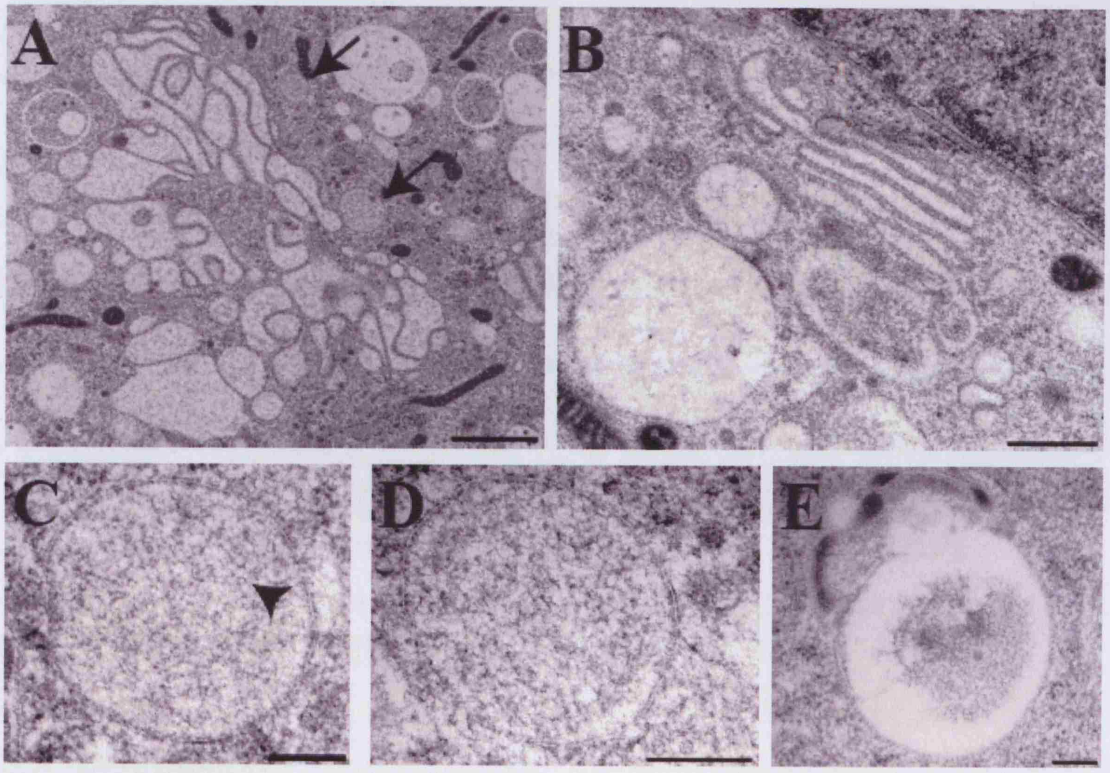

Figure 3.17 ***Monensin treated WPB.***

HUVEC were grown on coverslips and treated for with 10μM monensin. After 1 hour the coverslips were rapidly fixed using HPF and processed using FS(A). Scale bars represent xxnm.

In Figure 3.18, the cells, also grown on the sapphire coverslips have been treated with 20μM DTT for 2 hours at 37°C, after which they were fixed using the high pressure freezer. Michaux et al. (2006) showed that there was no effect at the light level after the HUVEC were exposed to the same treatment conditions. At first glance there seems to

be, likewise, no effect at the ultrastructural level; the WPB are electron dense, and as expected the characteristic VWF striations are clearly visible. However, closer examination suggests that the striations are narrower when comparing the distance between the lighter parts of the striations in the DTT treated WPB and the untreated, mature WPB. In concert there appears to be more striations in the DTT treated WPB, when taking into account the width of the organelle in question. This difference must be due to lower multimerisation state of VWF after the disulfide bonds have been disrupted by the DTT. Presumably the maintenance of the high degree organisation between the tubules is a reflection of the tight packing of VWF within the organelle despite the loss of the intermolecular bridges.

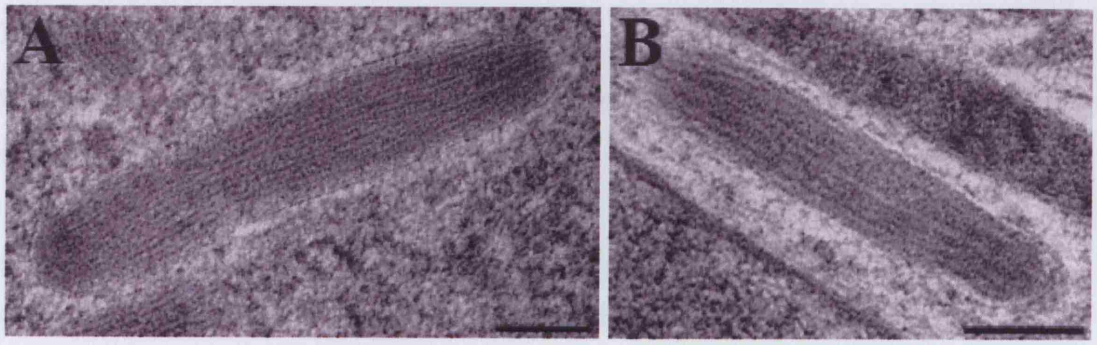

Figure 3.18 ***DTT treated WPB have narrower tubules than untreated WPB.***
HUVEC were grown on coverslips and treated with 20μM DTT. After 2 hours the cells were rapidly frozen and processed using FS(A). Scale bars represent 200nm.

3.3 Discussion

The recent discovery by Michaux et al. 2006 of the functional importance of the storage of VWF as tubules prompted the need for a more detailed analysis of the relationship between the tubules and the formation of the organelle. The development and availability of the new fixation technique for EM, HPF, has made it possible to undertake such a study. As well as uncovering new details about the relationships between the tubules themselves and the tubules and the membrane there have been other key findings from the use of this technique. The most striking finding is probably the increase in density of the organelle as it matures, suggesting that like conventional

secretory granules, VWF undergoes progressive condensation. Additional new findings include a second, later, role for clathrin in the maturation and a strong suggestion that the WPB undergo homotypic fusion.

Aspects of some of these issues are addressed in the early literature (increasing density, appearance of tubules in the Golgi; (Matsuda and Sugiura, 1970) but in no system have all the intimately related aspects been examined together. Crucially, the study shows that the use of HPF is able to capture more information than previously possible on the biogenesis and maturation of WPB in a well-characterised cell culture system, which is accessible to subsequent experimental investigation by modern molecular tools

3.3.1 Tubule formation

Whilst Michaux et al. (2006) demonstrated that tubulation is essential for the shape of WBP and function of VWF, using light microscopy it is not possible to determine when the tubulation of VWF first occurs. The use of HPF-FS indicates that tubulation occurs at the earliest stage of WPB formation, at the TGN. Indeed the presence of the tubule within the protrusion may be indicative of VWF being a driving force in the formation of the organelle. This is consistent with the importance of the interaction between the pro-peptide and mature VWF, in forming WPB. Since the interactions are pH-dependent and the cleavage of the VWF by furin likely occurs within the TGN, a first appearance of the tubules shortly thereafter is in line with these observations (Mayadas and Wagner, 1989; Wagner et al., 1986; Wise et al., 1991; Wise et al., 1988). The shape of the membrane surrounding the tubule shown in Figure 3.4 is of interest - it is not tightly wrapped around the tubule. There must be some factor(s) controlling its dimensions beyond the visible VWF tubule.

3.3.2 Clathrin coating

Lui-Roberts et al. recently discovered a novel role for a clathrin/AP-1 coat in the formation of WPB. They speculated that the coat was needed to act as an external

scaffold in forming the structures (Lui-Roberts et al., 2005). However, use of HPF reveals at least two functions that require clathrin coating during WPB maturation. One is a lattice along the axis or around the end of an elongated structure - the immature WPB, where it resembles the coating seen by chemical fixation and identified as clathrin/AP-1. This sometimes very extensive, partially curved coating is neither the flat lattices seen on the inner face of the plasma membrane nor the tightly curved coated buds seen on the TGN and the plasma membrane. One particularly interesting example of this is the presence of coating on the projection seen in Figure 3.4. Whether its failure to deform the TGN membrane into a classical budding profile is prevented by the presence of the VWF tubule is an attractive hypothesis, but as yet unconfirmed. However, the micrograph in Figure 3.5D is more reminiscent of a classical budding profile, although somewhat larger, perhaps indicating that the presence of the tubule is important to block scission rather than affecting the curvature of the membrane. This coating of the tips extends the known forms that clathrin can take within cells.

The other form of WPB-associated coat is on small traditionally shaped buds, likely involved in removal of material from the maturing granule, as has been found in other secretory granule model systems. The machinery used to recruit the coat is as yet unknown for this system, as are the contents. If these structures are similar to those observed elsewhere then they might be involved in removal of proteins such as the mannose 6-phosphate receptor or furin (Dittie et al., 1999; Klumperman et al., 1998), and indeed the proximity of the WPB with a budding profile to the Golgi in Figure 3.8B suggests that this recycling occurs early in the maturation process. Whether they are particularly labile is not known, but they have been observed in other systems using chemical preservation; perhaps they are much less common in WPB and this particular trafficking pathway plays a minor role in maturation of the endothelial granule. Another possible explanation for these vesicles is they contain material destined for release in a 'constitutive-like' manner, since it is known that a significant proportion of low molecular weight VWF is released constitutively (Kuliawat and Arvan, 1992; Mayadas et al., 1989; Tsai et al., 1991). It will be interesting to identify the adaptor protein that is involved in this budding. The GGA proteins are required for sorting events in other

systems and thus would be compelling candidates (Kakhlon et al., 2006). The depletion of these proteins from endothelial cells would also indicate whether this removal of material is functionally important in the maturation of WPB.

3.3.3 Tubules and the membrane

The relationship between the tubules and the membrane is far more complex than had previously been found using conventional chemical fixation. It is perhaps surprising given the importance of the tubules in the formation and maintenance of the elongated shape of the WPB that the membrane is not simply wrapped directly around the tubules, as has been observed after chemical fixation. However, further analysis of the micrograph produced after HPF-FS comparing the width of the WPB and the number of tubules incorporated indicate that a relationship does exist albeit a slightly more complex one. The graph in Figure 3.7 indicates that the width of the WPB is determined by the number of tubules incorporated and the regularity of the tubules viewed in cross-section in Figure 3.6E. It is interesting to speculate on the cause of this apparent repulsion between the tubules. A favoured hypothesis is that there is repulsion between the tubules and between the tubules and the membrane. The repulsion could arise because VWF is highly decorated by the negatively charged carbohydrate moiety, sialic acid (Samor et al., 1982). In support of this hypothesis is the finding that patients suffering from VWD can have mutations that affect the addition of sialic acid to the protein and the finding in the ST3GalIV mutant mouse has similar symptoms as VWD (Ellies et al., 2002). Of course this could be due to an inability of VWF to bind components in the blood rather than affecting the formation of the WPB. There are two main avenues that could be used to test this hypothesis, although both will require the use of HPF-FS followed by EM. Firstly, the use of 2,3-Dehydro-2-Deoxy-N-AcetylNeuraminic acid, which blocks the sialic acid transferases required for the addition of sialic acid. The second method will involve the expression of constructs replicating the VWF patient mutations discussed earlier in HEK293 cells. Of course a second hypothesis for the regular spacing of the tubules could be the presence of a matrix created by other content proteins that are incorporated into WPB.

Thus far the relationship between the shape of the membrane and the tubules has centred on the width of WPB rather than the length. This relationship may be somewhat less complex. Indeed it is apparent that the VWF is actually able to contact the membrane at the tips of the WPB and whilst there seems to be no requirement for a single tubule to run the whole length of the WPB, there are no regions in the WPB that are completely devoid of tubules.

3.3.4 Maturation

Most secretory granules undergo ultrastructural changes as they mature after budding. This can include an increase in density and changes in shape or the development of highly ordered, even crystalline cargo (Eaton et al., 2000; Greider et al., 1969; Kuliawat and Arvan, 1992). Such change has been reported for WPB in endothelial cells of the rabbit eye, where electron-lucent WPB - reminiscent of the immature WPB shown in this study, are reported to be adjacent to the Golgi, whereas other WPB within which the tubules are "embedded in a moderately dense matrix of fine particles" (Matsuda and Sugiura, 1970). The latter appear similar to the mature WPB found peripherally in endothelial cells after HPF. Interestingly, based on the distribution of the two types of WPB in different cells, Matsuda and Sugiura suggest that the organelles take more than 2 weeks to mature. Following preparation of HUVEC by HPF, a dramatic difference between the pericentriolar electron-lucent structures and the more peripheral WPB with their electron dense interior, within which the tubules can hardly be discerned, is seen. Both the former and the latter are very different to the WPB commonly seen in samples prepared by chemical fixation. Exactly how this change occurs is not understood. This apparent compaction may be a result of the compression required to produce functional VWF strings upon exocytosis (Michaux et al., 2006a). If the 'repulsion' hypothesis is correct it may be that the tubules are able to overcome the repulsion because of the increase in positive charge in the organelle as the WPB becomes more acidic. Of course, the increase in charge would also account for some of the increase in electron density that is observed. The time taken to become "mature", or at least the presence of

electron-dense WPB in rapidly growing HUVEC in culture, suggests that maturation time is a few hours rather than two weeks. This estimate would be in line with the time taken for WPB to acquire membrane protein markers of maturation such as Rab27 (Hannah et al., 2003). The exact correlation in time or any functional relationship between acquisition of CD63, Rab27 and the shift in morphological density is not yet clear. However, the intracellular distribution of the electron-lucent versus the dense WPB strongly implies that the former will be among the Rab27-negative population and the latter will be the mature, Rab27-positive population.

In addition to the more obvious mature WPB, there also appear to be a second population of WPB-like organelles. Whilst these organelles are of similar size and shape to the mature WPB they have no obvious tubular content. Perhaps as a result of this they are often less electron dense. It is impossible to say if these are truly WPB, but their shape and distribution alongside the mature WPB population suggests that they are. It may be most likely that the tubules are blocked from view by the incorporation of one of the alternatively included content proteins, discussed in the introduction, since Michaux et al. (2006) have shown that tubulation is required to support the elongated shape. Determination as to whether these organelles truly are WPB may rely on the use of immunoEM after HPF, which is in the early stages of development.

3.3.5 Fusion and flexion

Measurements taken from both electron micrographs and confocal images suggest that there is an overall increase in surface area between the mature and immature WPB, despite the removal membrane by the clathrin-coated buds discussed earlier. This suggests either that there are vesicles delivering proteins and membrane to the WPB as they mature, or homotypic fusion. The later hypothesis is favoured for a number of reasons: firstly, the amount of membrane delivered is significant but it is extremely rare to see uncoated buds associated with the WPB; secondly, as presented in this chapter, the electron micrographs that suggest fusion (Figure 3.15); and thirdly, the timelapse imaging also represented in this thesis (Figure 3.14). Valentijn et al. have also recently

claimed to have demonstrated that homotypic fusion occurs using EM tomography (Valentijn et al., 2007). Whilst agreeing with their hypothesis, some of the images shown seem more reminiscent of the bending of WPB, demonstrated by the Cutler lab (Zenner et al. 2007) using timelapse microscopy as well as EM, and in Figure 3.16. However, neither this thesis, nor Valentijn et al. have formally proven that fusion does occur. This could be investigated using two channel FRAP, or correlative live microscopy with EM, probably utilising HPF to ensure fast fixation. The tools that will make this possible are currently being developed by Paul Verkade (University of Bristol). The functional importance of homotypic fusion may be more difficult to assess since blocking global fusion will also block VWF release, which is measured to assay WPB function. To address this it may be necessary to identify the SNAREs specific to this process.

3.3.6 Use of HPF in analysis of WPB formation

These data reveal answers to some of the questions raised in the introduction relating to the relationship between the tubules and the membrane, yet the first detailed look at WPB formation by HPF also reveals many more intriguing features that demand further studies. Whether the use of HPF will be as productive for studying all organelles is not yet clear, but the preservation achieved by this method makes it a good choice for anyone interested in cell morphology / organelle formation and function. HPF has allowed for the confirmation that tubulation of VWF occurs in the TGN and that the forming WPB often remain intimately connected with the TGN whilst already in their elongated form. Two additional maturation steps have also been identified: the presence of clathrin-coated buds which are surmised to be involved in retrieval of missorted proteins and the concentration of cargo, observed by an increase in electron density. The finding of the second population of WPB suggests there may be another alternative route of maturation not previously considered. Finally, the observations after DTT treatment confirm that HPF-FS is the ideal technique to consider small differences that cannot be discerned with other techniques and also supports the importance of the disulfide bonds even after the organelle has formed.

4 Formation of WPB at the TGN

4.1 Introduction

HPF-FS has allowed for a more complete ultrastructural study of the biogenesis of WPB, but it has also raised many questions that still need to be addressed. Firstly, events at the Golgi; the electron micrographs indicate that formation of the WPB is a dynamic event rather than a cisternae becoming filled with tubules and pinching off from the rest of the TGN (Figure 3.5). As discussed earlier, the cytoskeleton has an important role to play at the Golgi and its potential role in deformation of the membrane to form WPB was examined. The formation of vesicles from the TGN has been demonstrated to require the actin cytoskeleton, whilst the formation of Golgi-to-plasma membrane carriers (GPCs) is dependent on microtubules and the microtubule-associated motor protein kinesin (Carreno et al., 2004; Musch et al., 1997; Polishchuk et al., 2003). Like WPB, GPCs are often tubular and the long-range movement of both GPCs and WPB is on microtubules (Manneville et al., 2003). These similarities may suggest that it is most likely that microtubules are the most likely candidate for involvement in WPB formation from the TGN. However, unlike GPCs, the shape of the WPB is dependent on the tubulation of VWF, as discussed in the introduction and the previous chapter. Therefore, it could be possible that the tubulation of the VWF is sufficient to generate a force to deform the membrane. This is an interesting hypothesis, especially since the only place the tubule is able to contact the membrane is at the tip where anchoring could occur. Of course it is more difficult to imagine where anchoring could occur within the TGN since it would be necessary for the tubule to have something to push against.

The electron micrographs generated after HPF-FS show a stalk-like structure connecting the forming WPB to the TGN (Figure 3.5). This stalk could be suggestive of a regulatory step before the WPB are able to undergo final scission from the TGN. It has been proposed that PI(4)P adaptor proteins (FAPP) co-ordinate the budding and fission apparatus of GPCs (Godi et al., 2004). The authors find that displacement or absence of FAPP proteins prevents the scission reaction from taking place. Godi et al. hypothesise

that the FAPPs may act as molecular switches to determine the state of GPCs as fission permissive or fission restrictive. Negative curvature is necessary to form this stalk and since it is known that FAPP2 has lipid transfer activity and is thus able to modify lipid compostition, it would be interesting to test if it plays a role in generating this curvature.

Finally, the scission machinery for WPB has not been described. The kinase activity of protein kinase D is required for transport to the basolateral surface from the TGN and thus could be implicated. Whilst the exact molecular mechanism for scission is unknown, it is well established that it is protein kinase D-dependent (Hausser et al., 2005; Liljedahl et al., 2001; Yeaman et al., 2004). The kinase dead mutant utilised in these studies will be used to determine if release of WPB from the TGN is dependent on kinase activity.

Another well-known scission mechanism is dependent on dynamin. The use of dynamin is often implicated in scission of coated structures, particularly those with a clathrin coat. The activity of dynamin, as it hydrolyses GTP, is thought to be sufficient to cause a conformational change, which in turn results in scission of the bud (Hinshaw and Schmid, 1995; Stowell et al., 1999; Takei et al., 1995). It is, therefore possible to use dynamin mutants that are unable to hydrolyse GTP to determine if dynamin is involved in the scission of WPB from the TGN. More recently a new reagent has become available for inhibiting the action of dynamin, the small molecule dynasore, which is a non-competitive inhibitor of the GTPase activity (Macia et al., 2006). However, since long-term inhibition of dynamin was required, it was not possible to use this inhibitor.

4.2 Results

4.2.1 Co-localisation between TGN, cytoskeleton and WPB

Since it is already known that the long-range movement of WPB is dependent on microtubules, fixed HUVEC were immunolabelled for tubulin, as well as for VWF to check for co-localisation in the peri-nuclear area (Figure 4.1).

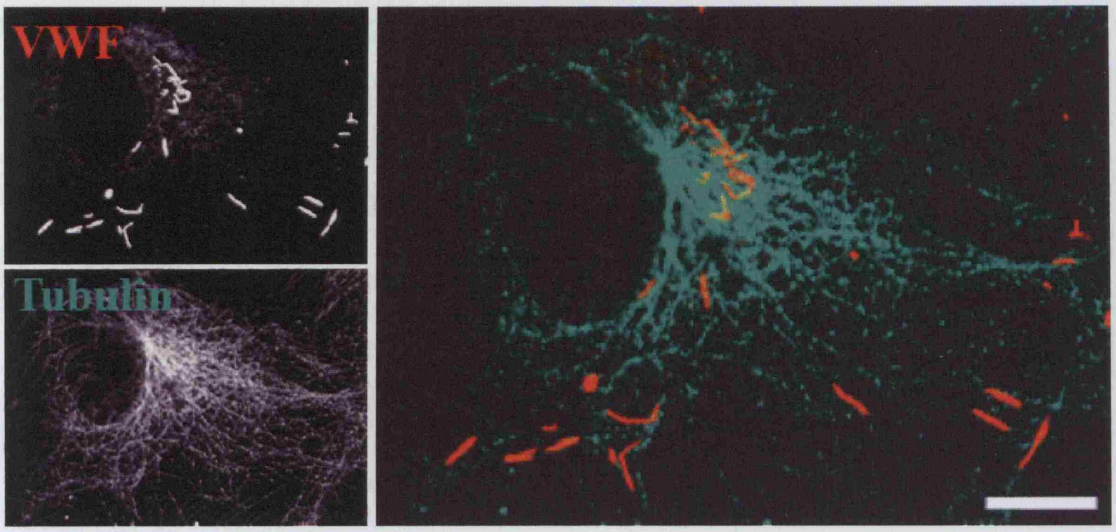

Figure 4.1 **VWF and tubulin co-localise next to the MTOC and in the cell periphery.**

HUVEC were grown on coverslips for 24 hours after which they were fixed, permeabilised and immunolabelled using anti-VWF (red) and anti-tubulin (green) antibodies. Images are confocal sections. Scale bar represents 10μm.

Perhaps unsurprisingly, there is an accumulation of staining of tubulin coincident with the cluster of immature WPB. This staining corresponds to the microtubule organising centre (MTOC), which is usually located adjacent to the Golgi and where the immature WPB cluster as they emerge from the TGN. Within this region there is some obvious overlap between tubulin and VWF indicating that microtubules might be a candidate for involvement in the earliest stage of WPB maturation. Interestingly, there seems to be more limited co-localisation between microtubules and WPB distant from the peri-Golgi, area, where it is known from timelapse experiments, they must interact for movement to occur.

The second candidate for involvement is actin: To investigate a possible role for actin in WPB formation, fixed HUVEC were labelled for actin and VWF. Figure 4.2 indicates that there is not the concentration of staining in the peri-Golgi region as there is for microtubules; there is some limited co-localisation more peripherally in the cell (panel A), but it not really apparent in the perinuclear region. Despite this, both microtubules and actin poisons were used to assess the involvement of cytoskeleton in WPB

formation.

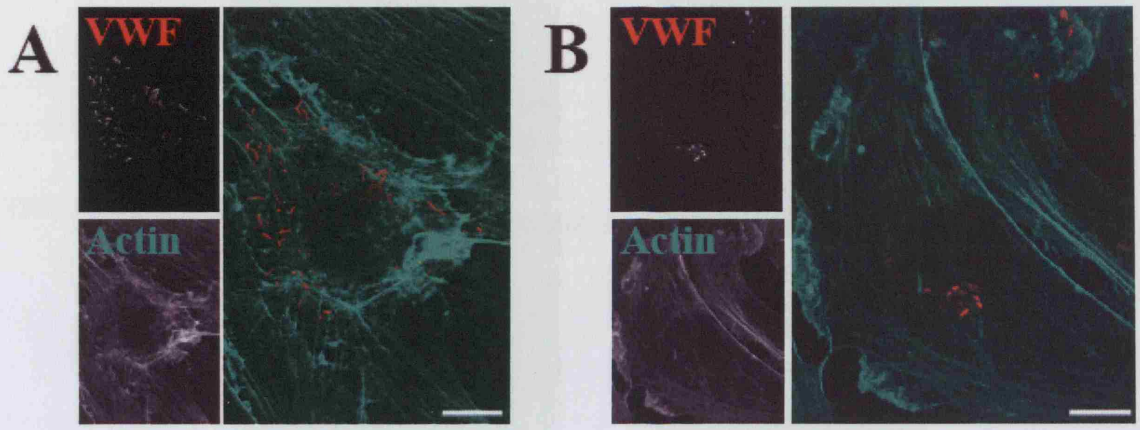

***Figure 4.2* Limited co-localisation between VWF and actin.**

HUVEC were grown on coverslips for 24 hours, after which they were fixed, permeabilised and labelled with anti-VWF antibody (red) and phalloidin (green). Images are confocal sections. Scale bars represent 10μm.

4.2.2 Formation of recombinant WPB

To focus on the earliest events in the biogenesis of WPB using acute drug treatment it is not possible to observe endogenous WPB since it is essential that only the WPB made during the treatments are considered. VWF-GFP (Romani de Wit et al., 2003) can be expressed in HUVEC; making it possible to distinguish newly formed WPB from those already in the cell. Attempts were then make to synchronise the formation of these GFP-positive WPB using temperature blocks so that drug treatments could be used both during the block and immediately after the cells are returned to 37°C. Incubation of cells at 20°C is commonly used to block exit from the TGN (Duden et al., 1991; Matlin and Simons, 1983). However, placing HUVEC at 20°C results in no obvious accumulation of protein in the TGN (Figure 4.3). It does seem that fewer WPB are formed, indicating that exit from the TGN is slowed to some extent, or that there is not sufficient energy to make WPB at 20°C.

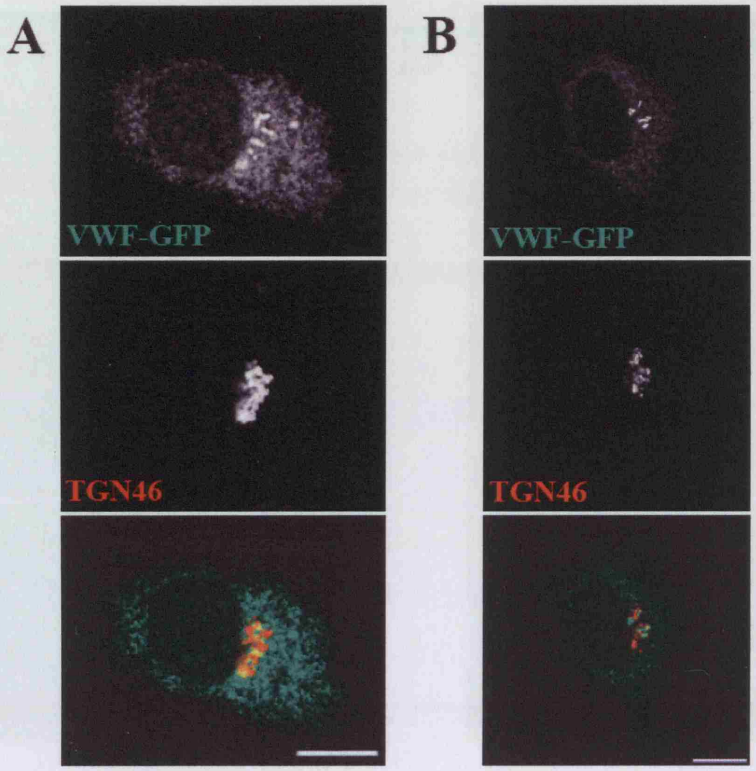

Figure 4.3 **WPB are able to form at 20°C**

HUVEC were nucleofected with a VWF-GFP construct. For panel **A** cells were incubated at 37°C for 4 hours. For panel **B** the cells were incubated at 37°C for 2 hours, then the media was replaced with CO_2-independent media at 20°C and incubated for 2 hour at 20°C. After the respective amount of time had elapsed the cells were fixed, permeabilised and immunolabelled with TGN46. Images are confocal sections. Scale bars represent 10μm.

This work was hampered by the fact it is very difficult to see VWF in the TGN, by immunolabelling or imaging GFP, except when it has also formed a tubular structure, thus there may be some accumulation that cannot be visualised at the light level. It will be interesting to look at these cells by EM after fixation using HPF-FS. Untransfected HUVEC were also incubated at 18°C and 21°C to see if a slight modification in temperature could produce a more dramatic phenotype (Figure 4.4). However, no obvious accumulation could be observed.

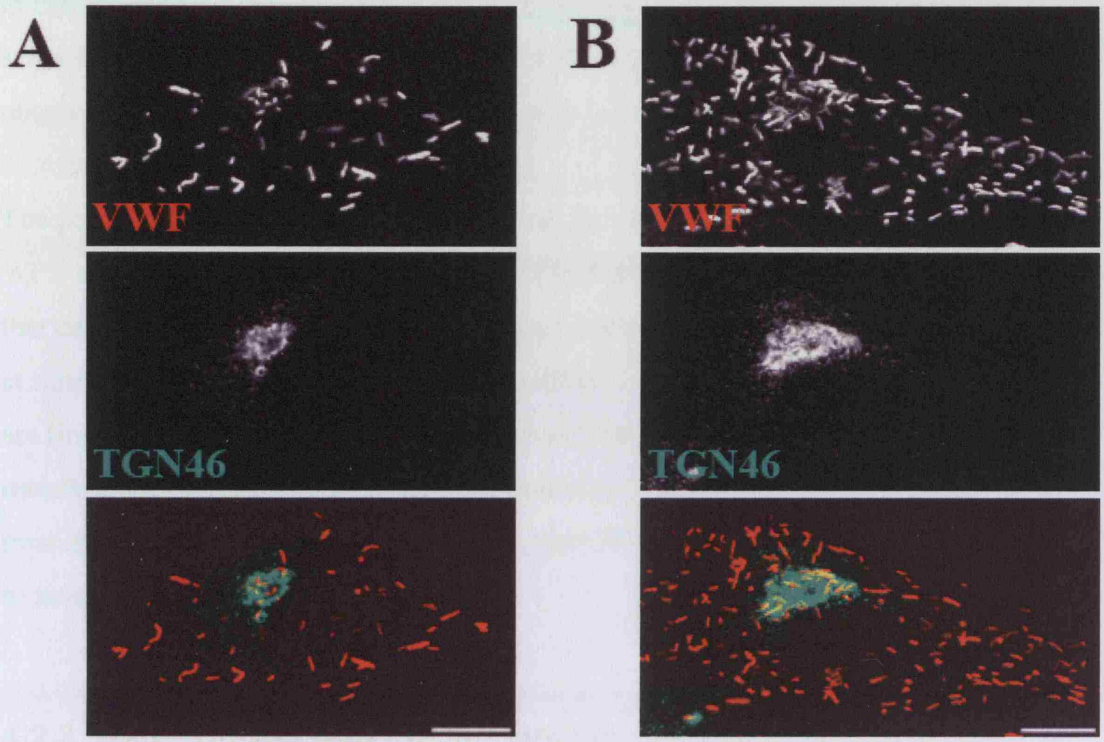

Figure 4.4 **Incubation of cells at 18°C or 21°C does not lead to an accumulation of VWF in the TGN.**

HUVEC were grown on coverslips. When they were approximately 90% confluent, the growth medium was replaced with CO_2-independent medium at 18°C (**A**) and 21°C (**B**). After 2 hours the cells were fixed, permeabilised and immunolabelled with anti-VWF (red) and TGN46 (green) antibodies. Images are confocal sections. Scale bars represent 10μm.

Since this method did not seem to be effective at blocking TGN exit, a different method was required. The use of VWF-GFP to follow the newly forming WPB meant that timelapse microscopy could be employed. Cells were either microinjected or nucleofected with VWF-GFP and then imaged by timelapse microscopy. Although VWF-GFP cannot be seen in the Golgi it is possible to see it within the ER, so this fluorescence was used to detect transfected cells. Cells with ER fluorescence but lacking characteristic WPB were imaged for up to four hours to detect the formation of new WPB. The images were taken relatively infrequently, at 30 minutes time intervals, since the HUVEC seemed to be very light sensitive. However, a WPB budding from an imaged cell was extremely rare for either transfection protocol and thus this method could not be used to study early biogenesis events. The absence of newly forming WPB

in the imaged HUVEC could be a result of the light exposure, since other cells on the same dish, not exposed to light, were for GFP-positive WPB. This may linked to the observation that when the HUVEC are stressed in culture they tend to make fewer WPB.

The presence of GFP-WPB in cells that were not illuminated indicates that the first WPB are formed soon after transfection; indeed previous experiments in the lab indicate that cells contain WPB four hours post transfection. Thus, nucleofected cells were fixed at time-points less than four hours post transfection to give an indication of when WPB are first formed. It was found that it is rare to find WPB in cells 2-2.5 hours post transfection, but that they are more common after 3 hours. It was therefore decided to treat the cells 2 hours after transfection so that GFP-WPB will not have been made prior to treatments, which are discussed below.

4.2.3 Microtubules and the biogenesis of WPB

Nocodazole is commonly used to depolymerise microtubules and thus it was added to the cells two hours after nucleofection, at which point they had already attached to the dish. After either one or two hours treatment, the cells were fixed, permeabilised and incubated with anti-GFP (green) and anti-GM130 (red) antibodies before processing for microscopic analysis. GM130 is used in this analysis because the GFP antibody and TGN46 antibody are both raised in sheep, precluding their use together. Figure 4.5 indicates that WPB are still able to form in the absence of microtubules. The GFP-positive WPB remain in close proximity to the Golgi, since their movement is dependent on microtubules. However, they are distributed throughout the cell since they are available to bud from the dispersed mini stacks created by the Golgi fragmentation. The fragmentation is due to a disruption in the relationship between the Golgi and ER exit sites by removal of microtubules, indicating that the inhibitor has worked.

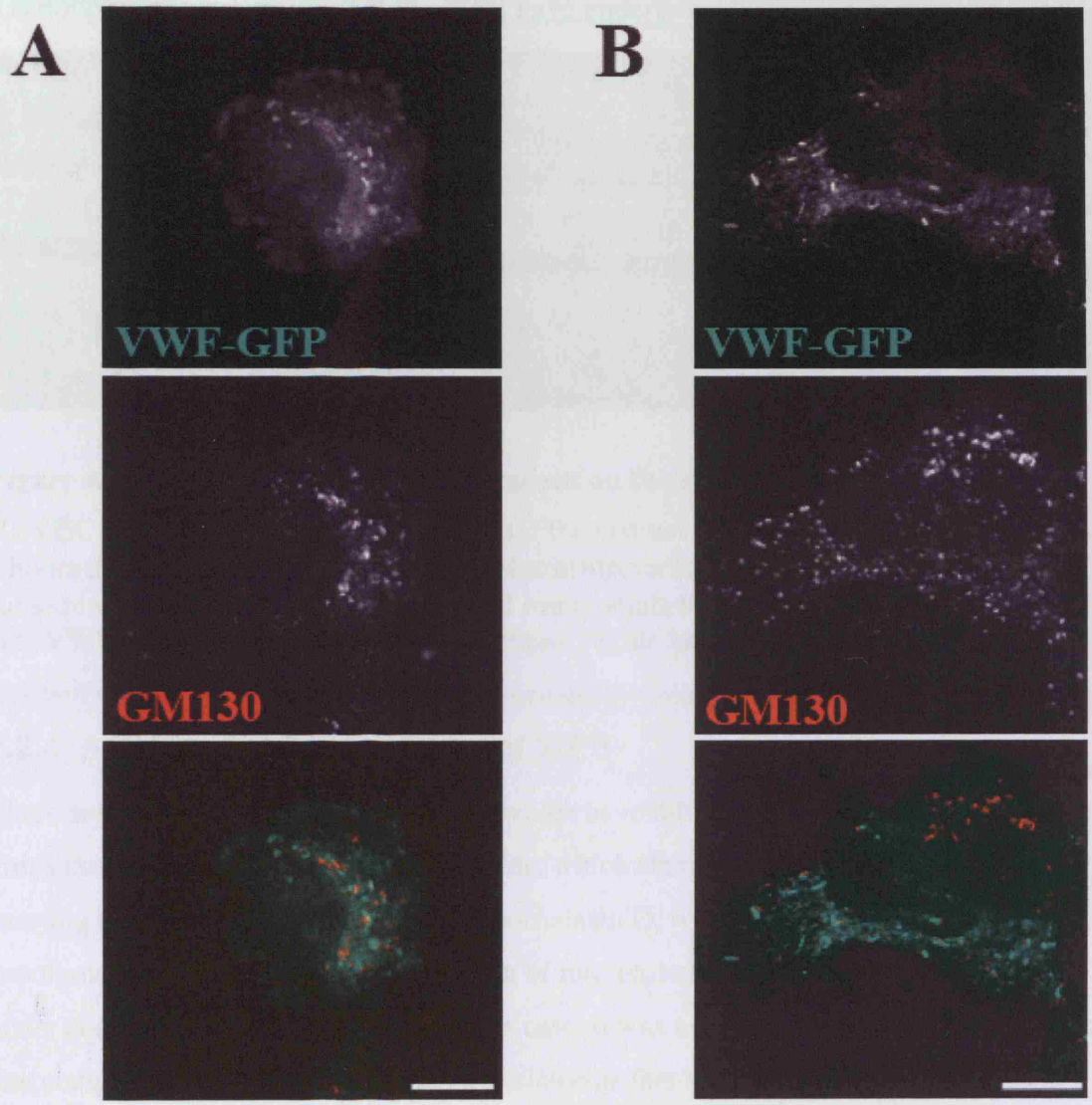

***Figure 4.5* WPB formation is not dependent on microtubules.**

HUVEC were nucleofected with a VWF-GFP construct. After 2 hours the cells were treated with 10μg/ml nocodazole for 2 hours (**A**) or 3 hours (**B**). The cells were subsequently fixed and permeabilised and immunolabelled with anti-GFP (green) and anti-GM130 (red). Images are confocal sections. Scale bars represent 10μm.

In addition, no effect was found when the cells were incubated in aurintricarboxylic acid, which inhibits the microtubule-dependent motor kinesin (Hopkins et al., 2000; Lalli et al., 2003), although again the WPB are unable to move away from the Golgi (Figure 4.6). Thus it would seem that microtubules and their associated motor, kinesin, are not required for the initial formation of WPB, although without electron microscopy

it is not possible to confirm that the WPB have undergone scission from the Golgi.

***Figure 4.6* WPB formation is not dependent on the activity of kinesin.**
HUVEC were nucleofected with a VWF-GFP construct and plated onto coverslips. After 2 hours the cells were treated with 100μM aurintricarboxylic acid. The cells were subsequently fixed and permeabilised and immunolabelled with anti-GFP (green) and anti-VWF (red). Images are confocal sections. Scale bars represent 10μm.

4.2.4 Actin and the biogenesis of WPB

There are numerous actin poisons, all of which have different effects on actin. The two drugs used in this study were jasplakinolide, which stabilises actin filaments, thus exerting its effect on active actin, and cytochalasin D, which causes actin depolymerisation. As with the disruption of microtubules, the cells were treated two hours post nucleofection; however, in this case, it was not possible to use concentrations that completely disrupted the actin cytoskeleton as this leads to a complete collapse of the cells making immunofluorescence microscopy impossible. Thus, a reduction in the number of WPB rather than a complete loss was expected. Figure 4.7 indicates that WPB are formed after treatment with either cytochalasin D or jasplakinolide. The concentration of jasplakinolide used at a concentration where the loss of actin caused the cells to partially collapse, but nevertheless WPB are still apparent within these cells, although perhaps these are formed before the collapse was so extensive. However, it is clear that there is a reduction in the number of WPB (panels B and C compared to A) and they are less elongated, after treatment with both drugs.

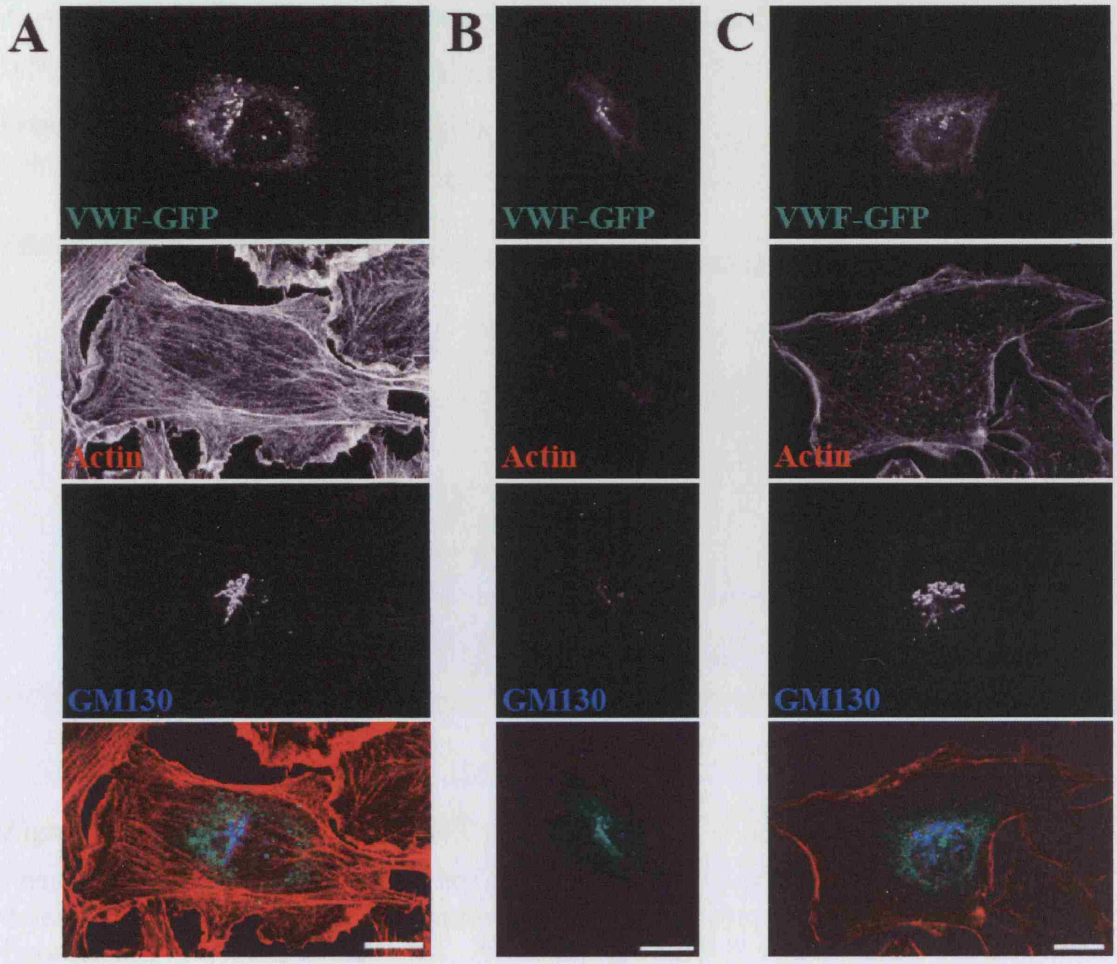

***Figure 4.7* Actin is involved in the formation of WPB.**

HUVEC were nucleofected with a VWF-GFP construct and plated onto coverslips. After 2 hours the cells are treated with either DMSO (**A**), 0.5μM jasplakinolide (**B**) or 200nM cytochalasin D (**C**). After a further 2 hours the cell are fixed, permeabilised and labelled with anti-GFP (green), phalloidin (red) and GM130 (blue). Images are confocal sections. Scale bars represent 10μm.

Cytochalasin D treated cells were used to quantify any deficiency in the number and size of WPB. This was analysised by comparing the total amount of GFP fluorescence in WPB or WPB-like structures per cell between the treated and untreated cells. The graph in Figure 4.8 indicates the average amount of non-ER fluorescence per cell (so, the fluorescence that is incorporated in WPB-like structures), normalised to the average non-ER in DMSO treated cells. It is apparent that there is almost 40% less non-ER fluorescence per cell in the cytochalasin D treated cells. The ER fluorescence is

discounted by thresholding, as it tends to be less bright than the fluorescence of the WPB. The macro used for this analysis was written by Miguel Branco (MRC CSC, London) and is available in Appendix I.

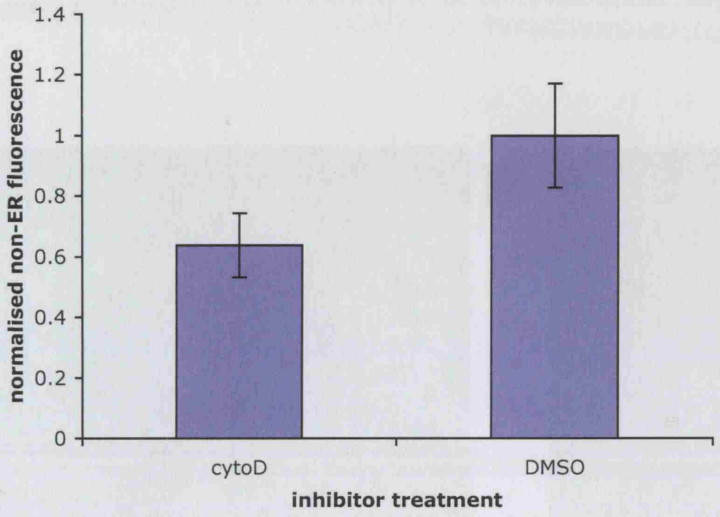

Figure 4.8 **Reduction in VWF-GFP positive WPB after cytochalasin D treatment.** Images from the experiment described in Figure 4.7 were analysed using ImageJ to determine GFP fluorescence per expressing cell. All values were normalised to average fluorescence in DMSO treated cells. Error bars represent standard error.

The fact that treated cells retain the ability to form WPB may be because some actin remains in the cells. However, since actin is important in many processes in the cell the effect seen on the biogenesis of WPB may be an indirect one. For example, this could be a failure to deliver other proteins required for Golgi function. To determine if the role of actin in the biogenesis of WPB is specific, the roles of the actin-dependent motors commonly found at the TGN were considered.

4.2.5 Motor proteins and WPB biogenesis

The best-studied motor protein at the TGN is the non-muscle Myosin II. The activity of this motor protein can be inhibited with the use of the drug blebbistatin, which blocks the myosin heads in a products complex with low actin affinity (Kovacs et al., 2004;

Straight et al., 2003). The same protocol discussed above was used, whereby blebbistatin was added to the cells two hours post nucleofection. The fluorescence images in Figure 4.9 show that GFP-positive WPB are present after treatment with blebbistatin (panel B). The change in actin morphology of the treated cells indicates that the drug is working. Thus Myosin II is unlikely to be involved in the biogenesis of WPB.

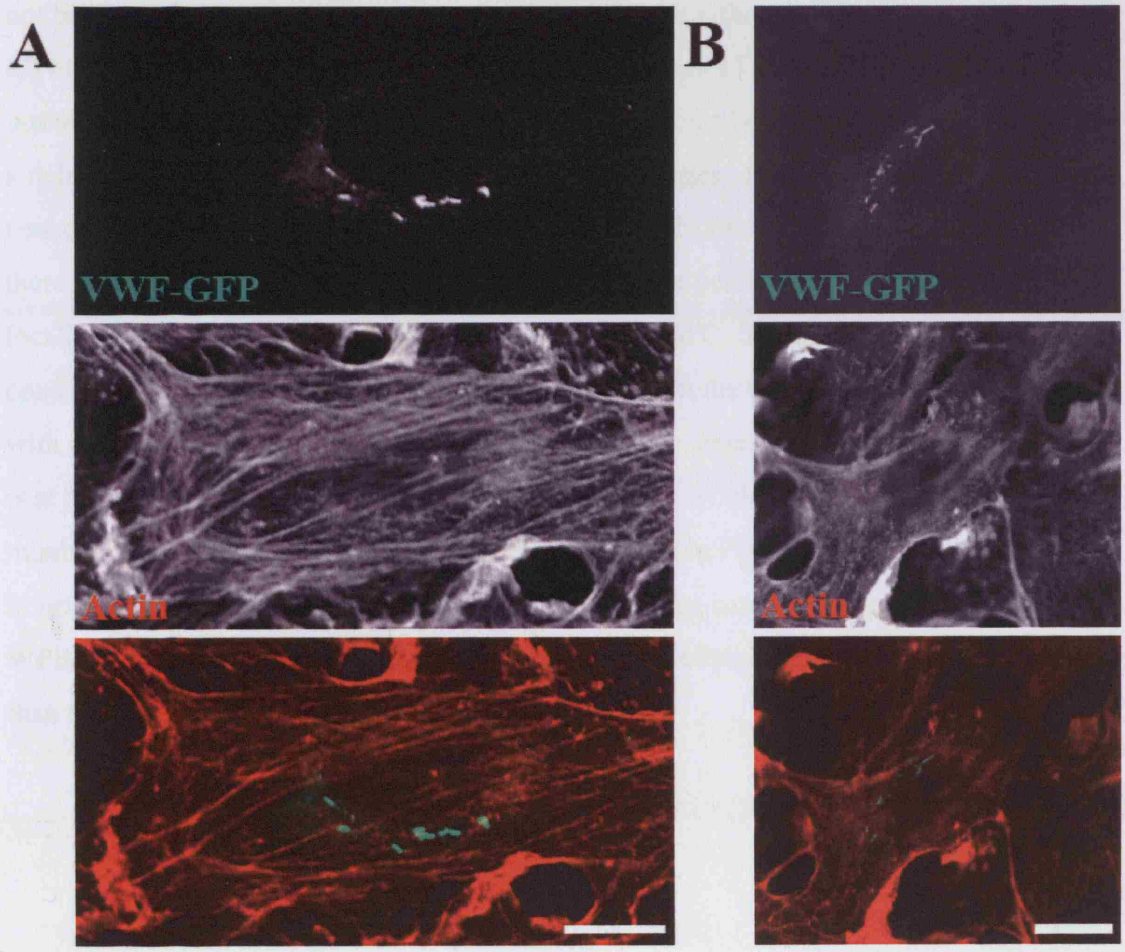

Figure 4.7 **Myosin II activity is not required for the formation of WPB.**

HUVEC were nucleofected with a VWF-GFP construct and plated onto coverslips. After 2 hours the cells were treated with 10μM blebbistatin (**B**) or DMSO (**A**) for a further 2 hours, whereupon the cells were fixed, permeabilised and labelled with anti-GFP (green) and phalloidin (red). Images are confocal sections. Scale bars represent 10μm.

Another motor protein found at the TGN, and which operates in concert with clathrin

and AP-1, is the atypical myosin, Myosin VI (Au et al., 2007; Spudich et al., 2007). This motor moves towards the minus end rather than the plus end of actin filaments. Whilst there is, as yet, no drug that specifically inhibits Myosin VI, the expression of a construct with only the tail domain should act as a dominant negative (Buss et al., 2001). There are two transcripts of Myosin VI, and it is the "no insert" transcript that is expressed in endothelial cells (Folma Buss, personal communication). The use of the constructs rather than the drug treatment meant that the protocol discussed above could not be used. Instead HUVEC were microinjected with either the wild type or tail-only Myosin VI (kind gifts of Folma Buss) and left for either 24 or 48 hours. It should be possible to determine if there is co-localisation between Myosin VI and VWF, as well as a reduction in the number of WPB present at these stages. In Figure 4.9A the wild type construct is expressed and there is no striking co-localisation with VWF. Furthermore there seems to be no enrichment of fluorescence in the perinuclear staining or co-localisation with the Golgi. However, Figure 4.9B and C, in which the tail-only construct is expressed, show that there is a reduction in the number of WPB compared with expression of the wild type construct. The fluorescence from the tail-only construct is at first suggestive of cell blebbing and death, which would, of course, affect the number of WPB present, yet the DAPI staining (blue) in Figure 4.9C appears to be normal. However, the expression level of GFP proteins can also affect the number of WPB produced and it is clear that the tail construct is expressed at a much higher level than the wild type construct.

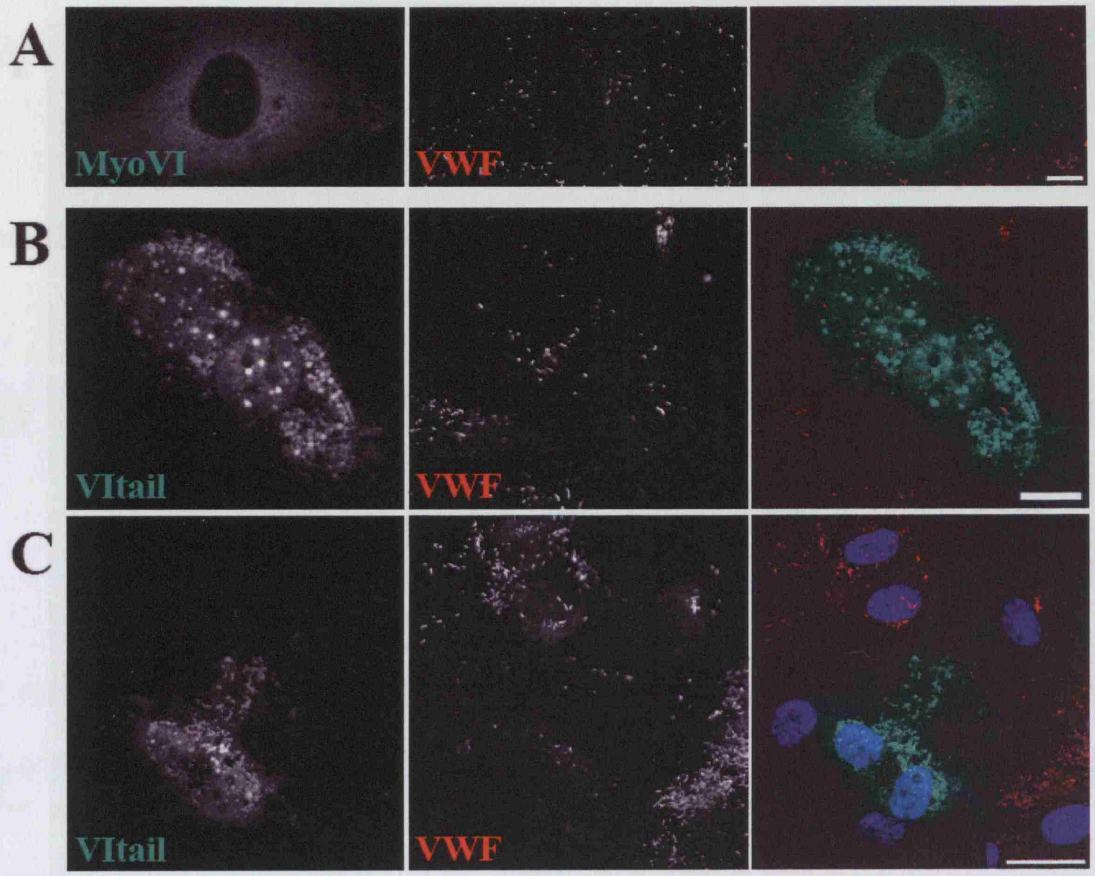

Figure 4.8 **Myosin VI may play a role in the biogenesis of WPB.**

HUVEC were microinjected with Myosin VI-GFP construct (no insert) (green - **A**) or Myosin VI tail-only-GFP construct (green - **B** & **C**). After 24 hours the cells were fixed, permeabilised and labelled with anti-VWF (red) and DAPI (blue – **C**). Images are confocal sections. Scale bars represent 10μm (**A** & **B**) and 25μm (**C**).

To address this the constructs were transfected into HEK293 cells to check expression levels after nucleofection rather than microinjection. The results are represented in Figure 4.9 and show that there is indeed a reduction in the number of WPB at high expression levels of both constructs (panel C compared with panel B). However, in panel D, a cell expressing the tail-only construct at a low level, there are multiple WPB.

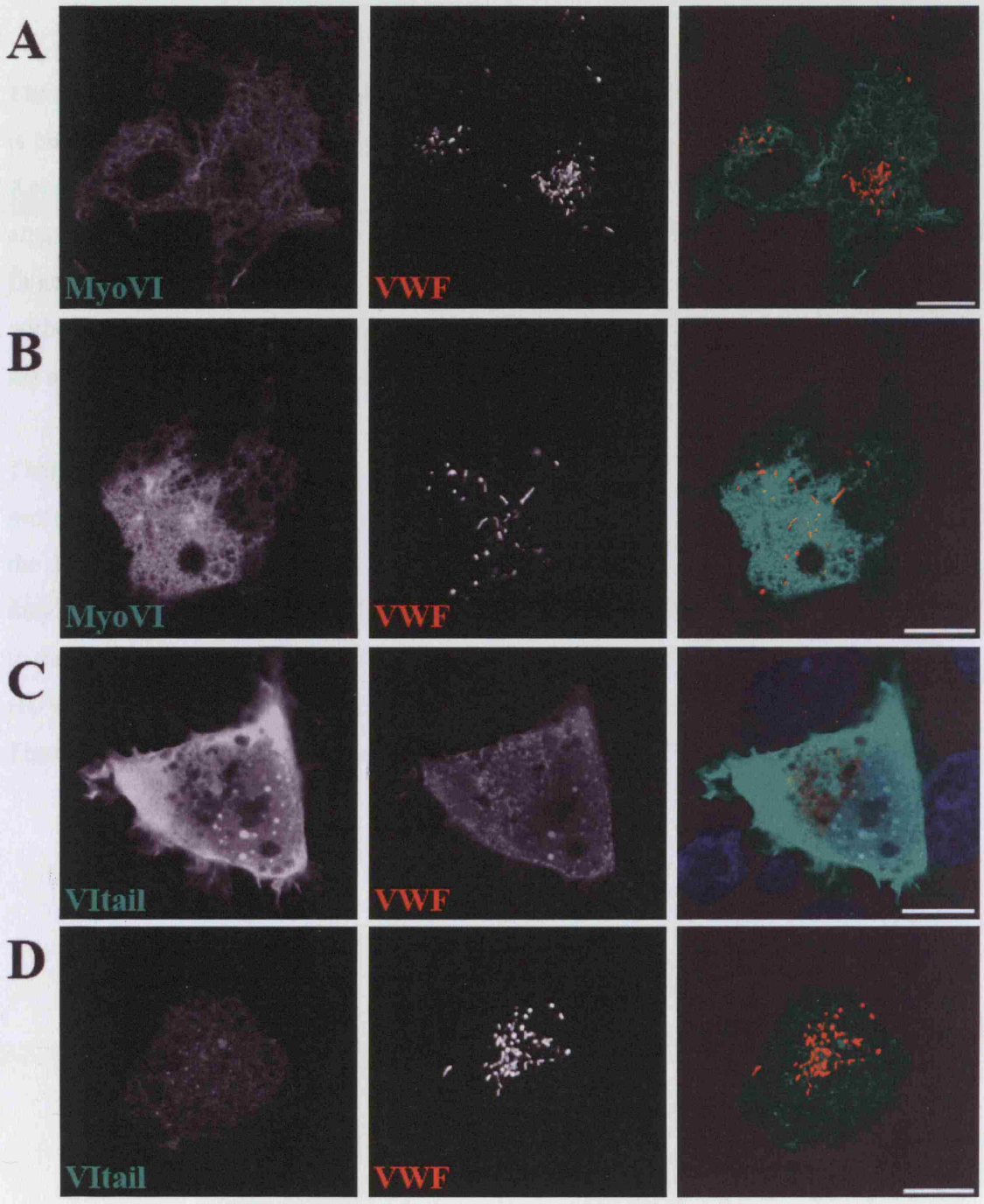

Figure 4.9 **Myosin VI may play a role in the formation of pseudo-WPB in HEK293 cells.**

HEK 293 cells were nucleofected with a VWF construct and Myosin VI(no insert)-GFP construct (green – **A** & **B**) or Myosin VI tail-only-GFP construct (green – **C** & **D**). After 2 days the cells were fixed, permeabilised and labelled with anti-VWF antibody (red). Images are confocal sections. Scale bars represent 10μm.

The transfection efficiency in the HEK293 cells, compared with the HUVEC, means that is possible to quantify the number of the cells with and without WPB in these cells. Approximately 50% of the cells expressing the tail-only construct contain WPB, whilst almost 100% of the cells expressing the wild type construct contain WPB (Figure 4.10). In general, the cells expressing a higher level of the tail-only mutant protein that where without WPB, but this was not always the case. Only cells that contained bothVWF and the appropriate GFP construct were included in this calculation.

There are a number of possible explanations for these results. Firstly, the tail-only protein may take longer to fold than VWF, thus allowing some WPB to be made before the dominant negative construct can have its effect. Secondly, the tail-only construct may have to be expressed above some threshold to allow it to act as a dominant negative to the endogenous protein within the cell. Finally, as discussed in relation to the HUVEC, a high expression level may non-specifically preclude the formation of WPB. These issues could be resolved using siRNA to knock down the endogenous Myosin VI.

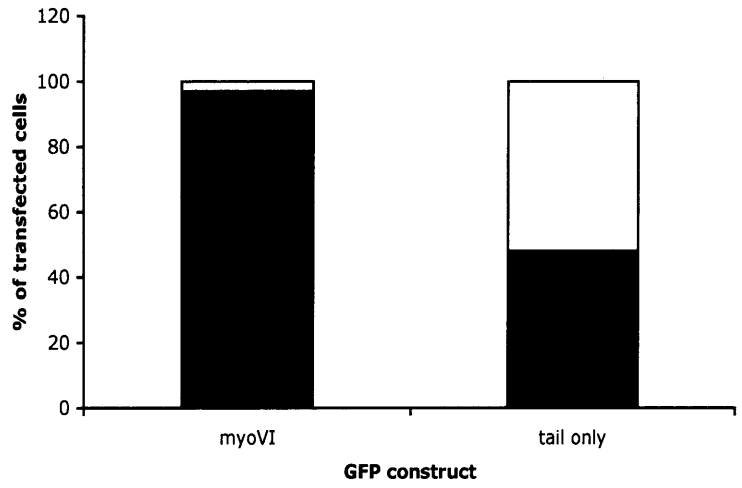

***Figure 4.10* Only 50% of cells expressing Myosin VI tail-only and VWF are able to make WPB.**

HEK293 cells from the experiment in Figure 4.9 were scored as to whether or not they

contained WPB. The cells had to be expressing VWF and the respective GFP protein. 100 cells were counted for each condition from 2 independent experiments.

It has been demonstrated that Rab8 is an interacting partner of Myosin VI (Sahlender et al., 2005) and since this Rab is found on TGN membranes it could provide a link between the VWF and Myosin VI. Thus Rab8-GFP (from Folma Buss) was also expressed in endothelial cells to check for co-localisation with WPB. Rab8-GFP (Figure 4.11 panel A) is largely cytosolic, but with an enrichment in staining in the perinuclear region. It is possible to see some potential co-localisation between Rab8 and VWF in the perinuclear area, especially around the perimeter of the WPB, but whether this is a result of the high expression levels is unclear. To further confirm if Rab8 does play a role in the biogenesis of WPB, the constitutively active Rab8 mutant, Q67L, which phenocopies the tail-only mutant of Myosin VI in MDCK cells with respect to VSV-G delivery to the basolateral surface (Au et al., 2007), was expressed in HUVEC (Figure 4.11B). It is clear that there are still WPB in these cells, perhaps not as many as in the panels A, but within the normal degree of variation from cell to cell. In panel B it is apparent that this construct causes a redistribution of the Golgi (blue), thus any affect on WPB biogenesis could due to a general Golgi defect rather than a specific effect.

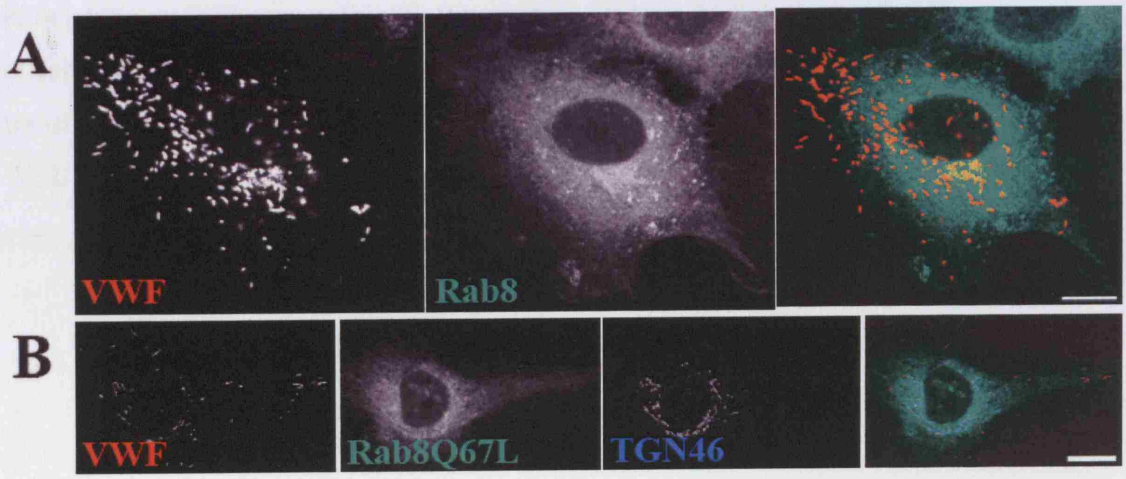

Figure 4.11 **Some limited co-localisation between Rab8-GFP and VWF, but expression of Rab8Q67L has no effect on biogenesis of WPB.**

HUVEC were microinjected with a Rab8-GFP construct (green – **A** and a Rab8Q67L-GFP construct (green – **B**). After 24 hours the cells were fixed, permeabilised and

labelled with anti-VWF (red) and anti-TGN46 (blue – **B**) antibodies. Images are confocal sections. Scale bars represent 10μm.

4.2.6 Hip1R and WPB biogenesis

Of course, the dynamic activity of actin means that a motor protein is not required to exert a force. One protein that provides a link between the vesicle coats and the actin cytoskeleton is Hip1R. It has previously been demonstrated that knocking down Hip1R reduces the delivery of lysosomal enzymes from the TGN to the lysosome by 40% (Carreno et al., 2004), where they publish an siRNA sequence that was used in this study. They also demonstrate that the use of actin poisons reduces delivery of the hydrolases by the same amount. This is a similar level as for cytochalasin D described above (Figure 4.8). The simplest way to test for a reduction in the number of WPB is a secretion assay; since cells can be depleted of Hip1R over a long period it is not necessary, or indeed possible, to consider early events only. In the assay, the cells are stimulated to release the VWF that is contained in WPB using the secretagogue PMA, whilst constitutive release in the absence of PMA is also measured. Before the stimulation of secretion the HUVEC were nucleofected with Hip1R siRNA and then, after 48 hours, the cells were transfected again with siRNA; this ensures that all the WPB present in the cells would have been produced after Hip1R depletion. The level of knockdown at 70% was assessed using qPCR. Figure 4.12 indicates that there is no difference in the amount of VWF secreted from the cells in comparison to mock-transfected cells. Thus it seems unlikely that Hip1R is involved in the biogenesis of WPB.

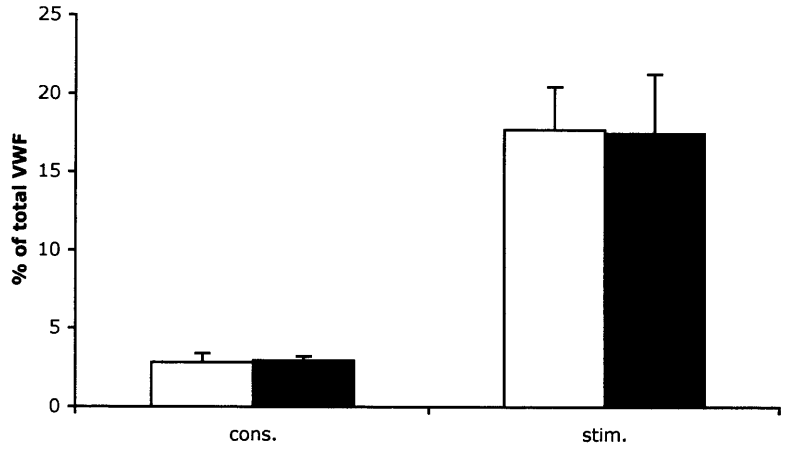

Figure 4.12 **Depletion of Hip1R has no effect on release of VWF from HUVEC.**
HUVEC were nucleofected with Hip1R siRNA (white bars) or scrambled siRNA (black bars) on day 0 and again on day 2. After a further 48 hours the cells were incubated with serum free medium, firstly without and subsequently with PMA for 30 minutes each to measure constitutive and stimulated release respectively. Finally, the cells were lysed so total cellular VWF could be measured. The amount of VWF in each sample was measured using a colorimetric ELISA and is expressed as a percentage of total VWF, and the constitutive portion (cons.) is subtracted from total stimulated release to calculate the PMA responsive pool (stim.). Error bars represent standard error.

4.2.7 Regulation of budding and scission

As discussed, the presence of the stalk in the HPF-FS images may be indicative of regulation in the scission of the WPB, presumably to ensure that all the necessary proteins have been incorporated. The FAPP proteins are good candidates for regulating this process (Godi et al., 2004). It is possible to interfere with these proteins by overexpressing only the PH domain of the protein; this will act as a dominant negative by binding the TGN and displacing the wild type protein. One drawback of using this method is that the PH domain binds to PI(4)P and may displace other proteins that bind the phosphoslipid such as AP-1. However, it should be possible to distinguish a phenotype caused by the loss of AP-1 described by Lui-Roberts et al. (2005) from the predicted phenotype of a failure to undergo scission. Therefore, FAPP-PH-YFP (a kind gift of John Lucocq and Dario Alessi, Dundee) was expressed in endothelial cells. The cells were fixed after two days and immunostained with anti-VWF and anti-TGN46 (panel A) antibodies. In Figure 4.13 it is clear the FAPP-PH domain does indeed

localise to the TGN. Also it seems that its expression leads to the block in the release of VWF from the TGN, with extensive co-localisation between the VWF and TGN46 staining (panel A). However, another, perhaps more interesting phenotype, was also observed (panel B). In panel B it is apparent that the WPB are beginning to form, but they appear unable to be released from the TGN (indicated by the FAPP-PH fluorescence) and compared with the adjacent untransfected cell visible in panel C, a lower magnification images of panel B, which has WPB throughout the cell. Indeed the WPB in the cell expressing the FAPP-PH appear to be slightly longer than the newly forming WPB in untransfected cells and they appear to be almost curling around the Golgi.

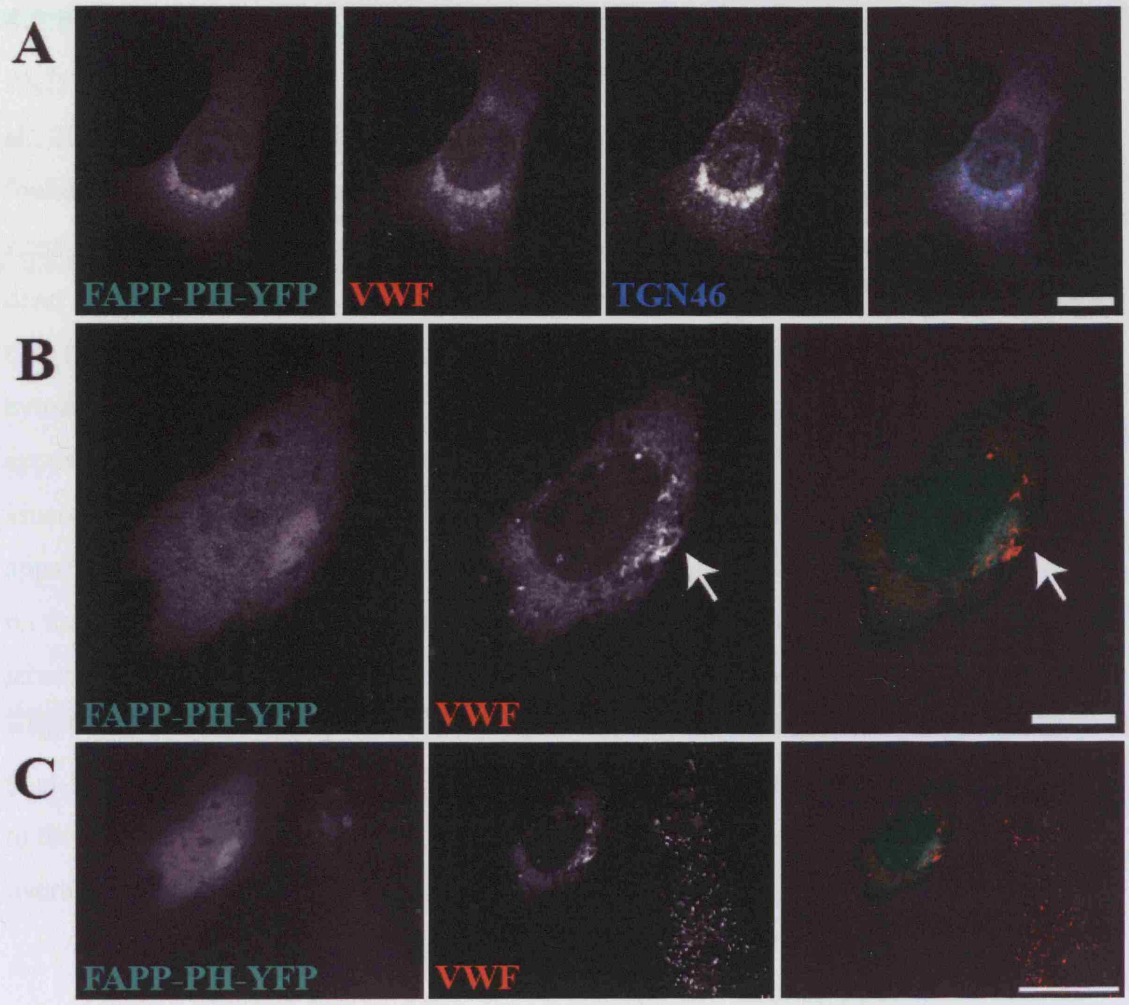

Figure 4.13 **FAPP may play a role in the regulation of scission of WPB.**

HUVEC were nucleofected with a FAPP-PH-YFP construct (green). After 48 hours the cells were fixed, permeabilised and labelled with anti-VWF antibody (red). Arrows point to WPB that appear to be forming from the Golgi but may be unable to undergo scission. Images are confocal sections. Scale bars represent 10μm for panels **A** & **B** and 25μm for panel **C**.

4.2.8 Scission from the Golgi

After elongation of the WPB, in order to become an independent organelle, the WPB has to undergo scission from the TGN. There are a number of proteins already implicated in scission from the Golgi. Two of those, PKD and Dynamin 2, were tested.

4.2.8.1 PKD and WPB

PKD has previously been implicated in the scission of GPCs from the Golgi (Liljedahl et al., 2001). Whilst the evidence for the role of PKD is clear, no mechanism has yet been found, since it is unlikely that PKD itself can exert the mechanical force required for scission to occur. The kinase activity of PKD is required for scission and thus kinase dead PKD (a kind gift of Vivek Malhotra) was expressed in HUVEC, alongside the wild type form. Expression of the wild type protein (Figure 4.14A and B) is mainly cytosolic, but some enrichment at the Golgi is apparent. The WPB is these images appear to be normal. Figure 4.13 panels C and D show the expression pattern of the kinase dead form of the protein. The Golgi localisation of this protein is even more apparent than for the wild type protein in panel C. In panel C, there is also a clear effect on the WPB. Instead of the characteristic elongated WPB, small punctate VWF-positive structures are seen throughout the cytoplasm. This phenotype is similar to that observed with knockdown of AP-1, which is known to support the formation of elongated WPB (Lui-Roberts et al., 2005). Interestingly when PKD-kinase dead protein is not localised to the TGN, as in panel D , the effect on WPB is lost. It is not clear why the overexpressed kinase dead PKD does not always localise to the Golgi.

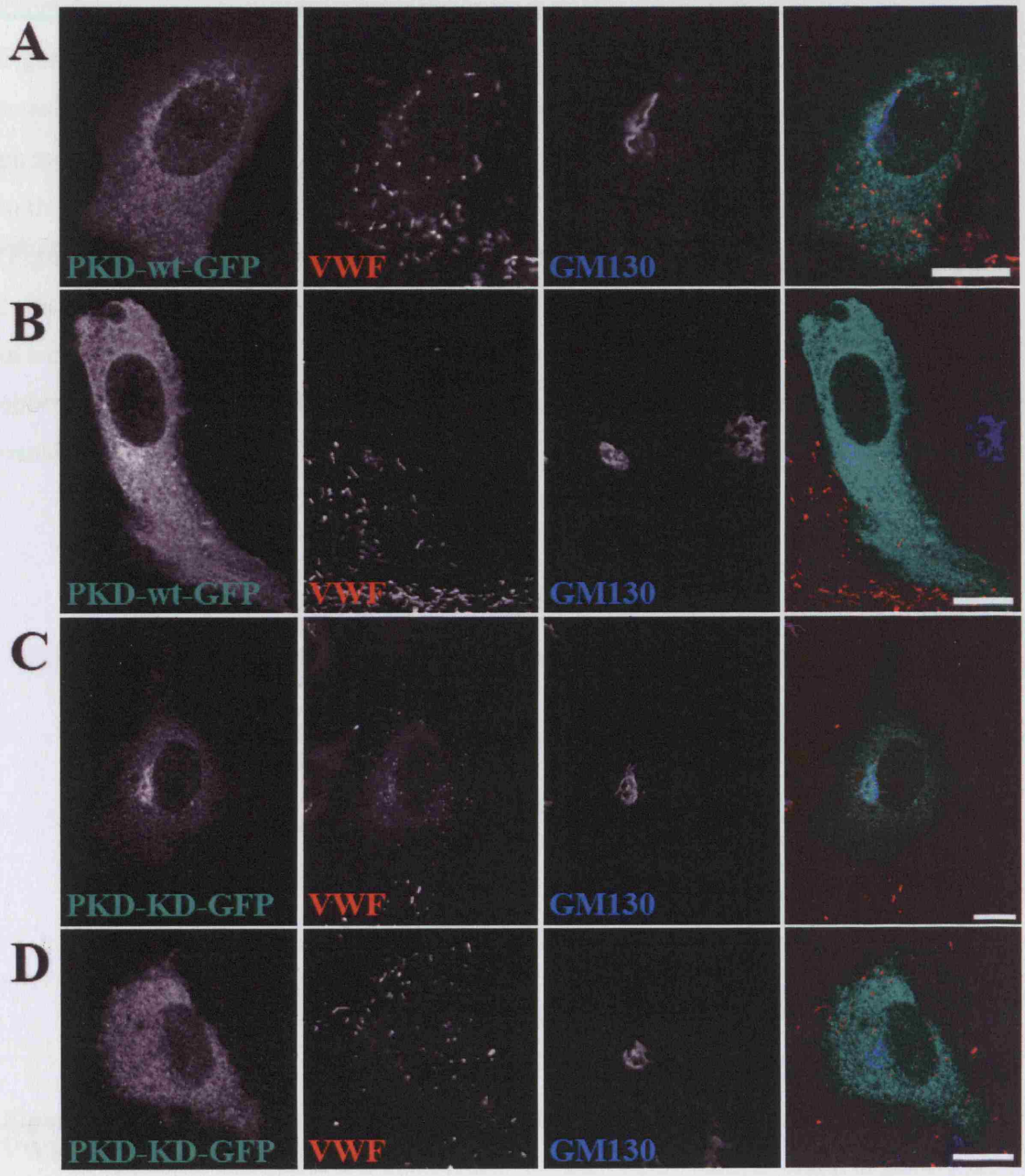

Figure 4.14 **Localisation of PKD-kinase dead to the Golgi results in a failure to make elongated WPB.**

HUVEC were nucleofected with a wild type PKD-GFP construct (green – **A** & **B**) or with a PKD-kinase dead-GFP construct. After 48 hours the cells were fixed, permeabilised and labelled with anti-VWF (red) and anti-GM130 (blue) antibodies. Images are confocal sections. Scale bars represent 10μm.

To confirm that this phenotype really is like the phenotype observed after AP-1

knockdown a secretion assay was performed using the same method as that discussed in Figure 4.12, except that HEK293 cells were used instead of HUVEC to achieve a high transfection efficiency, thus making a biochemical analysis possible. Similarly to the phenotype observed after AP-1 depletion it is apparent that the VWF puncta visualised in the cells after expression of kinase dead PKD are not responsive to secretagogue (Figure 4.15). There is a reduction of 50% in the amount of stimulated release coincident with an increase in constitutive release, indicating that the puncta are released in a constitutive manner. The reduction in stimulated release is not as large as that observed following AP-1 knockdown but this may well be due to the difference in transfection efficiency of the siRNA compared to that of the kinase dead construct.

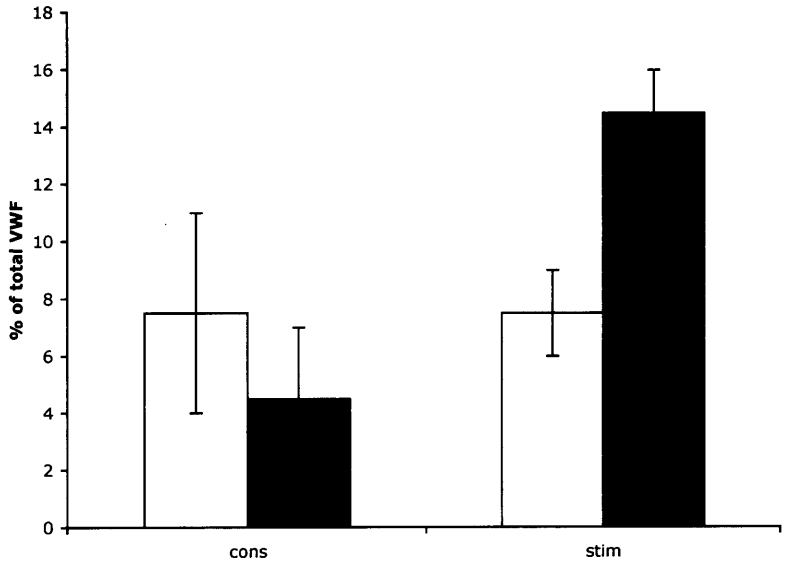

***Figure 4.15* Stimulated release of VWF is reduced in HEK293 cells expressing VWF and PKD kinase dead, compared with wild type.**

HEK293 cells were nucleofected with a VWF construct and a PKD-KD construct (white bars or a wild type PKD construct (black bars). 48 hours after transfection the secretion assay described in Figure 4.13 was performed. Error bars represent standard error.

An obvious explanation for this phenotype is that PKD acts upstream of AP-1. Indeed one of the suspected downstream targets of PKD is PI(4)kinase, which is responsible for maintaining the high PI(4)P concentration characteristic of the TGN and required for the recruitment of AP-1 to the TGN. Unfortunately this makes it impossible to distinguish if

PKD plays a role in scission, which is downstream of the requirement of AP-1.

4.2.8.2 Dynamin-2 and Scission from the TGN

Dynamin-2 has also been implicated in budding from the TGN. Unlike PKD, dynamin is thought to be able to provide the force necessary for the scission reaction, although the exact mechanism is disputed. The energy for the reaction is provided by the hydrolysis of GTP to GDP, which results in a conformational change that causes scission. Thus it is possible to block scission from the TGN by expressing a GDP locked form of dynamin 2 (K44A) (Altschuler et al., 1998; Cao et al., 2000). Both wild type and the K44A mutant were microinjected into HUVEC along with a VWF-GFP construct to increase the chance of co-expression. The cells were then fixed either after 24 (Figure 4.16 panels A & C) or 48 hours (panels B & D) and immunolabelled with anti-TGN46 antibody. After one day it is apparent that the GFP-positive WPB remain attached to the TGN when coinjected with Dyn2K44A. However, although not the case in panel A, often the GFP-positive WPB even remain in close proximity to the TGN when coinjected with wild type Dyn2, making it difficult to distinguish whether they are unable to detach, or have simply not had sufficient time to move far from the Golgi. Therefore looking at the cells after two days should give a clearer view. It is immediately obvious that even two days post-transfection the GFP-positive WPB remain attached to the TGN (Figure 4.16D), and indeed there is a significant reorganisation of the TGN. Whether this reorganisation is a specific effect on the Golgi, or a result of a failure for the WPB to undergo scission from the TGN is not clear. However, the fact these cells are in the process of dividing may also be a contributory factor, since such a dramatic phenotype is not always observed.

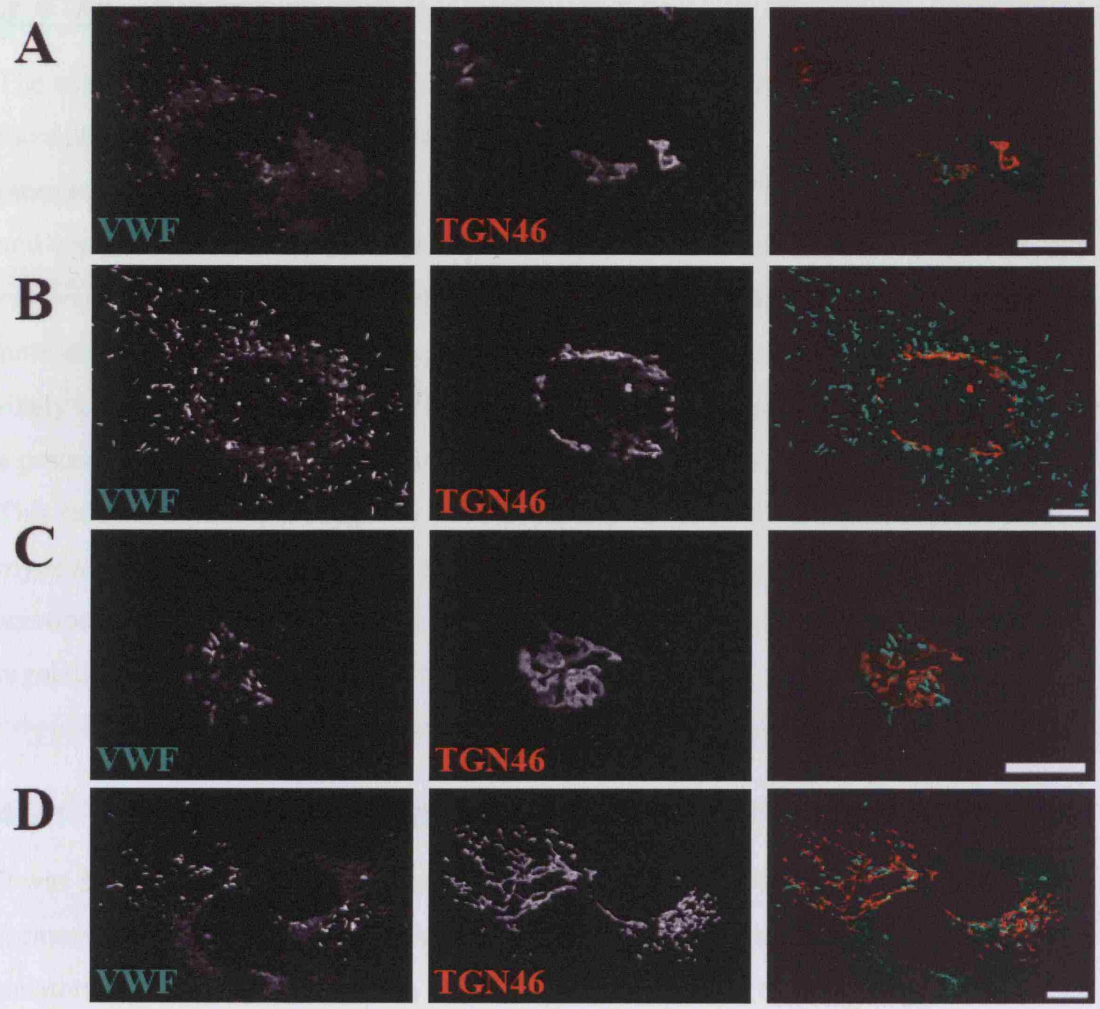

Figure 4.16 **Dynamin 2 may be required for scission of WPB from the TGN.**
HUVEC were microinjected with a VWF-GFP construct (green), as well as a dynamin 2 construct (**A** & **B**) or a dynamin 2 K44A construct (**C** & **D**). After 24 hours (**A** & **C**) or 48 hours, (**B** & **D**) the cells were fixed, permeabilised and labelled with an anti-TGN46 antibody (red). Images are confocal sections. Scale bars represent 10μm.

Of course even though these cells have been microinjected it would be preferable to have an indication that the cells are indeed expressing the Dynamin constructs as expected. In addition siRNA against dynamin 2 would be useful to further confirm a role for dynamin 2 in scission of WPB from the TGN.

4.3 Discussion

The use of high pressure freezing and freeze substitution to study events at the TGN has increased interest in the budding of the WPB from the Golgi. It has been shown by other members of the Cutler lab that both tubulation of VWF (Michaux et al., 2006a) and clathrin together with its adaptor protein AP-1 (Lui-Roberts et al., 2005) are required for the formation of elongated WPB. However whether tubulation of VWF provides sufficient force to generate this elongated shape is unclear. Perhaps more likely is that there is at least some involvement of the cytoskeleton, and there is certainly a precedent for this, with both actin and tubulin having roles in the formation of vesicles. This study suggests that actin may have a role to play, possibly alongside the atypical myosin, Myosin VI. In addition, this study shows that the apparatus required for scission of the WPB is likely to be dynamin 2 and FAPP may be playing a role in the regulation of this scission event.

4.3.1 The cytoskeleton and the biogenesis of WPB

It was hypothesised that it was most likely that microtubules would play a role in the formation of WPB because of their role in the formation of the tubular Golgi to plasma membrane carriers (GPCs), which like WPB, are transported on microtubules. However, it is clear that after treatment with nocodazole to depolymerise microtubules WPB were still able to form. This was despite the redistribution of the Golgi into mini stacks as a result of the nocodazole treatment (Figure 4.4). This also indicates that the integrity of the Golgi ribbon is not necessary to form WPB, which are actually significantly larger than the mini stack. Unsurprisingly given this result, the activity of the microtubule motor, kinesin, is not required for the formation of WPB (Figure 4.5).

In contrast, it seems that actin does play a role in the formation of WPB. However, whether it is strictly necessary is not obvious. In Figure 4.6 it is clear that WPB can still be formed after treatment of the cells with either jasplakinolide or cytochalasin D. There is a significant reduction in the amount of non-ER GFP fluorescence (i.e. that in WPB) after treatment with cytochalasin D. The reason for the reduction in number,

rather than a total absence of WPB may be because not all of the actin has been depolymerised. Of course another explanation could be that actin aids the formation of WPB but is not strictly necessary. Finally, it is also possible that the reason for the reduction in the number of WPB formed is that, in the absence of the actin cytoskeleton, there is a failure to deliver another component that is key to the budding of the WPB. A final point of interest is that the WPB formed after treatment with the actin poisons are more rounded than the untreated cells. This could be because the absence of actin means that full elongation is not possible, or because, as mentioned in the introduction, there is a increase in the pH of the Golgi after cytochalasin D treatment, although since the increase is only 0.23 this may be unlikely (Lazaro-Dieguez et al., 2006). It has not been possible to assess the role of tubulation of VWF in providing the force for the deformation of the membrane, but it seems possible that this could contribute, alongside the actin cytoskeleton.

4.3.2 Actin motors and the biogenesis of WPB

In order to address whether the reduction of actin is specific, the roles of two actin motors, known to function at the TGN, were tested. Firstly, the action of Myosin II was inhibited with the drug blebbistatin, using the same protocol as that used to test the involvement of both actin and tubulin. However, the similarity between the size and number of WPB between the treated and untreated samples suggests that Myosin II is not involved in the biogenesis of WPB.

The other actin motor that functions at the TGN is Myosin VI. Unfortunately there is not a simple drug treatment that could be used to assess the role of Myosin VI in the formation of WPB, but it was possible to use a tail-only mutant, which acts as a dominant negative to block the function of endogenous Myosin VI. After expression of this construct in HUVEC there are fewer WPB formed and those that are formed tend to be smaller and consequently more rounded (Figure 4.7). This is a similar phenotype to that observed in the presence of actin poisons. In addition, this experiment was repeated in HEK293 cells, where it was possible to distinguish between newly forming WPB and

those that were already present in the cell before transfection of the tail-only construct. It was found that 50% of the HEK293 cells expressing the tail-only construct alongside VWF failed to form WPB, whilst the other 50% were able to form WPB. There was a correlation between the expression levels of the tail-only mutant and whether the cell was able to form WPB, with the highly expressing cells being the ones that are unable to make the elongated organelle. It could be it is that the high expression level of the tail-only mutant, rather than it acting as a domain negative that is causing the defect in biogenesis. However, another possibility is that the tail-only construct must be expressed at a significant level to block the function of all of the endogenous protein. It will be necessary to use siRNA against Myosin VI to distinguish between these two possibilities. Furthermore, it would be interesting to test the bleeding time of the Snell Waltzer mouse.

4.3.3 Hip1R and the biogenesis of WPB

Since it has previously been demonstrated that clathrin is essential for the biogenesis of WPB (Lui-Roberts et al., 2005), and this study suggests that actin may also play an important role, the involvement of Hip1R, which interacts with both of these proteins has been tested. This is particularly important since it has recently been demonstrated that Hip1R is involved in the delivery of lysosomal hydrolases from the TGN to the lysosome. The secretion assay performed after depletion of Hip1R showed no defect in the release of WPB, which suggests that Hip1R does not play a role in the biogenesis of the WPB. This assay was used instead of the standard assay using VWF-GFP because the Hip1R can be depleted from the cells for a longer period of time, over which a significant number of WPB are turned over.

4.3.4 Regulation of scission

That there is regulation of scission to ensure that all the necessary components are recruited into a forming secretory vesicle is not a surprise. The presence of the stalk-like structure between the TGN and the forming WPB could perhaps represent a regulatory

step before final scission can occur. It has been hypothesised that the FAPPs may be responsible for determining whether a secretory vesicle is competent for scission. Thus, in this study the role of FAPP in the scission of WPB has been investigated. The expression of the PH domain of the FAPP protein in endothelial cells results in a failure to make WPB. Two phenotypes are observed, firstly an accumulation of VWF in the Golgi (interestingly, the only time that such significant co-localisation with TGN46 has been observed), and secondly the formation of WPB that appear unable to undergo scission from the TGN (Figure 4.13A and B respectively). The second phenotype is particularly interesting, as this is what would be expected if FAPP was important in the regulation of scission. It will be interesting to look at both of these phenotypes using EM after HPF-FS, to see whether the VWF in the TGN in panel A is tubulated, and in panel B to see if it is possible to distinguish between a block in scission and a defect in the regulation of scission. If the stalk observed connecting the WPB to the TGN is indeed involved in this regulation it may be absent after expression of FAPP-PH.

However, an important caveat to this experiment is that the overexpression of the PH could displace other PI(4)P binding partners from the TGN membrane. Whilst it does not seem to effect the recruitment of AP-1, since the observed phenotypes are very different, it does not preclude the phenotype being due to the lack of other PI(4)P binding partners. siRNA against FAPP could be used to address this problem, although the published SMARTpool targeted against FAPP does not appear to work well with HUVEC and further optimisation is necessary.

4.3.5 Scission from the Golgi

The final event before the WPB becomes an independent organelle is, of course, scission. There are three processes described that lead to scission at the TGN, two of which have been investigated in this study. Firstly, the expression of a PKD kinase-dead mutant in HUVEC indicates that PKD plays a role upstream of scission of elongated WPB. The resulting phenotype is similar to that observed after HUVEC have been depleted of AP-1, with small VWF puncta distributed through the cell (Figure 4.14). As

in the AP-1 depleted cells, these puncta are not able to undergo regulated release (Figure 4.15). The presence of these puncta in the cytosol at least precludes a role for PKD in their scission.

However, it is not possible to formally discount a role for PKD in the scission of WPB from the TGN, although the finding that dynamin 2 is involved in this scission event certainly suggests it is unlikely (Figure 4.16). It is apparent that upon co-expression of both VWF-GFP and dynamin 2 K44A that the GFP-positive WPB remain in close proximity to the TGN. This phenotype should be further confirmed with the use of tagged constructs and siRNA targeted against dynamin 2. Furthermore, it would be interesting to test whether the dynamin 2 knockout mouse has a prolonged bleeding time. Finally, the examination of this phenotype using EM after HPF-FS would be very interesting.

4.3.6 Roles for other proteins at the TGN

Of course, many other proteins will have roles to play at the TGN. One obvious protein to investigate in further detail is clathrin. Whilst it is already known that clathrin is necessary in the biogenesis of WPB (Lui-Roberts et al., 2005) and that it coats tubule-containing protrusions at the TGN ((Zenner et al., 2007) and Figure 3.x), it would be interesting to determine if clathrin was required for tubulation, and whether clathrin is required for the initial budding or maintainence the shape of the organelle whilst the tubules are still being arranged. In addition, it would be investigate whether any, and which of the BAR-domain containing protein are involved in WPB biogenesis. Thus, whilst this study indicates roles for actin, FAPP and dynamin at the TGN, many further experiments are required to present a full itinerary of events at the TGN.

5 Hermansky-Pudlak Syndrome and WPB

5.1 Introduction

Aberrant formation of lysosome-related organelles (LRO) is a hallmark of Hermansky-Pudlak syndrome (HPS) and implicates the mutated proteins in LRO biogenesis. Indeed the role of HPS2, more commonly known as AP-3beta, in the biogenesis of WPB has already been demonstrated, with delivery of CD63 perturbed in HUVEC depleted of HPS2 ((Harrison-Lavoie et al., 2006) and Figure 5.13). More recently a role for BLOC-1 proteins in WPB formation, the BLOC resulting in the most severe phenotype in terms of pigmentation has been demonstrated to have an effect on WPB. Simultaneous knockdown of three components of BLOC-1, snapin, pallidin and muted, in human umbilical vein endothelial cells results in a reduction in stimulated release of VWF (unpublished results – Figure 5.1, with kind permission from Tom Nightingale). Thus BLOC-1 must play an important, but as yet undescribed role, in the biogenesis of WPB. However, the roles the BLOC-2 and BLOC-3 have not been considered in HUVEC.

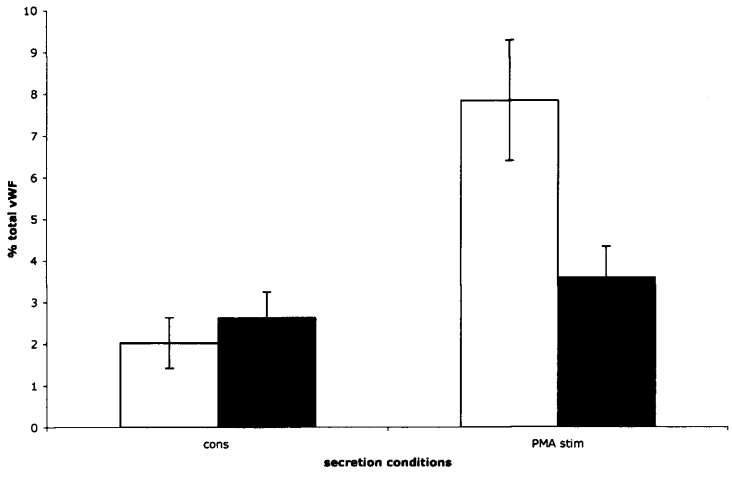

Figure 5.1 **Knockdown of BLOC-1 results in a greater than two-fold reduction in stimulated release.**

HEK293 cells were first transfected with siRNA oligos against Snapin, Pallidin and Muted mRNA and then after 48 hours transfected again with the siRNA cocktail and a VWF construct. After a further 48-72 hours a secretion assay was performed indicating a reduction in stimulated release compared to mock transfected cells. All values are

normalised to total cellular VWF and the constitutive portion is subtracted from total stimulated release to calculate the PMA responsive pool.

In order to investigate the roles of BLOC-2 and –3 in WPB biogenesis, the various BLOC components were knocked down individually and in concert in human endothelial cells using siRNA. In order to ascertain whether any of the BLOC-2 or BLOC-3 proteins are required a number of criteria were examined; whether WPB are formed, whether the WPB still recruit the expected membrane proteins, and whether the WPB are able to undergo stimulated release. Finally, since a role for BLOC-3 has previously been demonstrated in the movement of LAMP-1 (Falcon-Perez et al., 2005; Nazarian et al., 2003), this was used as a control to check that the siRNA oligos were sufficiently depleting the cells of BLOC-3.

The membrane-associated proteins known to be recruited to WPB as discussed in the Introduction are P-selectin, which is recruited at that TGN, and CD63 and Rab27a, which are recruited as the WPB mature (Bonfanti et al., 1989; Hannah et al., 2003; McEver et al., 1989; Vischer and Wagner, 1993). Figure 5.2 is a series of confocal images from a control experiment where HUVEC were nucleofected twice with scrambled siRNA, highlighting this recruitment. These images should be referred back to throughout this chapter as examples of normal WPB expression of these proteins.

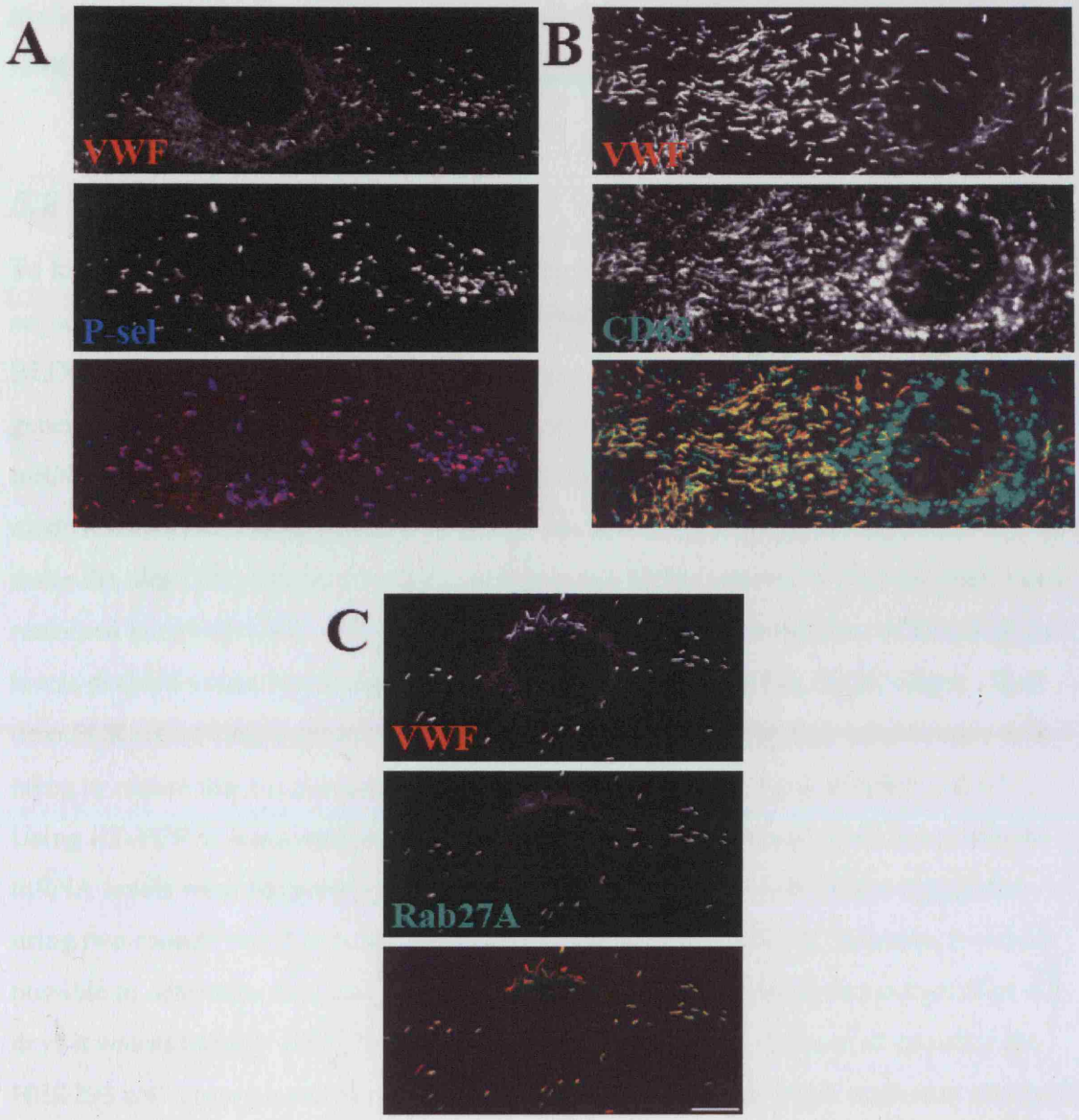

Figure 5.2 ***Recruitment of membrane proteins to WPB.***

HUVEC are nucleofected with scrambled siRNA on day 0 and day 2, along with Rab27a-GFP (green) in panel **C**. On day 4, the cells are fixed, permeabilised and immunolabelled with VWF (red, **A-C**), P-selectin (blue, **A**) and CD63 (green, **B**).

The secretion assay to test for stimulated release of VWF was performed in both HUVEC and HEK293 cells, making use of the finding that VWF is able to drive the formation of WPB in HEK293 cells (Michaux et al., 2003). This allows the protein to be depleted prior to expression of such that no WPB made in the presence of the protein are seen within the cells as a confounding background, thus no subtle effects are

masked. The quantity of VWF, in both the constitutively released samples and those released after stimulation, will be assessed by ELISA.

5.2 Results

To knockdown most of these proteins, the Qiagen design tool was used to generate sequences that, according to their algorithms, should target the mRNA of the BLOC-2 or BLOC-3 components and recruit the RISC apparatus most efficiently. The sequence generated was put into the BLAST program to ensure that it only targets the specific mRNA required. HPS1 siRNA was purchased from Invitrogen and included chemical modifications that are designed to eliminate the induction of cellular stress pathways and make the oligo more stable in serum, thus prolonging the amount of time that that RNA remained knocked down. However, whilst slightly prolonging the time of knock down, it was decided to use two rounds of nucleofection with the siRNA for all oligos. Real-time PCR (RT-PCR) was used to assess the level of knockdown and suitable care was taken to ensure that the primers for the RT-PCR amplified only the specific mRNA. Using RT-PCR it was established that the knockdown was optimal at 48 hours and the mRNA levels were beginning to slightly increase at 72 hours. The major reason for using two rounds was that in the absence of antibodies to the BLOC proteins, it wasn't possible to determine the turnover of the protein and by performing the assays after 4-5 days it was extremely unlikely that any protein remained. In addition when using the HEK293 cells, two rounds are essential so a VWF construct can be transfected alongside the second round of siRNA. A table indicating the average level of knockdown for each of the components of BLOC-2 and BLOC-3 is shown below for both HEK293 cells and HUVEC since as level of knockdown were similar (Table 5.1).

***Table 5.1* Percentage knockdown of HPS mRNA compared to cells mock transfected with either water or scrambled siRNA.**
Efficiency of knockdown is assessed using qPCR. siRNA oligos resulting in a less than 70% knockdown were discarded.

mRNA		% knockdown
BLOC-2	HPS3-1	95%
	HPS3-2	95%
	HPS3-4	91%
	HPS5	80%
	HPS6	76%
BLOC-3	HPS1	75%
	HPS4	82%

5.2.1 BLOC-2 localisation

Mutation of the HPS3 gene in the cocoa mouse result in the loss both HPS5 and HPS6 proteins, suggesting this is the key component in the complex, therefore HPS3 was the first protein investigated. All HPS proteins, including HPS3, have been reported to be cytosolic with some membrane association. Thus, two HPS3-GFP constructs were made (Materials and Methods) and microinjected into HUVEC to determine HPS3 localisation in endothelial cells and in particular to establish if there is any co-localisation with VWF in WPB. Figure 5.3 shows that HPS3 is indeed cytosolic. In Figure 5.3A, HPS3-GFP (16) construct was microinjected into HUVEC, the cells were fixed after 24 hours and processed for immunofluorescence microscopy. An image from this experiment shows that the protein is mainly cytosolic, although there is a slight increase in intensity around the perinuclear cluster of WPB, possibly corresponding to the Golgi. However, a cell microinjected with the other HPS3-GFP (20) construct and fixed after 48 hours showed no such enrichment. In addition, this cell has a lower level of HPS3-GFP expression. In neither case is any co-localisation with WPB apparent. Furthermore, overexpression of HPS3 appears to have no effect on the formation or maintenance of WPB. This was not tested using the secretion assay due to the low transfection efficiency of this construct.

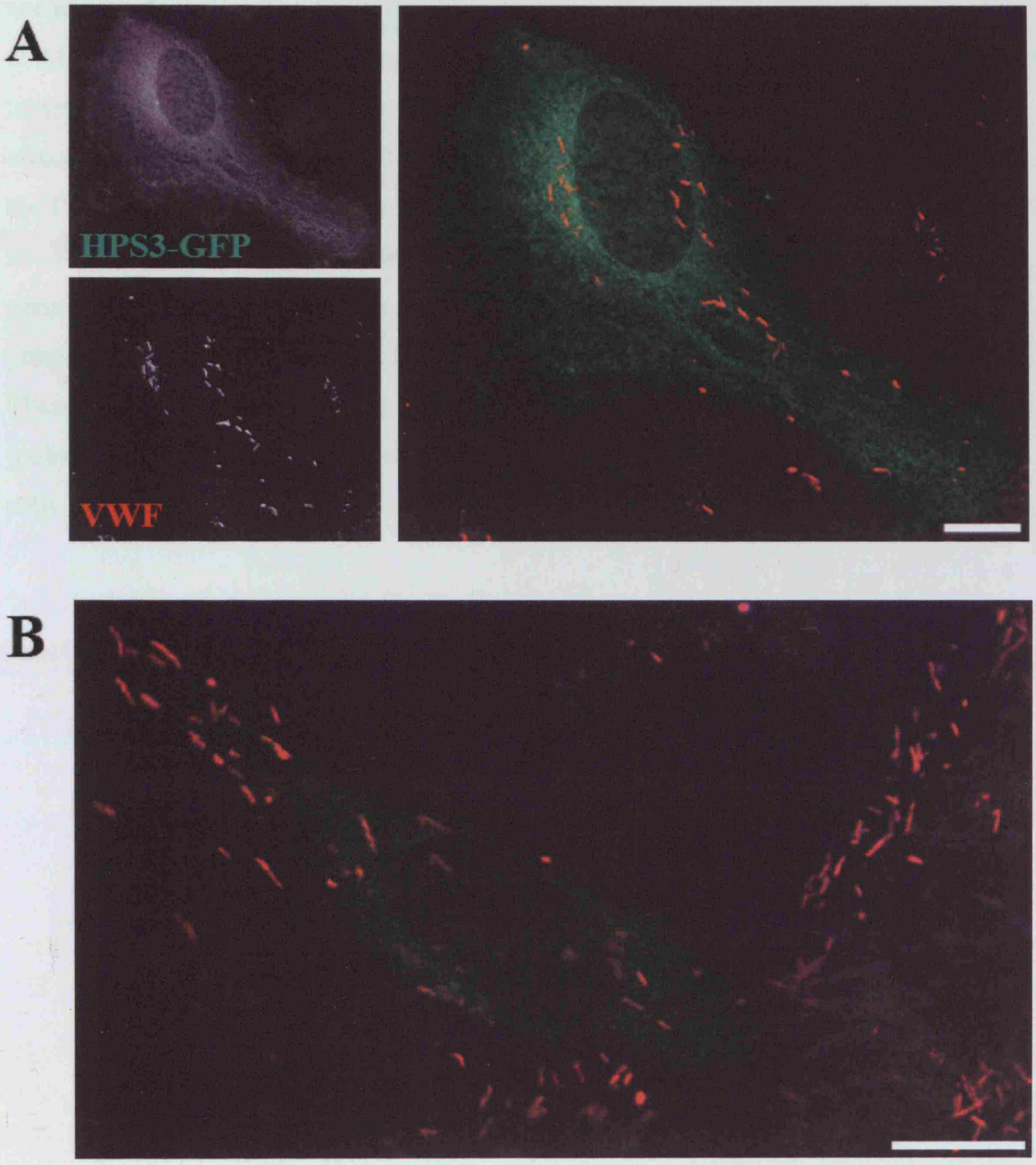

Figure 5.3 **HPS3-GFP is cytosolic and does not colocalise with VWF-positive WPB.** HPS3-GFP constructs were microinjected into HUVEC and fixed after 24 hours (**A**) and 48 hours (**B**) respectively and labelled for VWF (red). Images are confocal sections. Scale bars represent 10μm.

Since it has been reported that HPS3 localisation requires a clathrin-binding domain (LLDFE), a construct with this region mutated (HPS3-CBD), a kind gift from Marjan

Huizing (Helip-Wooley et al., 2005), was used as a comparison for the localisation study and also to determine any effect on WPB formation (Figure 5.4). Given that expression of AP180 C-terminus, which acts as a dominant negative to the formation of clathrin lattice, prevents formation of new elongated WPB (Lui-Roberts et al., 2005), a similar effect might be expected if HPS3 is acting in concert with clathrin in this early step at the TGN. However, it is apparent in Figure 5.4 that overexpression of HPS3-CBD has no effect on the formation of new WPB, as indicated by the presence of the normal perinuclear cluster of WPB and no disruption of the preformed WPB. The HPS3-CBD protein has a similar expression pattern to the wild type HPS3-GFP fusion proteins. There is some very slight overlap between HPS3-CBD and VWF in panel A, but this is probably due to the high concentration of protein in the cytosol and is not present in all cells (panel B).

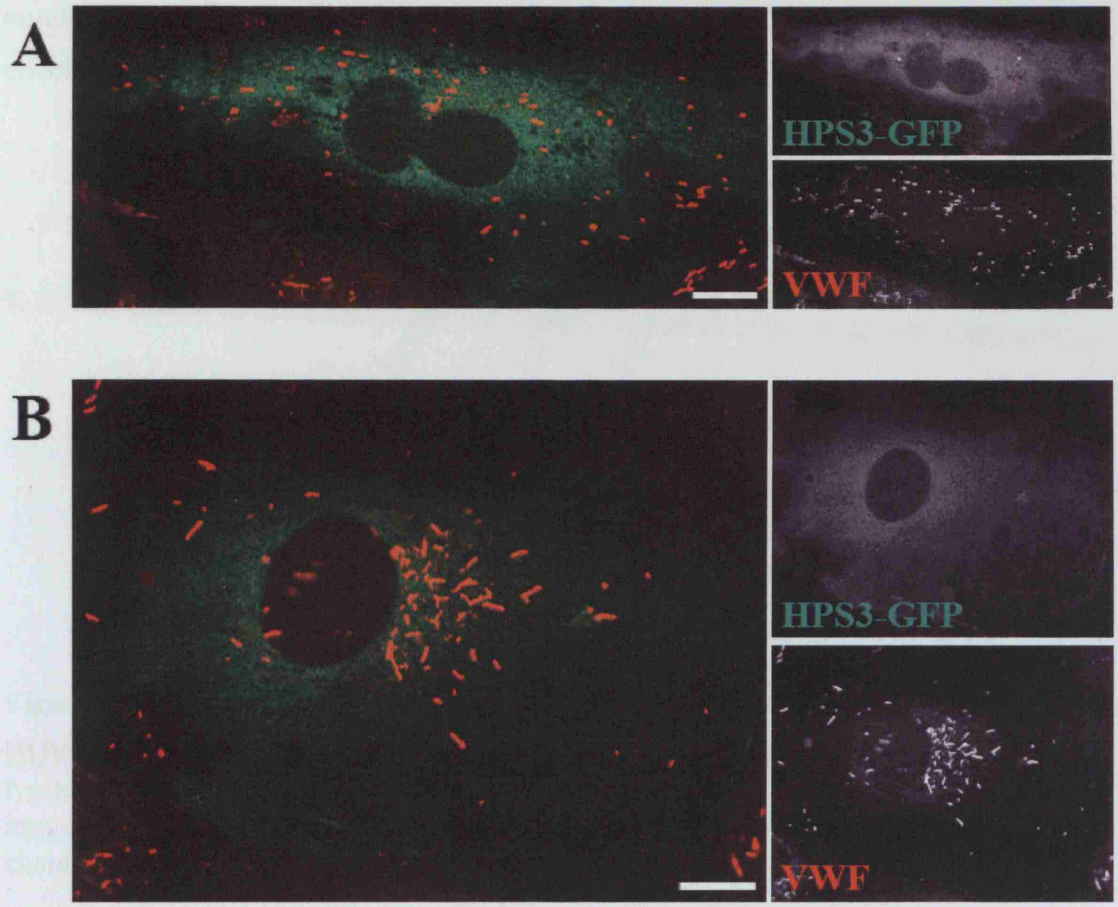

Figure 5.4 ***Expression of mutant HPS3 construct lacking the clathrin binding domain has no effect on the biogenesis of WPB.***

In panels **A** and **B** HUVEC were microinjected with HPS3-CBD and fixed after 48 hours. The cells were labelled with an anti-VWF antibody (red). Images are confocal sections. Scale bars represent 10μm.

Further, a co-immunoprecipitation (co-IP) indicated that HPS3 does not bind to clathrin in endothelial cells. In the absence of an antibody against HPS3, an antibody against GFP was used for the co-IP. After immunoprecipitating with the GFP antibody the samples were subsequently western blotted with an anti-clathrin antibody. The upper panel in Figure 5.5 shows that clathrin was only present in the cell lysate and not in the lanes after IP. The lower panel indicates significant enrichment of HPS3-GFP in the IP compared to the lysate. Indeed the absence of the band in the lysate is probably due to the low transfection efficiency of the HPS3-GFP construct. Since only a relatively small fraction of HPS3 is bound to clathrin in fibroblast, it may be necessary to increase the

number of transfected cells in order to determine if there really is an interaction in endothelial cells.

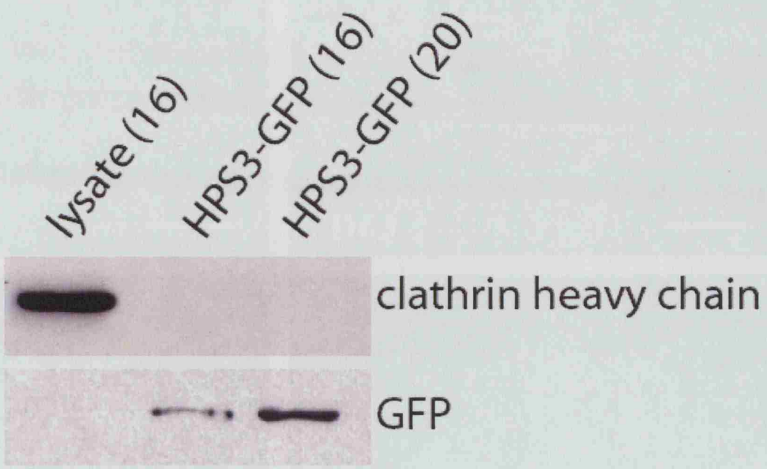

Figure 5.5 ***HPS3 does not interact with clathrin in endothelial cells.***
HUVEC were nucleofected with HPS3-GFP, after 48 hours the cells were lysed and lysates incubated with anti-GFP immobilsed on dynabeads. The lysate and immunoprecipitate was run on an SDS gel and western blotted with anti-clathrin heavy chain antibody and an anti-GFP antibody.

5.2.2 BLOC-2 knockdown and association of membrane proteins

Whilst it is unlikely that HPS3 works in concert with clathrin in endothelial cells, it does not preclude the involvement of HPS3 in the biogenesis of WPB. Therefore HPS3 was knocked down in HUVEC using the two round protocol 4-5 days later the mRNA was prepared for RT-PCR analysis, and the cells were fixed for immunofluorescence, where the cells were labelled with an anti-VWF antibody to assess the formation and localisation of the WPB. The initial siRNA used (HPS3-1) caused a loss of VWF-positive WPB, CD63 staining is shown that cells are present (Figure 5.6).

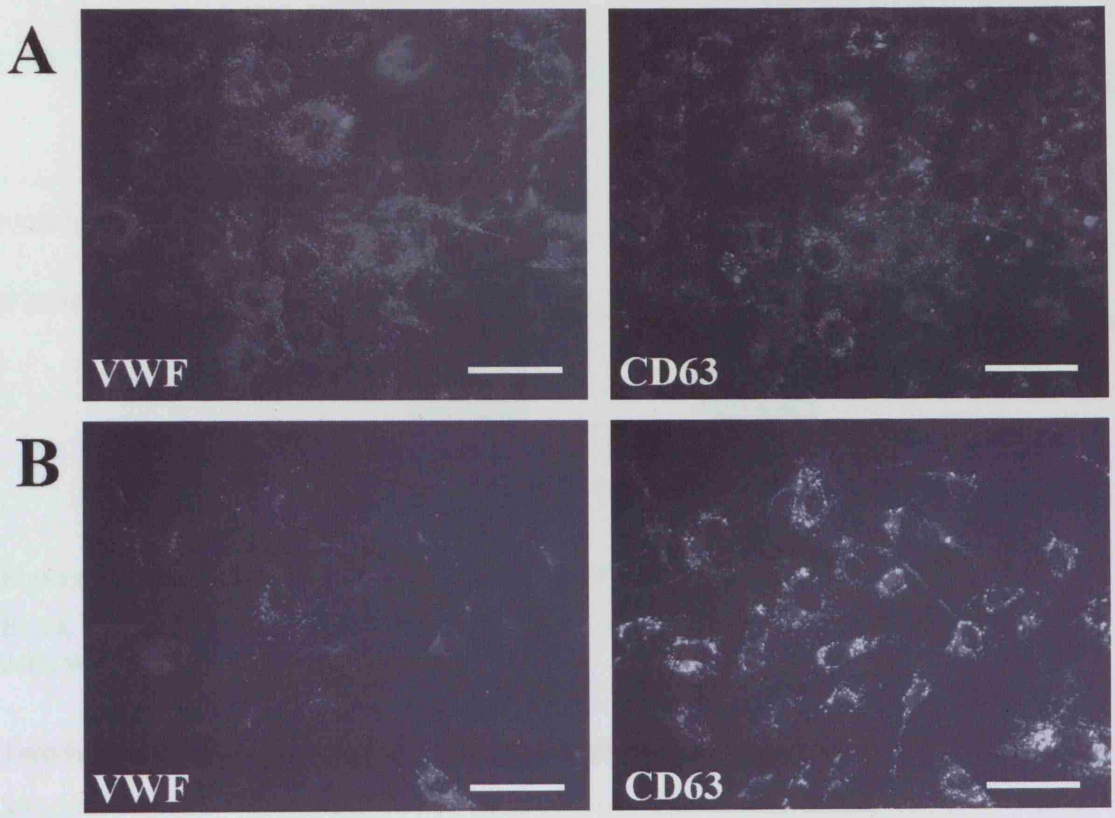

Figure 5.6 ***Nucleofection of HPS3-1 siRNA causes a loss of WPB from HUVEC.***
HUVEC were nucleofected twice with HPS3-1 siRNA on day 0 and day 2, and fixed on day 5. The cells were subsequently labelled with anti-VWF and anti-CD63 antibodies. Images are confocal sections. Scale bars represent 50μm.

Quantification of the number of cells containing WPB is shown in Figure 5.7, indicates that after knockdown of HPS3 that less than 50% of the cells contain WPB as compared with nearly 90% after mock transfection of HUVEC.

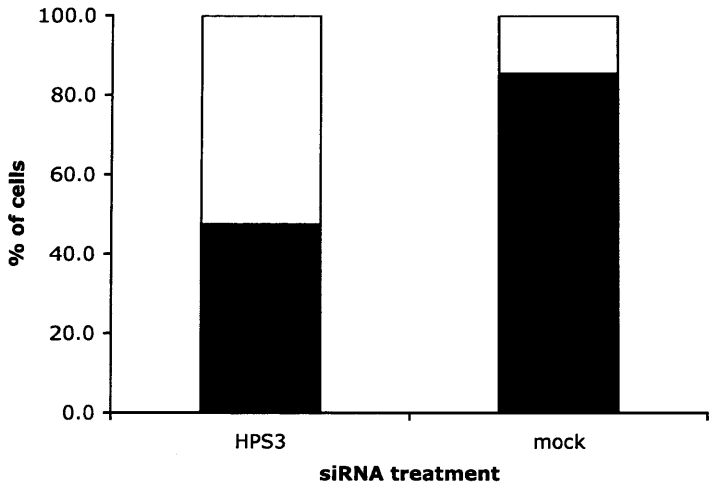

Figure 5.7 ***Knockdown of HPS3 results in a 50% reduction of WPB in HUVEC***
Black bars indicate number of cells with WPB and white bars, the number without. 150 cells were counted for each condition.

Two further siRNAs targeted against HPS3 were used to confirm this result. Whilst the knockdown achieved using either of these siRNAs was similar to that for HPS3-1 (see table 3.1), neither showed the dramatic loss of VWF-positive WPB as observed with HPS3-1 or indeed any change in the localisation of WPB. The effect of HPS3-1 must, therefore, be an off-target effect and not due to the specific loss of HPS3 protein. This cannot be due to the targeting of another protein within the coding region, as this would have been identified using the BLAST program. However, more recently it has been reported that a match between residues 2-8 of the siRNA and the 3'UTR of any mRNA can result in an efficient knockdown (Birmingham et al., 2006). Dharmacon have developed software to detect these so called 'seed matches' (http://www.dharmacon.com/seedlocator/default.aspx) and when the appropriate region of HPS3-1 is put into the program there are multiple possibilities of mRNAs that could be affected. There are 38 mRNAs containing multiple seed matches including VWF A domain containing variant 1 and Rab36. These proteins will discussed later. Of course the finding of the off-target effect meant that HPS3-2 and HPS3-4 were used for all further experiments.

To test whether HPS3 plays an important role in the recruitment of any of the known

membrane proteins to WPB, HUVEC were subjected to the standard double round of knockdown and when appropriate the second round was accompanied by expression of a Rab27a-GFP construct in the second round of nucleofection. This was followed by fixation, permeablisation and immunolabelling for the membrane proteins usually associated with WPB. The localisation of CD63 was of particularly interest, since in melanocytes BLOC-2 deficiency seems to affect proteins that are often delivered in an AP-3-dependent fashion, although through an independent route (Di Pietro et al., 2006). Furthermore, the correct localisation of CD63 and Rab27a is also an indication that the WPB are maturing (Figure 5.8). Using either siRNA HPS3-2 or HPS3-4 all membrane-associated proteins seemed to be normally localised to WPB and in the expected position within the cell (Figure 5.8 compared with Figure 5.2). This is in contrast to observations made after knockdown of HPS2 or AP-3beta using the same nucleofection protocol, a condition in which CD63 is no longer localised to WPB and found only in late endosomes/lysosomes (Harrison-Lavoie et al., 2006).

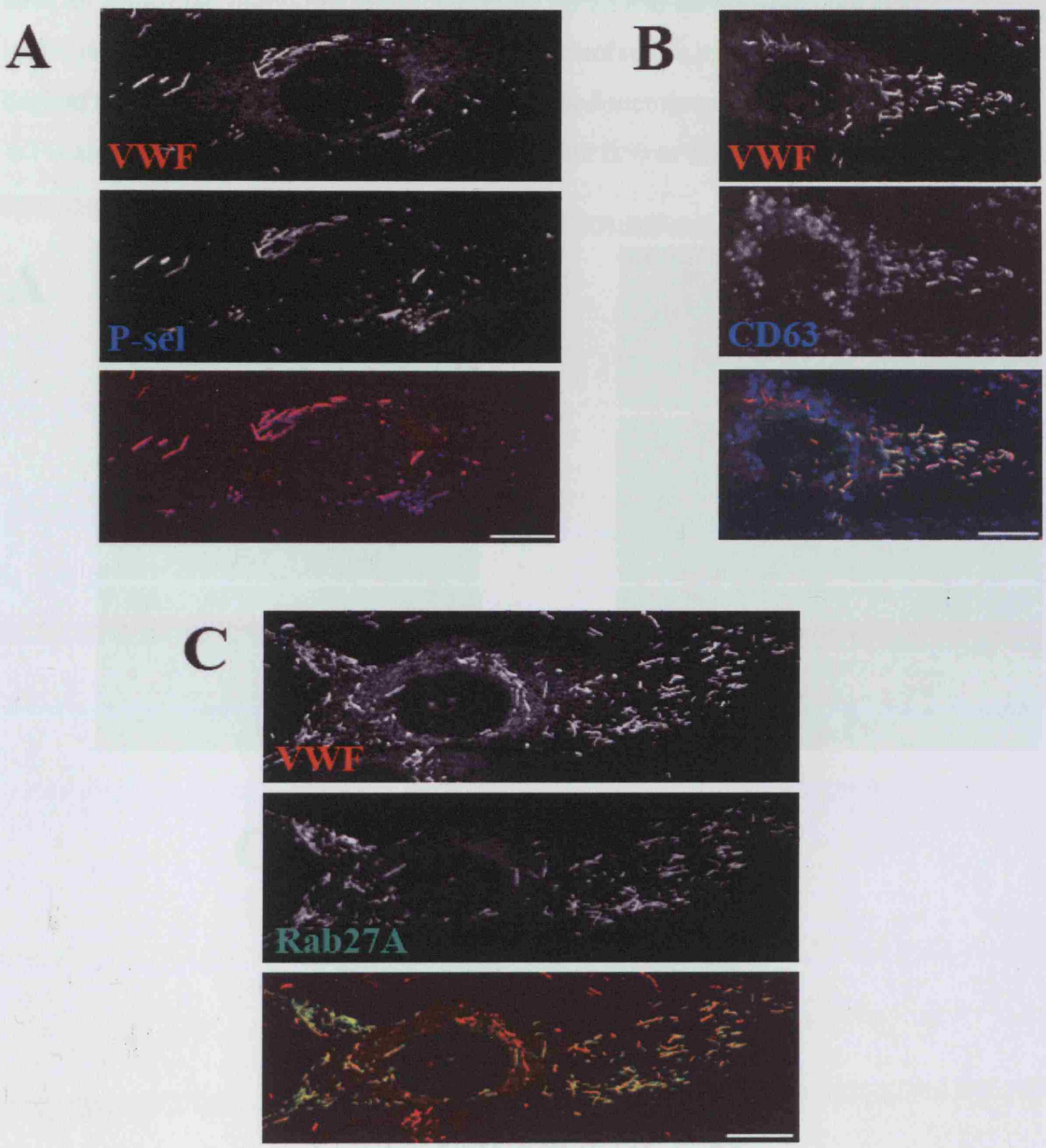

Figure 5.8 ***HPS3 knockdown in HUVEC has no effect on the localisation of membrane proteins.***

HUVEC were nucleofected with HPS3-4 siRNA (**A** & **C**) and HPS3-2 siRNA (**B**) on day 0 and day 2, along with Rab27a-GFP (green) in panel **C**. On day 4 the cells where fixed, permeablised and immunolabelled with VWF (red), P-selectin (blue – **A**) and CD63 (green – **B**). Images are confocal sections. Scale bars represent 10μm.

Whilst the HPS proteins are often found in complexes, subtle differences in phenotypes between proteins found in the same complex exist. This may be because the proteins

have an additional individual effect, therefore HPS5 and HPS6 were both also individually knocked down. Using the same nucleofection protocol as that used to deplete the cells of HPS3, none of the well-studied membrane-associated proteins of WPB are affected by knockdown of HPS5 (Figure 5.9) or HPS6 (Figure 5.10).

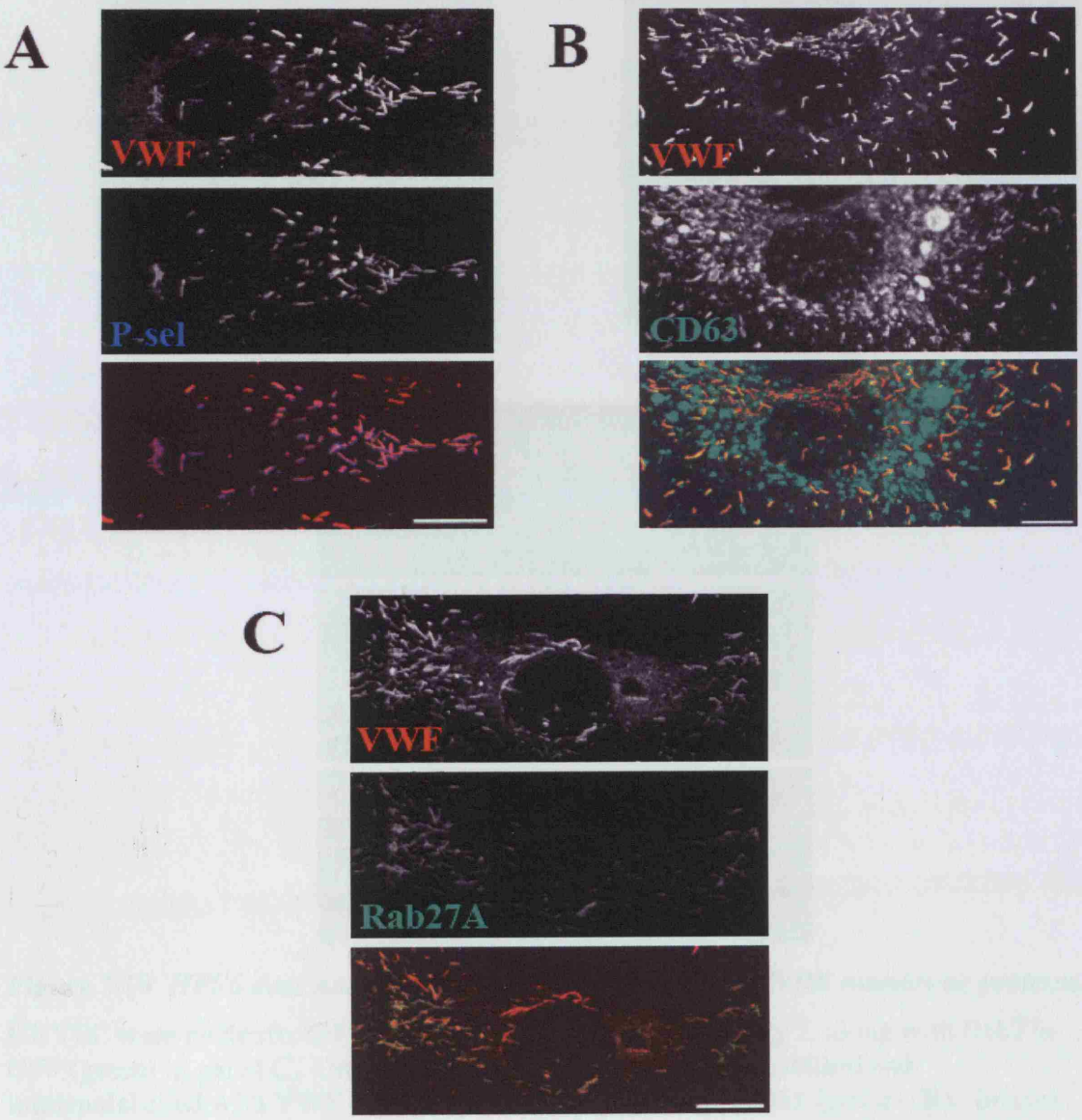

Figure 5.9 ***HPS5 does not play a role in the localisation WPB membrane proteins.***
HUVEC were nucleofected with HPS5 siRNA on day 0 and day 2, along with Rab27a-GFP (green) in panel **C**. On day 4 the cells where fixed, permeablised and immunolabelled with VWF (red), P-selectin (blue – **A**) and CD63 (green – **B**). Images are confocal sections. Scale bars represent 10μm.

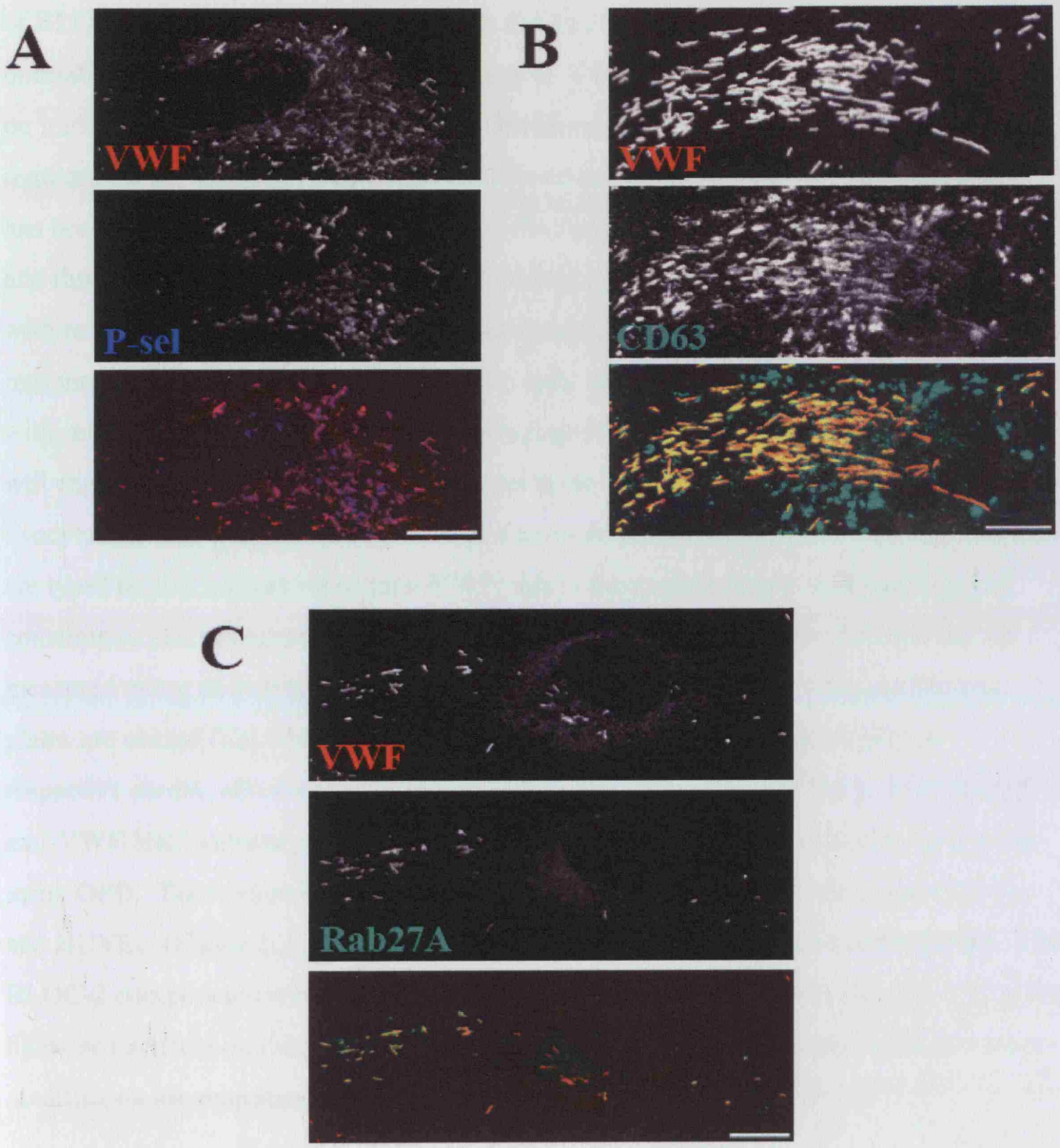

Figure 5.10 ***HPS6 does not play a role in the localisation of WPB membrane proteins.***

HUVEC were nucleofected with HPS6 siRNA on day 0 and day 2, along with Rab27a-GFP (green) in panel **C**. On day 4 the cells where fixed, permeablised and immunolabelled with VWF (red), P-selectin (blue – **A**) and CD63 (green – **B**). Images are confocal sections. Scale bars represent 10μm.

5.2.3 BLOC-2 knockdown and exocytosis

As all the proteins involved in WPB exocytosis/function are not, as yet, characterised

there is a chance that BLOC-2 may have a functional effect. Indeed, upon knockdown of BLOC-1 there is no apparent effect on the localisation of membrane proteins, but a dramatic reduction in the stimulated release of VWF. BLOC-1 could have a direct effect on maturation or release by localising to WPB, or, perhaps more likely, it could be required for the trafficking of an as yet undescribed WPB protein. A secretion assay has been used to determine whether the WPB are able to undergo regulated exocytosis, and thus functioning as expected. This involves incubating the nucleofected cells first with release medium that does not contain serum (a source of VWF), this will be used to measure constitutive release of VWF. The cells are then incubated for 30-45 minutes with release medium containing the secretagogue PMA (this is non-physiological but will ensure maximum release of VWF from those WPB competent to undergo regulated exocytosis), this medium will be used to determine stimulated release. Finally, the cells are lysed to give a measure of total VWF; this is then used to normalise the levels of constitutive and stimulated release. The relative amounts of VWF in the medium are measured using an enzyme-linked immunosorbent assay (ELISA), whereby 96 well plates are coated first with anti-VWF antibody, and then are incubated with the respective media, allowing the VWF present to bind, after washing the plate is probed anti-VWF-HRP antibody. The plate is subsequently developed in a colorimeteric assay using OPD. These experiments were carried out in both HEK293 cells (Figure 5.11A) and HUVEC (Figure 5.11B) and no effect on stimulated release could be identified. The BLOC-2 components were also depleted simultaneously in HUVEC (Figure 5.11B'), but likewise no effect on release could be detected. Furthermore, the triple knockdown has no effect on the recruitment of P-selectin, CD63 or Rab27a (Figure 5.12).

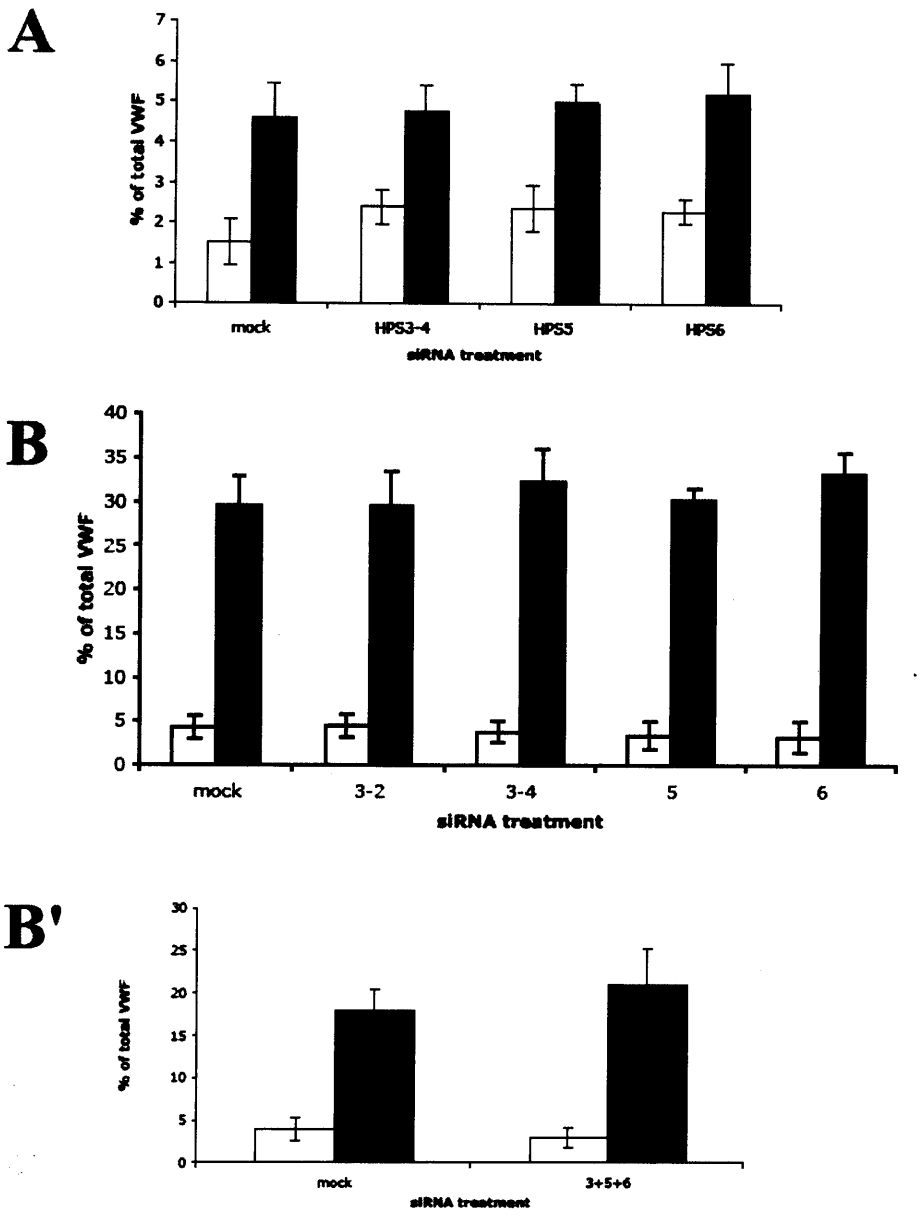

Figure 5.11 ***Depletion of BLOC-2 has no effect on stimulated release of VWF.***

HEK 293 cells (**A**) and HUVEC (**B**) were nucleofected with HPS3, 5 and 6, individually and in concert, on day 0 and day 2, and alongside VWF in the HEK293 cells. On day 4 the cells were incubated in release medium, firstly without and then with PMA for 45 minutes (**B**) and 30 mins (**B'**), then finally the cells were lysed to allow total VWF to be measured. All values are normalised to total cellular VWF and the constitutive portion is subtracted from total stimulated release to calculate the PMA responsive pool.

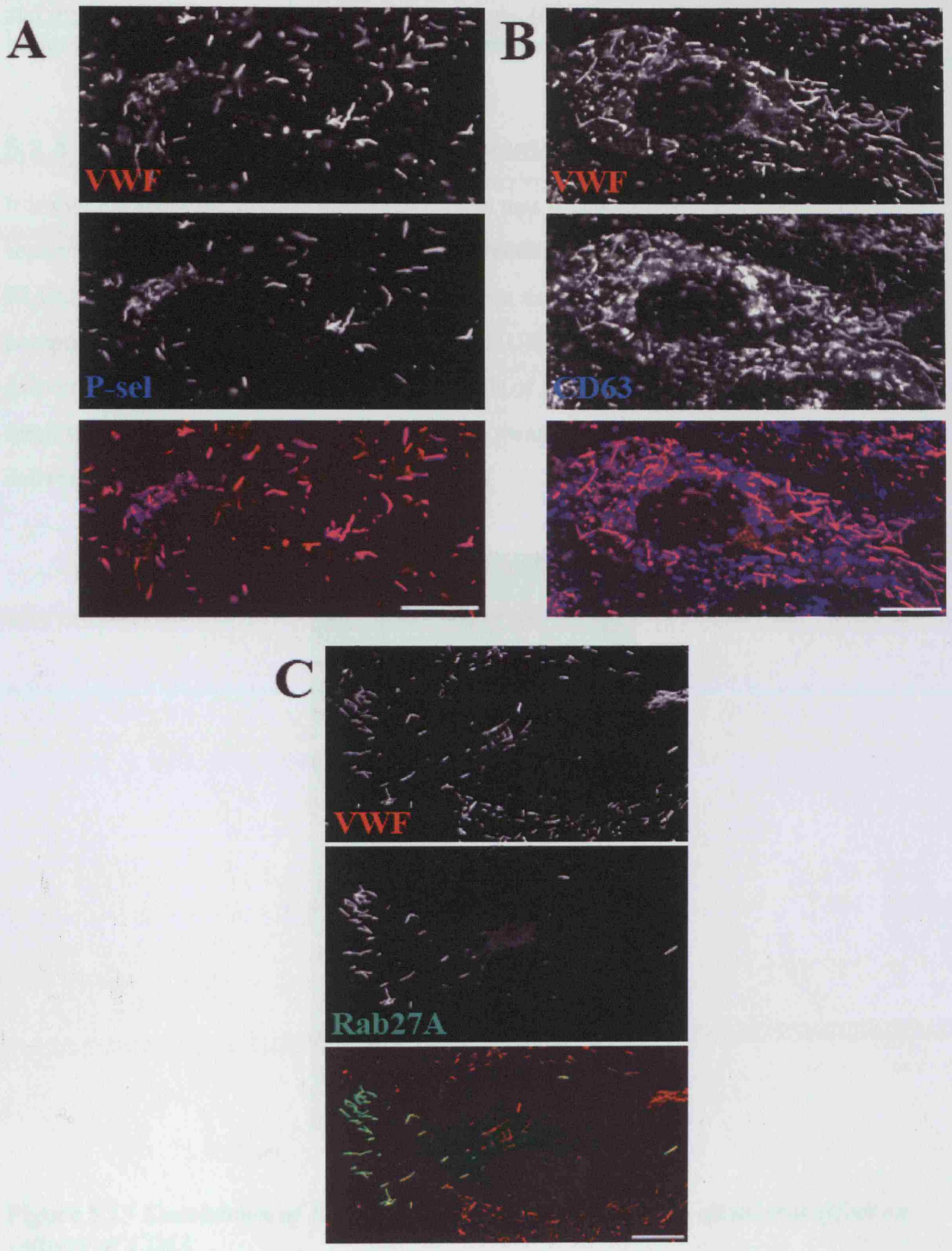

Figure 5.12 ***BLOC-2 depletion has no effect on localisation of WPB membrane proteins.***

HUVEC were nucleofected with HPS3, HPS5 and HPS6 siRNA on day 0 and day 2, along with Rab27a-GFP (green) in panel C. On day 4 the cells were fixed, permeablised

and immunolabelled with VWF (red), P-selectin (blue – A) and CD63 (blue – B). Images are confocal sections. Scale bars represent 10μm.

5.2.4 BLOC-2 and AP-3 double knockdown

It is evident from the double knockout mouse that BLOC-2 and AP-3 operate on separate pathways thus resulting in a more severe phenotype, in this case similar to BLOC-1. Therefore BLOC-2 components were depleted alongside HPS2, the beta component of AP-3. As discussed earlier, in HUVEC, AP-3 depletion results in reduced delivery of CD63 to WPB. Depleting the cells of BLOC-2 alongside AP-3 does not seem to result in any additional effect, with a minimal amount of CD63 still being delivered to WPB (Figure 5.13).

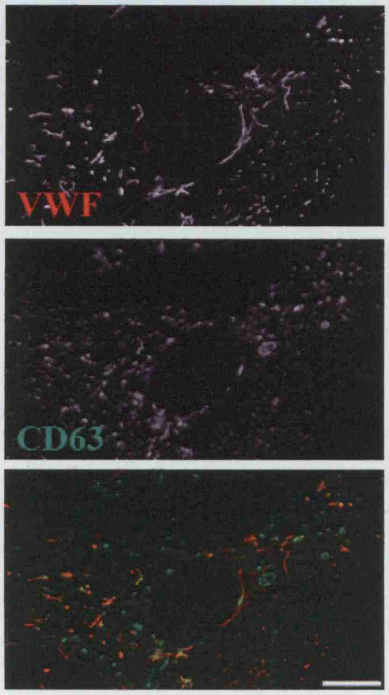

Figure 5.13 ***Knockdown of BLOC-2 and AP-3 together has no additional effect on delivery of CD63.***

HUVEC were nucleofected with HPS3 and HPS2 (AP-3beta) siRNA on day 0 and day 2. On day 4 the cells were fixed, permeablised and immunolabelled with VWF (red) and CD63 (green). Images are confocal sections. Scale bar represents 10μm.

5.2.5 BLOC-3 knockdown and the recruitment of WPB-specific membrane-associated proteins

BLOC-3 is a heterodimeric complex made up of HPS1 and HPS4 proteins (Martina et al., 2003; Nazarian et al., 2003). Unlike the case for BLOC-2, neither protein seems to be 'dominant', HPS1 protein is absent in the light ear (HPS4) mouse and HPS4 protein is absent in the pale ear (HPS1) mouse. Therefore both proteins were knocked down side by side to determine if either the complex or the individual proteins played a role in the biogenesis of WPB. The same transfection protocol of two nucleofections separated by 48 hours was used (with the Rab27a-GFP construct expressed as required), although this time using the Stealth siRNA in the case of HPS1. The localisation of the membrane proteins, P-selectin, CD63 and Rab27a was observed. Figures 3.15 – 3.17 shows that none of these membrane proteins are mislocalised in either HPS1 (Fig. 3.15) or HPS4 (Fig.3.16) knockdown, or indeed when they are knocked down together (Fig.3.17).

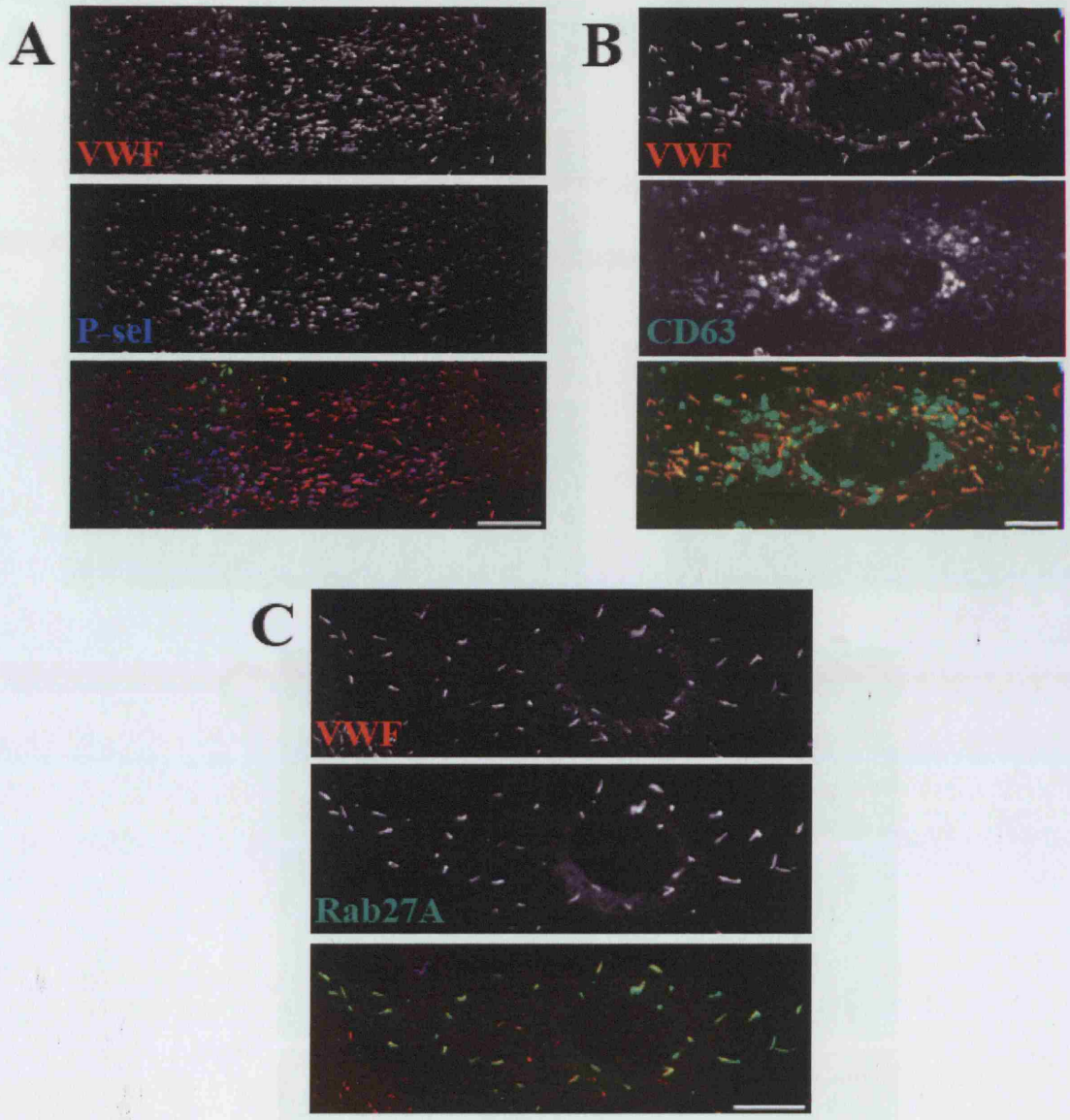

Figure 5.14 ***WPB membrane proteins are localised normally in the absence of HPS1.***

HUVEC were transfected with HPS1 siRNA on day 0 and again on day 2, alongside Rab27a-GFP (green) in panel C. Cells were fixed, permeabilised and immunolabelled for VWF (red), P-selectin (blue – A) and CD63 (green – B). Images are confocal sections. Scale bars represent 10μm.

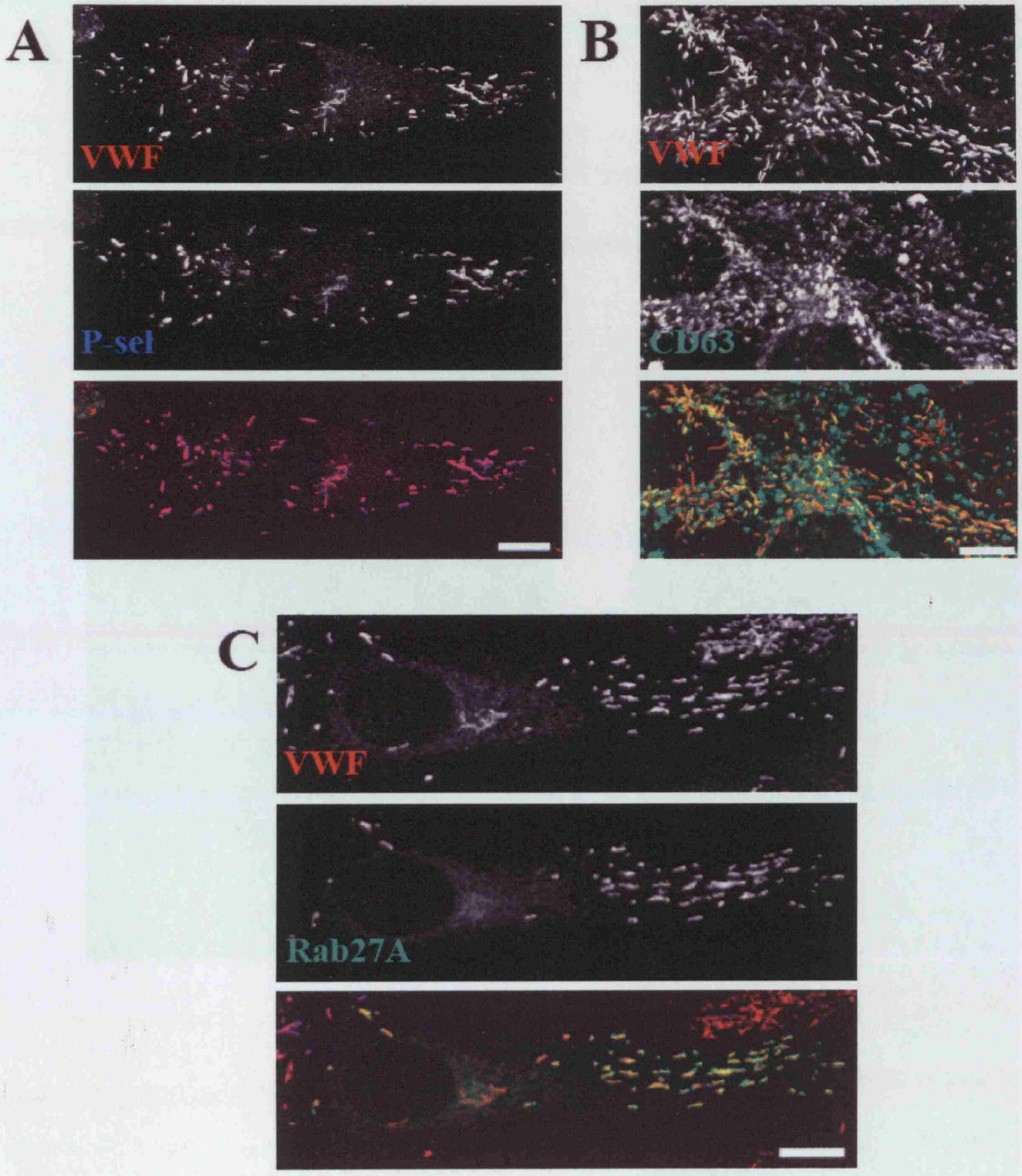

Figure 5.15 ***WPB membrane proteins are localised normally in the absence of HPS4.***

HUVEC were transfected with HPS4 siRNA on day 0 and again on day2, alongside Rab27a-GFP (green) in panel **C**. Cells were fixed, permeabilised and immunolabelled for VWF (red), P-selectin (blue – **A**) and CD63 (green – **B**). Images are confocal sections. Scale bars represent 10μm.

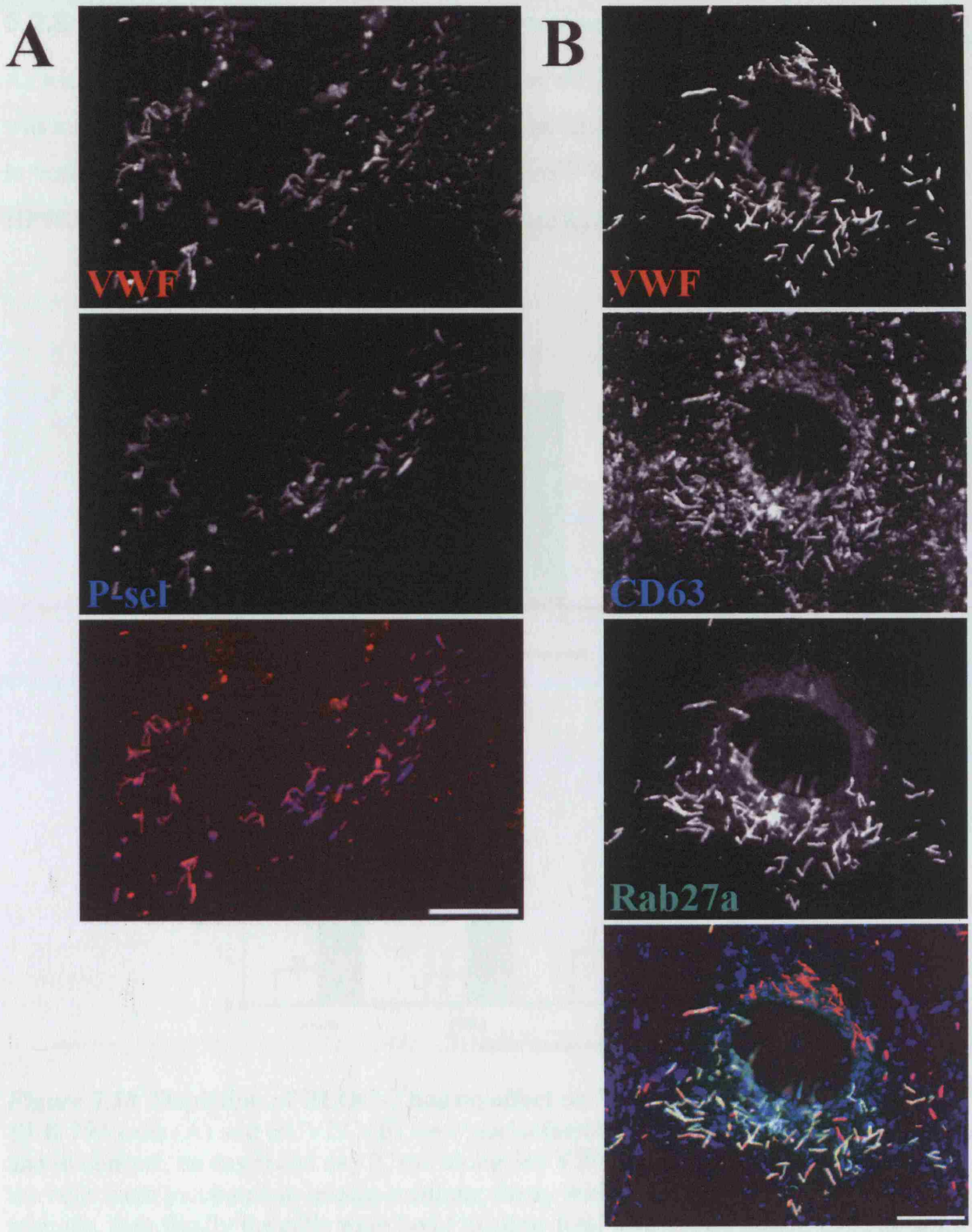

Figure 5.16 **WPB membrane proteins are localised normally after depletion of both HPS1 and HPS4.**
HUVEC were transfected with both HPS1 and HPS4 siRNA on day 0 and again on day2, alongside Rab27a-GFP (green) in panel **B**. Cells were fixed, permeabilised and immunolabelled for VWF (red), P-selectin (blue – **A**) and CD63 (blue – **B**). Images are confocal sections. Scale bars represent 10μm.

5.2.6 BLOC-3 and exocytosis

As with BLOC-2, the effect of BLOC-3 depletion on the regulated exocytosis of WPB was analysed. The secretion assay followed by an ELISA was used to analyse function in both HEK293 cells and HUVEC. No effect could be observed for either HPS1 or HPS4, or when both components of BLOC-3 were knockdown together (Figure 5.17).

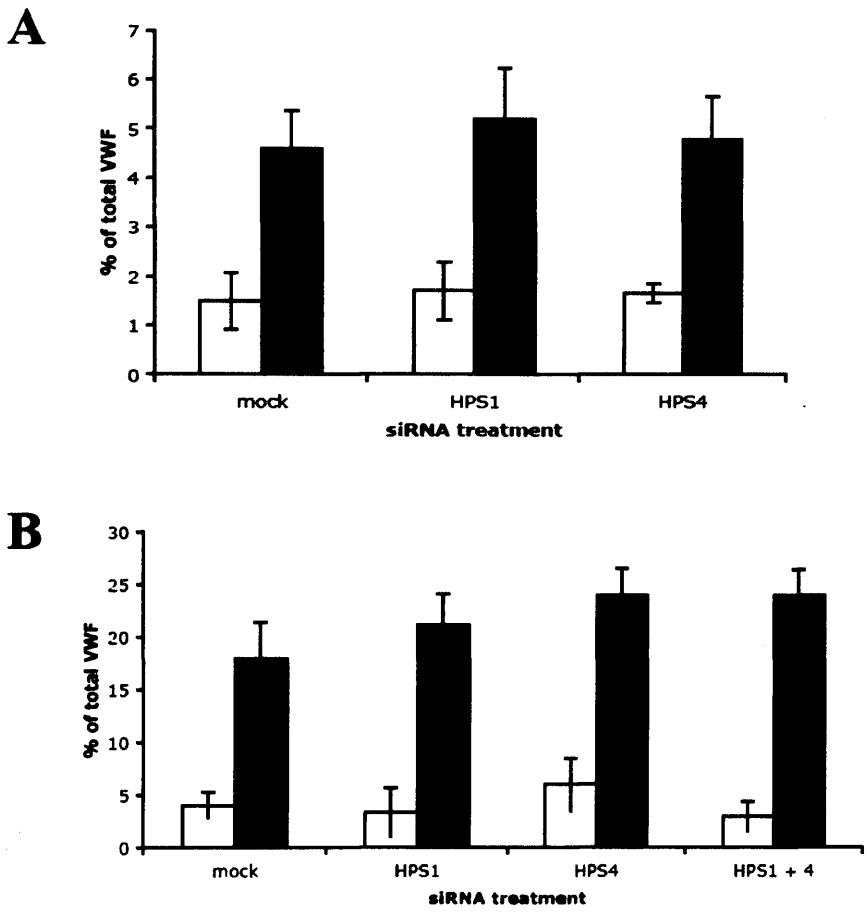

Figure 3.18 **Depletion of BLOC-3 has no effect on WPB exocytosis.**
HEK 293 cells (A) and HUVEC (B) were nucleofected with HPS1 and 4, individually and in concert, on day 0 and day 2, and alongside VWF in the HEK293 cells. On day 4 the cells were incubated in release medium, firstly without and then with PMA for 30 minutes, then finally the cells were lysed to allow total VWF to be measured. All values are normalised to total cellular VWF and the constitutive portion is subtracted from total stimulated release to calculate the PMA responsive pool.

5.2.7 BLOC-3, LAMP-1 and CD63

The best-studied defect resulting from an absence of either BLOC-3 protein is the

altered localisation of the LAMP-1 protein. It was shown that LAMP-1 is still targeted to lysosomes but the lysosomes themselves are found to be more perinuclear (Falcon-Perez et al., 2005; Nazarian et al., 2003). Therefore the LAMP-1 localisation was established in BLOC-3 knockdown cells. In the fibroblasts, LAMP-1 shows a more perinuclear localisation in the knockout cells compared with control cells and this is caused by a defect in the movement of the lysosomes. Interestingly, in the BLOC-3 knockdown cells, where both HPS1 and HPS4 are knockdown together there seems to be an increased clustering of the lysosomes compared with mock transfected cells (Figure 5.18). The pattern of localisation is also likely to be a result of a defect in the movement of the lysosomes.

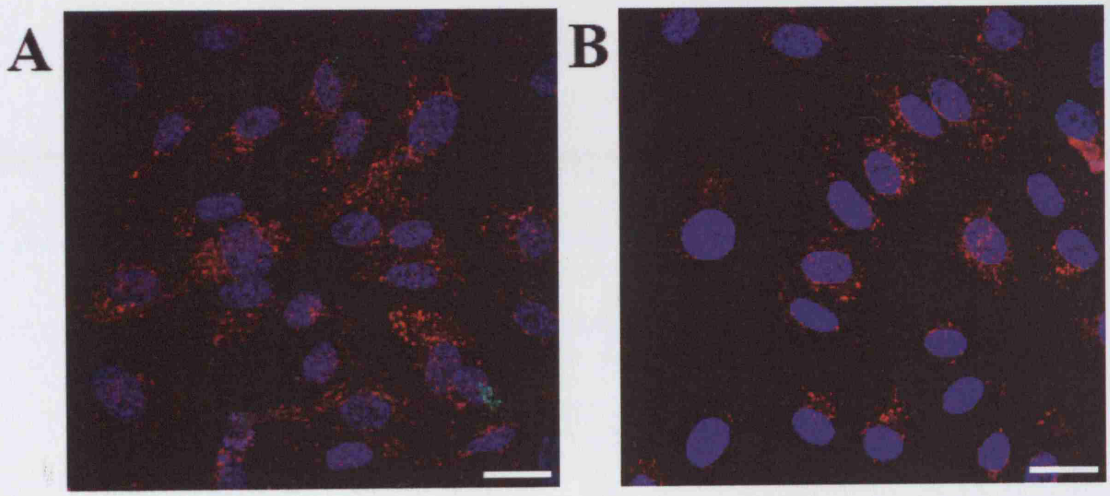

Figure 5.18 **LAMP-1 positive lysosome are more clustered after BLOC-3 knockdown**
Cells were treated with two rounds of nucleofection with scrambled siRNA (**A**) and HPS1 and HPS4 siRNA (**B**) after which they were analysed by immunofluorescence and labelled for LAMP-1 (red) and stained with DAPI (blue). Scale bars represent 25μm.

This suggests that the knockdown is effective at the protein level as well as at the mRNA level and these two cells types have a common mechanism for the movement of lysosomes, which is dependent on BLOC-3. However, this mechanism is not required for the movement of WPB since Figure 5.16 shows no perinuclear clustering of VWF positive structures. Likewise no perinuclear clustering of melanosomes or lytic granules has been reported.

5.2.8 BLOC-2 and BLOC-3 double knockdown

Finally, HPS3 and HPS1 of BLOC-2 and BLOC-3 respectively were knocked down in concert to elucidate if there is any redundancy between the two complexes that could mask any effects seen in the single knockdowns. However, Figure 5.19 shows that P-selectin (A), CD63 (B) and Rab27a (C) are all localised normally to WPB and the distribution of WPB throughout the cell is similar to the mock transfected cells (Figure 5.19).

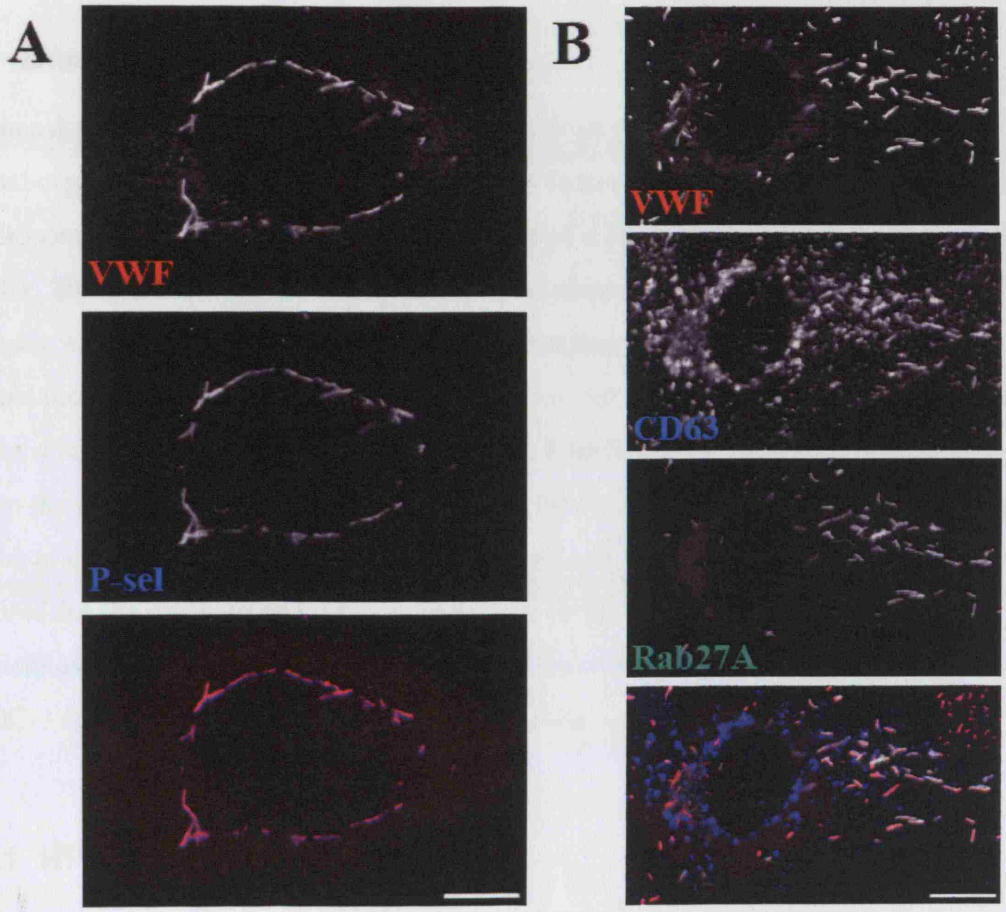

Figure 5.19 **Simultaneous depletion of BLOC-2 and BLOC-3 has no effect on recruitment of membrane proteins to WPB**
HUVEC were transfected with both HPS3 and HPS1 siRNA on day 0 and again on day2, alongside Rab27a-GFP (green) in panel **B**. Cells were fixed, permeabilised and immunolabelled for VWF (red), P-selectin (blue – **A**) and CD63 (blue – **B**). Images are confocal sections. Scale bars represent 10μm.

confocal sections. Scale bars represent 10μm.

5.3 Discussion

Hermansky-Pudlak syndrome is one of a number of syndromes affecting lysosome-related organelles. This, along with the shared features such as low pH and recruitment of lysosomal membrane proteins, is suggestive of a common mechanism for biogenesis (Cutler, 2002; Dell'Angelica et al., 2000). The most outwardly obvious feature of these diseases, and in particular HPS, is albinism Thus much of the research has focussed on the melanosome, given the obvious pigmentation defect, involving the use of mouse coat colour mutants. HPS patients also suffer from bleeding disorders, which is thought to be due to the absence of platelet dense granules. Of course a bleeding disorder could also be due to defects in the biogenesis and exocytosis of WPB. Indeed HPS2 (AP-3beta) is required for the delivery of CD63 to WPB and HPS2 and BLOC-1 are required for efficient exocytosis (Harrison-Lavoie et al., 2006). However, neither BLOC-2 nor BLOC-3 seem to be required for WPB biogenesis.

5.3.1 HPS3 and clathrin

Whilst the BLOC proteins have been described as containing no recognisable domains, this is not completely accurate. HPS3 has a predicted clathrin-binding domain (NCBI prediction) and more recently has indeed been shown to interact with clathrin through this domain in fibroblasts (Helip-Wooley et al., 2005). This is particularly interesting since, as discussed in the introduction and in chapter 3, WPB biogenesis requires clathrin and the adaptor AP-1. The initial co-localisation studies in Figure 5.3 show no obvious overlap between HPS3 and VWF, however the association of clathrin itself is relatively transient. In contrast, the finding that the depletion of HPS3 mRNA with HPS3-1 siRNA results in the loss of WPB from HUVEC (Figure 5.6 and 5.7) suggested that perhaps HPS3 might have a role to play alongside clathrin. However, further investigations found that HPS3 and clathrin do not interact in endothelial cells (Figure 5.5) and the effects of HPS3-1 siRNA were off target effects. Treatment of HPS3-1 transfected HUVEC with MG-132, a proteasome inhibitor, caused the accumulation of

VWF in small clustered puncta (data not shown). Two of the proteins flagged by the seed locator may be of interest. Firstly, the VWF A domain containing variant 1, which is a member of a superfamily of proteins containing the VWF A domain. However, whether this protein has any role in the formation of WPB is unclear, since the family member are involved in a number of cellular processes including cell adhesion, the immune response and, of course haemostasis (Colombatti and Bonaldo, 1991). Another seed match for the HPS3-1 siRNA is Rab36. Whilst the function of Rab36 has not been described it is localised to the Golgi (Mori et al., 1999) and thus may be required for Golgi function and thus the off-target phenotype could result from a generally Golgi defect. This could be tested by determining ssHRP release in these HPS3-1 siRNA treated cells.

5.3.2 BLOC-2 is not involved in WPB biogenesis

The results of both the secretion assay (Figure 5.11) and the normal localisation of the known WPB membrane proteins (Figures 5.8 – 5.10 and 5.12) indicates that BLOC-2 is not required in the biogenesis of WPB. This is in contrast to that observed in the melanocytes, where delivery of CD63 to the melanosome is, in part, dependent on BLOC-2 (Di Pietro et al., 2006). In WPB, it seems that only AP-3 is required for the delivery of CD63 and there is no additive effect of knockdown of AP-3 and BLOC-2.

5.3.3 The function of BLOC-3 in endothelial cells

The assays used in this study also indicate BLOC-3 is not involved in the biogenesis of WPB (Figures 5.15 – 5.19). However, it does seem to affect the localisation of lysosomes (Figure 5.20). In contrast to the observed result in the knockout fibroblasts that the lysosomes are less clustered around the nucleus in the knockout cells, the lysosomes in the BLOC-3 depleted endothelial cells are more clustered around the nucleus compared to the cells treated with control siRNA. It is likely that this represents the same defect in movement, but simply reflects a cell type specific variation in the 'normal' localisation of lysosomes. Falcon-Perez et al. suggest that BLOC-3 is involved

in linking the lysosomes to the cytoskeleton and find that the lysosomes in the knockout cells have a lower frequency of movement than the wild type cells (Falcon-Perez et al., 2005). The movement of the LRO must be regulated in a different fashion since there has been no reports of melanosomal clustering and Figures 5.15-5.17 show no abnormal clustering of WPB. Furthermore, any defect in movement would likely be identified by a decrease in stimulated release of VWF, which is not found. It is perhaps unsurprising that an organelle such as the WPB, which must be primed for immediate release, requires different machinery for movement than the lysosome. It is possible that BLOC-3 also plays a role in the movement of WPB, but that there is greater redundancy in this pathway so defects would be more difficult to detect.

5.3.4 LRO – the differences

The initial hypothesis, and the reason for initiating this study was because there are a number of diseases that effect multiple LRO. The BLOC proteins, which are implicated in Hermansky-Pudlak syndrome, were good candidates for involvement in the biogenesis of WPB since it had already been demonstrated that HPS2 (AP-3beta) was required for the delivery of CD63 to the WPB. However, whilst BLOC-1 is implicated in WPB exocytosis, this study could find no role for either BLOC-2 or BLOC-3. Therefore, whilst there may be some shared features amongst LRO, the overall molecular mechanism and the relative importance of individual components is quite different. This is perhaps unsurprising given the difference in biogenesis between melanosomes and WPB. Whilst the melanosome matures from an endosome, the WPB forms more directly from the TGN and recruits VWF and P-selectin at this early stage (Marks and Seabra, 2001; Raposo and Marks, 2007; Sengel and Stoebner, 1970; Vischer and Wagner, 1994). Indeed the essential role that VWF plays in the formation of the WPB, highlighted by the fact it is sufficient to drive formation in a heterologous system (Blagoveshchenskaya et al., 2002; Michaux et al., 2003; Wagner et al., 1991) and the importance of tubulation of VWF for the elongation and function of the WPB, may mean that other cytoplasmic components are less important. However, despite the finding that neither BLOC-2 or BLOC-3 are not required for WPB formation and

function, it would be interesting to image the WPB depleted of the BLOC-2 and BLOC-3 proteins, using EM after HPF-FS to see if they become electron dense.

5.3.5 Use of siRNA

Of course there are some obvious weaknesses in this study that could contribute to the finding that neither BLOC-2 or BLOC-3 are required for WPB biogenesis. Firstly the use of siRNA rather than true knockouts means that some protein would remain in the cells, and since it is known that these proteins are expressed at low levels, a small amount of protein may be sufficient to perform the function of the protein. Furthermore, the use of qPCR to detect knockdown at the mRNA level rather than using antibodies means it is impossible to quantify exactly how much protein remains in the cell. Antibodies against BLOC-2 and BLOC-3 were obtained from E. Dell'Angelica. However when the cell lysates were western blotted there were a lot of non-specific bands, but no bands of the expected sizes (see Appendix II). Nevertheless, the effect on the lysosome localisation in the BLOC-3 knockdown cells suggests that the knockdown is sufficient to have an effect at the protein level. Also the successful use of this technique in elucidating the role of HPS2 (AP-3beta) in the delivery of CD63, as well as the requirement for BLOC-1 in efficient stimulation exocytosis indicates that the use of this technique is valid.

6 Summary and Discussion

In this thesis, the formation and maturation of WPB is described at the ultrastructural level, using HUVEC fixed by high pressure freezing and processed by freeze substitution. The major new findings from using this technique, rather than conventional chemical fixation are: 1) VWF tubulates in clathrin-coated protusions in the TGN; 2) the WPB remain attached to the TGN via stalk-like structures before final scission occurs; 3) tubules in the immature WPB are disorganised; 4) VWF undergoes progressive condensation, leading to denser and denser WPB; 5) clathrin has a second role in biogenesis, hypothesised to be retrieving missorted material, as well as a scaffold for WPB formation. Finally, in concert with light microscopy, measurement of immature and mature WPB suggests that WPB may undergo homotypic fusion. This data is supported by movies of VWF-GFP, and EM micrographs suggestive of fusion (Chapter 3).

A key of advantage of the use of HPF-FS, is the ability to preserve the relationship between the forming WPB and the TGN and gave an indication of the complexity of the process. However, no description of molecular machinery involved in the initial formation of WPB, with the exception of clathrin and AP-1, has been made. The experiments described in this thesis suggest a role for actin, possibly alongside Myosin VI, FAPP and dynamin 2 in WPB biogenesis (Chapter 4).

In addition, a candidate approach was taken to identify other proteins that are involved in the maturation of WPB. The Hermansky-Pudlak syndrome proteins are implicated in the biogenesis of other LRO and thus are good candidates. Indeed BLOC-1, as well as HPS2, the beta subunit of AP-3, have been shown to be required for exocytosis. However, the experiments in this thesis indicate that neither BLOC-2 nor BLOC-3 are important in WPB biogenesis (Chapter 5).

6.1 High pressure freezing and WPB biogenesis

There have been some notable advances in recent years in the understanding of WPB

biogenesis. The finding that tubulation of the main component protein, VWF is required for the formation of this uniquely-shaped elongated organelle is particularly interesting (Michaux et al., 2006a). Furthermore, the authors demonstrate that storage of VWF as tubules is functionally important, critical to the orderly release of long platelet-capturing strings of VWF upon exocytosis. In addition, Lui-Roberts et al. (2005) found that AP-1 and clathrin are required for the formation of WPB. These findings indicated a need to examine the relationship between tubules themselves and the tubules and the membrane in the formation of WPB, and to consider the coating of the membrane in the context of tubulation.

It is only possible to examine these relationships using electron microscopy. In HUVEC, fixed using conventional chemical methods, the relationship is uncomplicated; the membrane wrapped directly around a bundle of tubules that are well aligned to each other. These samples also show that it is the immature WPB that are coated with clathrin, but since the connections to the TGN are not well preserved it is not possible to assess the earliest point at which it is required. However, as described in this thesis (Chapter 3), in HUVEC fixed and dehydrated using high pressure freezing and freeze substitution respectively, the findings are somewhat different. The tubulation of VWF within the TGN is consistent with the importance of the interaction between the pro-peptide and mature VWF, in forming WPB. Since the interactions are pH-dependent and the cleavage of the VWF by furin likely occurs within the TGN, a first appearance of the tubules shortly thereafter is in line with these observations (Wagner et al., 1986; Wise et al., 1991; Wise et al., 1988).

The protrusion shown in Figure 3.4 is extensively clathrin-coated, and it would be interesting to investigate if the formation of tubules is dependent on AP-1 and clathrin, given the observation by Lui-Roberts et al. (2005). This could be examined in AP-1 depleted HUVEC or AP-180-C-expressing HUVEC using high pressure freezing and freeze substitution. It is interesting to speculate how AP-1 or clathrin could interact with a secretory protein. It has been demonstrated that VWF can bind P-selectin (Michaux et al., 2006b), which as a membrane protein could potentially interact with AP-1.

However, there is no requirement for P-selectin in HEK293 cells to form WPB upon expression of VWF.

The most dramatic finding of the analysis of HUVEC after HPF-FS is the difference in organelle density between the immature and mature WPB. This seems to be, at least in part due to the loss of the electron-lucent space between the tubules. One attractive hypothesis, as discussed, is that the tubules in the immature WPB are held apart because of the negatively charged sialic acids that they are decorated with, but as the pH becomes more acidic as WPB mature, the repulsion between the negative charges is overcome, allowing the tubules to come into closer contact. This hypothesis could be tested by treated the cells with inhibitors that block the addition of sialic acid such as 2,3-dehydro-2-deoxy-N-acetyl-neuraminic acid, however, upon inhibition of all N-glycosylation using tunicamycin, VWF fails to exit the ER (Wagner et al., 1986). Another hypothesis, although not one that is mutually exclusive of the aforementioned hypothesis, is that some of the increase in density is due to the increased level of multimerisation state from immature to mature WPB. Indeed, the DTT-treated mature WPB are less dense than the untreated mature WPB, but still more dense than the immature ones, however they also demonstrate a loss of the electron-lucent space between the WPB. Finally, increase in electron density could be due to the delivery of additional proteins to the maturing WPB.

Whilst it is known that proteins are delivered to the WPB as they mature, the finding of clathrin-coated buds on the WPB indicate that there is also removal of components from the WPB. This could be retrieval of missorted proteins back to the TGN or constitutive-like secretion, as occurs from the immature secretory granule in AtT20 cells (Dittie et al., 1999; Klumperman et al., 1998; Kuliawat and Arvan, 1992). The GGA proteins are attractive candidates for involvement in the budding events, since the formation of clathrin-coated bud in the secretory granules of neuroendocrine cells is dependent on the GGA proteins. Furthermore, these budding events are essential for the maturation of the secretory granules (Kakhlon et al., 2006). It would be possible to test this either by knocking down the GGAs or by expressing the mutants used in the aforementioned

paper. A secretion assay could be used to determine if the WPB from GGA-deficient cells are no longer able to undergo exocytosis. As well as GGA function, homotypic fusion is also required for the maturation of secretory granules in neuroendocrine cells (Wendler et al., 2001). It would be interesting to investigate whether this is also the case for WPB. Homotypic fusion of the secretory granule is dependent on syntaxin 6. Therefore it would be prudent to determine if syntaxin 6 is localised to WPB and whether either depletion of syntaxin 6 or injection of anti-syntaxin 6 antibodies block WPB fusion. However, it will first be necessary to demonstrate that fusion of WPB occurs using a more robust assay.

It would be intriguing to study other LRO and secretory lysosomes using HPF-FS. It would be particularly interesting to observe the platelet alpha granules, since like the WPB, the alpha granules also contain the highly multimerised form of VWF. The VWF in the alpha granules is also able to form into tubules but granules are round rather than rod shaped, (Cramer et al., 1985) suggesting that it is more than just tubulation that is required to form the elongated WPB. Finally, VWF mutants affecting tubulation and glycosylation should be expressed in HEK293 cells so that the ultrastructure of the resultant WPB can be determined.

6.2 Formation of WPB at the TGN

The improvement in the preservation of the connections between forming WPB and TGN prompted an investigation of the molecular machinery required for the budding of WPB from the TGN. The results in this thesis indicate that the actin cytoskeleton, possibly alongside Myosin VI, FAPP and dynamin 2 may be involved in the formation of WPB. Further experiments are required to confirm the role of the latter components in WPB biogenesis, and this has been previously discussed (Chapter 4). Whilst the elongation of the initial protrusion may depend, in part on the actin cytoskeleton, it is tempting to speculate that the tubulation of VWF may contribute to this process by pushing from within. If tubulation assists actin cytoskeleton, then disrupting tubulation could lead to an increased dependency on the actin. Whilst tubulation is, of course,

required to form elongated WPB, it is not necessary for storage. Thus it should be possible to determine if the formation of the VWF-positive structures formed by expression of the Y87S mutant of VWF, which cannot form tubules, is more or less dependent on the presence of the actin cytoskeleton. Preliminary experiments involving treatment of the cells with cytochalasin D were performed in HEK293 cells with expression of wild type VWF and Y87S, which fails to tubulate (data not shown). However, the kinetics of formation of the VWF-positive structures after the expression of Y87S is somewhat slower than the wild type construct, possible due to slower folding of the mutants proteins, thus experiments will need to be repeated with actin poisons being added later after transfection of the Y87S construct. Of course, it is not possible to formally discount that the effect of loss of actin is not an indirect one. Better characterisation of the role of Myosin VI in the formation of WPB could, if positive, make this possibility less likely.

After elongation of the forming WPB, it is necessary for the WPB to undergo scission from the TGN. Finding that the WPB remains attached to the TGN by a stalk-like structure when they are apparently formed is intriguing. It seems possible that scission from the TGN is a two-step process, possibly because of the width of the WPB compared with a characteristic clathrin-coated vesicle. It would, therefore, be interesting to look at the phenotypes resulting from the expression of FAPP-PH or dynamin 2 K44A mutant proteins at the ultrastructural level. If the hypothesis from Godi et al. (2004) that FAPPs are involved in specification of competency for scission is correct, then it could be that FAPPs are involved in the initial step of the scission reaction, the formation of the stalk. If so, then the cells expressing dynamin K44A may be able to form the stalk, but unable to complete the scission reaction. In this case, it might be predicted that the stalk would be longer in the cells expressing the wild type dynamin. However, this is all highly speculative and the first priority should be to confirm the phenotypes, as discussed in Chapter 4.

Another superfamily of proteins involved in the generation of membrane tubulation that has not been discussed, are the BAR (Bin-Amphiphysin-Rvs) domain proteins, including

amphiphysin and endophilin (Gallop and McMahon, 2005). It is the N-terminal BAR domain of these proteins that are responsible for the membrane binding and deformation, whilst the C-terminal SH3 domain interacts with other proteins, including dynamin 2. Indeed, it has been shown that an antagonist relationship exists between the BAR domain protein (and the F-BAR proteins) and the actin cytoskeleton, plus dynamin, whereby BAR domain proteins promote membrane tubulation, whilst the actin cytoskeleton and dynamin restrict it (Itoh et al., 2005). This thesis suggest a positive role for the actin cytoskeleton in the formation of WPB, however, this does not preclude the need for actin reorganisation in both the initial deformation of the membrane and prior to the fission event. It would be interesting to determine if any of the BAR domain proteins or F-BAR proteins are localised to WPB and play a role in their formation.

6.3 Hermansky-Pudlak syndrome, WPB and other LRO

The designation of WPB as lysosome-related organelles, along with the finding by Harrison-Lavoie et al. (2006), that HPS2 (AP-3 beta) is required for the delivery of CD63 to WPB, make the Hermansky-Pudlak syndrome proteins compelling candidates for involvement in the biogenesis of WPB. However, as described in this thesis (Chapter 5), neither BLOC-2 nor BLOC-3, or any of the individual proteins composing these complexes play a role in the biogenesis of WPB. This must reflect differences in the biogenesis between WPB and melanosomes. Indeed, it has been shown that, not all of the HPS proteins are involved in the formation of other LRO and secretory lysosomes. This includes no requirement for any of the BLOC proteins in the biogenesis of lytic granules, of cytotoxic T-lymphocytes (CTL) (Bossi et al., 2005). It has been suggested that it is because the lytic granule is a secretory lysosome (i.e. there are no separate lysosomes in the CTL) rather than a LRO that its biogenesis machinery differs. However, the finding in this thesis, alongside a newly published result that the platelet alpha granules are unaffected in patients suffering from HPS, caused by defects in BLOC-2 and BLOC-3 components (Huizing et al., 2007), suggest that the molecular machinery is not the same even in systems where the organelle is distinct from the lysosome.

The finding of no requirement for BLOC-2 or BLOC-3 to form alpha granules in platelets is particularly surprising, since the dense granules are absent in the same patients. Both of the platelet granules are formed from multivesicular bodies in the megakarocyte, after which their biogenesis itinerary diverges. The absence of an effect on the alpha granules is interesting since they also contain tubular VWF (Cramer et al., 1985). Of course, tubulation in this case does not drive the formation of an elongated organelle, although the extent of tubulation is not known, as the tubules have only be observed in cross-section. Thus, VWF could be an important driving force in their formation.

Finally, whilst it is obvious by the criteria discussed above that WPB are LRO and they share some of the same molecular machinery with other LRO, their route of formation is very different. Unlike the other LRO, WPB are formed directly at the TGN, where tubulation of VWF is directly responsible for their formation (Michaux et al., 2006a; Sengel and Stoebner, 1970; Vischer and Wagner, 1994). Indeed it could be that the importance of VWF, which means that fewer cytosolic proteins, such as BLOC-2 and BLOC-3 are required for their formation. This final hypothesis, albeit based negative entirely on negative results, brings this study full circle; back to the importance of VWF tubulation in driving the formation of the WPB.

7 Appendix

7.1 Appendix I

```
Path="/Users/Helen/Desktop/200707/cytodactinx_Series00"

for (im=6; im<=7; im++) {

open(Path+im+".tif");
run("Properties...", "unit=pixel pixel_width=1 pixel_height=1");
run("RGB Split");
B=getImageID();
close;
selectImage(B+1);
run("Threshold..."); while (isKeyDown("space")==0) {wait(100);}
run("Create Selection");
getStatistics(a, m);
int=a*m;
print(int);
close;
close;

}
```

7.2 Appendix II

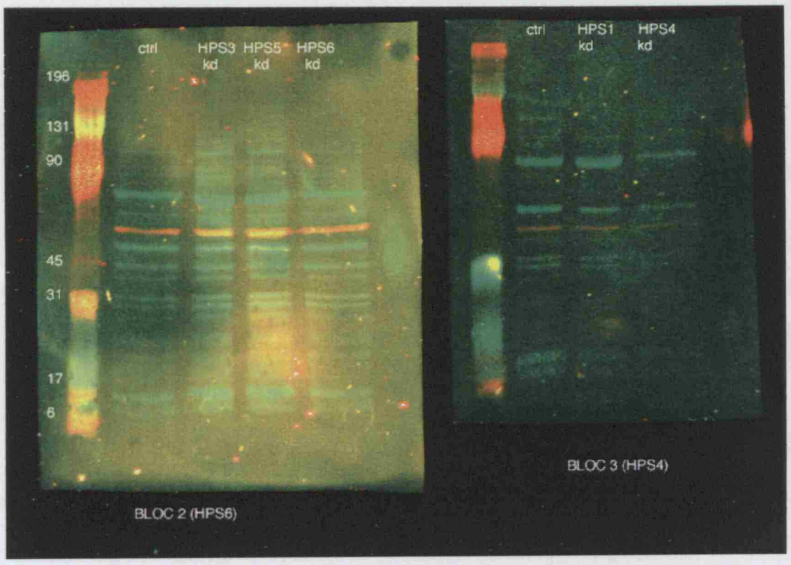

Figure 7.1 ***Antibodies to HPS6 and HPS4 do not recognise specific bands.***

HUVEC were nucleofected with the respective siRNA oligos twice, separated by 48 hours. After a further 48 hours the cells were lysed, and run on a reducing gel. After protein transfer on to nitrocellose the cells were incubated with an anti-HPS6 antibody (green) and anti-actin antibody (red on left) or anti-HPS4 antibody (green) and an anti-tubulin antibody (red on right).

References

Ali, B. R. and Seabra, M. C. (2005). Targeting of Rab GTPases to cellular membranes. *Biochem Soc Trans* **33**, 652-6.

Allen, S., Abuzenadah, A. M., Blagg, J. L., Hinks, J., Nesbitt, I. M., Goodeve, A. C., Gursel, T., Ingerslev, J., Peake, I. R. and Daly, M. E. (2000a). Two novel type 2N von Willebrand disease-causing mutations that result in defective factor VIII binding, multimerization, and secretion of von Willebrand factor. *Blood* **95**, 2000-7.

Allen, S., Abuzenadah, A. M., Hinks, J., Blagg, J. L., Gursel, T., Ingerslev, J., Goodeve, A. C., Peake, I. R. and Daly, M. E. (2000b). A novel von Willebrand disease-causing mutation (Arg273Trp) in the von Willebrand factor propeptide that results in defective multimerization and secretion. *Blood* **96**, 560-8.

Altschuler, Y., Barbas, S. M., Terlecky, L. J., Tang, K., Hardy, S., Mostov, K. E. and Schmid, S. L. (1998). Redundant and distinct functions for dynamin-1 and dynamin-2 isoforms. *J Cell Biol* **143**, 1871-81.

Au, J. S., Puri, C., Ihrke, G., Kendrick-Jones, J. and Buss, F. (2007). Myosin VI is required for sorting of AP-1B-dependent cargo to the basolateral domain in polarized MDCK cells. *J Cell Biol* **177**, 103-14.

Band, A. M., Maatta, J., Kaariainen, L. and Kuismanen, E. (2001). Inhibition of the membrane fusion machinery prevents exit from the TGN and proteolytic processing by furin. *FEBS Lett* **505**, 118-24.

Birmingham, A., Anderson, E. M., Reynolds, A., Ilsley-Tyree, D., Leake, D., Fedorov, Y., Baskerville, S., Maksimova, E., Robinson, K., Karpilow, J. et al. (2006). 3' UTR seed matches, but not overall identity, are associated with RNAi off-targets. *Nat Methods* **3**, 199-204.

Blagoveshchenskaya, A. D., Hannah, M. J., Allen, S. and Cutler, D. F. (2002). Selective and signal-dependent recruitment of membrane proteins to secretory granules formed by heterologously expressed von Willebrand factor. *Mol Biol Cell* **13**, 1582-93.

Boissy, R. E., Richmond, B., Huizing, M., Helip-Wooley, A., Zhao, Y., Koshoffer, A. and Gahl, W. A. (2005). Melanocyte-specific proteins are aberrantly trafficked in melanocytes of Hermansky-Pudlak syndrome-type 3. *Am J Pathol* **166**,

231-40.

Bonazzi, M., Spano, S., Turacchio, G., Cericola, C., Valente, C., Colanzi, A., Kweon, H. S., Hsu, V. W., Polishchuck, E. V., Polishchuck, R. S. et al. (2005). CtBP3/BARS drives membrane fission in dynamin-independent transport pathways. *Nat Cell Biol* **7**, 570-80.

Bonfanti, R., Furie, B. C., Furie, B. and Wagner, D. D. (1989). PADGEM (GMP140) is a component of Weibel-Palade bodies of human endothelial cells. *Blood* **73**, 1109-12.

Borner, G. H., Harbour, M., Hester, S., Lilley, K. S. and Robinson, M. S. (2006). Comparative proteomics of clathrin-coated vesicles. *J Cell Biol* **175**, 571-8.

Bossi, G., Booth, S., Clark, R., Davis, E. G., Liesner, R., Richards, K., Starcevic, M., Stinchcombe, J., Trambas, C., Dell'Angelica, E. C. et al. (2005). Normal lytic granule secretion by cytotoxic T lymphocytes deficient in BLOC-1, -2 and -3 and myosins Va, VIIa and XV. *Traffic* **6**, 243-51.

Brown, J. A., Novak, E. K. and Swank, R. T. (1985). Effects of ammonia on processing and secretion of precursor and mature lysosomal enzyme from macrophages of normal and pale ear mice: evidence for two distinct pathways. *J Cell Biol* **100**, 1894-904.

Burkhard, P., Stetefeld, J. and Strelkov, S. V. (2001). Coiled coils: a highly versatile protein folding motif. *Trends Cell Biol* **11**, 82-8.

Buss, F., Arden, S. D., Lindsay, M., Luzio, J. P. and Kendrick-Jones, J. (2001). Myosin VI isoform localized to clathrin-coated vesicles with a role in clathrin-mediated endocytosis. *Embo J* **20**, 3676-84.

Cao, H., Thompson, H. M., Krueger, E. W. and McNiven, M. A. (2000). Disruption of Golgi structure and function in mammalian cells expressing a mutant dynamin. *J Cell Sci* **113 (Pt 11)**, 1993-2002.

Carreno, S., Engqvist-Goldstein, A. E., Zhang, C. X., McDonald, K. L. and Drubin, D. G. (2004). Actin dynamics coupled to clathrin-coated vesicle formation at the trans-Golgi network. *J Cell Biol* **165**, 781-8.

Clark, R. H., Stinchcombe, J. C., Day, A., Blott, E., Booth, S., Bossi, G., Hamblin, T., Davies, E. G. and Griffiths, G. M. (2003). Adaptor protein 3-dependent microtubule-mediated movement of lytic granules to the immunological synapse. *Nat*

Immunol **4**, 1111-20.

Colombatti, A. and Bonaldo, P. (1991). The superfamily of proteins with von Willebrand factor type A-like domains: one theme common to components of extracellular matrix, hemostasis, cellular adhesion, and defense mechanisms. *Blood* **77**, 2305-15.

Cook, T. A., Urrutia, R. and McNiven, M. A. (1994). Identification of dynamin 2, an isoform ubiquitously expressed in rat tissues. *Proc Natl Acad Sci U S A* **91**, 644-8.

Cramer, E. M., Meyer, D., le Menn, R. and Breton-Gorius, J. (1985). Eccentric localization of von Willebrand factor in an internal structure of platelet alpha-granule resembling that of Weibel-Palade bodies. *Blood* **66**, 710-3.

Cutler, D. F. (2002). Introduction: lysosome-related organelles. *Semin Cell Dev Biol* **13**, 261-2.

Datta, Y. H., Youssoufian, H., Marks, P. W. and Ewenstein, B. M. (1999). Targeting of a heterologous protein to a regulated secretion pathway in cultured endothelial cells. *Blood* **94**, 2696-703.

de Leeuw, H. P., Wijers-Koster, P. M., van Mourik, J. A. and Voorberg, J. (1999). Small GTP-binding protein RalA associates with Weibel-Palade bodies in endothelial cells. *Thromb Haemost* **82**, 1177-81.

Dell'Angelica, E. C. (2004). The building BLOC(k)s of lysosomes and related organelles. *Curr Opin Cell Biol* **16**, 458-64.

Dell'Angelica, E. C., Mullins, C., Caplan, S. and Bonifacino, J. S. (2000). Lysosome-related organelles. *Faseb J* **14**, 1265-78.

Di Pietro, S. M. and Dell'Angelica, E. C. (2005). The cell biology of Hermansky-Pudlak syndrome: recent advances. *Traffic* **6**, 525-33.

Di Pietro, S. M., Falcon-Perez, J. M. and Dell'Angelica, E. C. (2004). Characterization of BLOC-2, a complex containing the Hermansky-Pudlak syndrome proteins HPS3, HPS5 and HPS6. *Traffic* **5**, 276-83.

Di Pietro, S. M., Falcon-Perez, J. M., Tenza, D., Setty, S. R., Marks, M. S., Raposo, G. and Dell'Angelica, E. C. (2006). BLOC-1 interacts with BLOC-2 and the AP-3 complex to facilitate protein trafficking on endosomes. *Mol Biol Cell* **17**, 4027-38.

Dittie, A. S., Klumperman, J. and Tooze, S. A. (1999). Differential distribution

of mannose-6-phosphate receptors and furin in immature secretory granules. *J Cell Sci* **112 (Pt 22)**, 3955-66.

Dong, J. F., Moake, J. L., Nolasco, L., Bernardo, A., Arceneaux, W., Shrimpton, C. N., Schade, A. J., McIntire, L. V., Fujikawa, K. and Lopez, J. A. (2002). ADAMTS-13 rapidly cleaves newly secreted ultralarge von Willebrand factor multimers on the endothelial surface under flowing conditions. *Blood* **100**, 4033-9.

Duden, R., Griffiths, G., Frank, R., Argos, P. and Kreis, T. E. (1991). Beta-COP, a 110 kd protein associated with non-clathrin-coated vesicles and the Golgi complex, shows homology to beta-adaptin. *Cell* **64**, 649-65.

Eaton, B. A., Haugwitz, M., Lau, D. and Moore, H. P. (2000). Biogenesis of regulated exocytotic carriers in neuroendocrine cells. *J Neurosci* **20**, 7334-44.

Edeling, M. A., Smith, C. and Owen, D. (2006). Life of a clathrin coat: insights from clathrin and AP structures. *Nat Rev Mol Cell Biol* **7**, 32-44.

Egea, G., Lazaro-Dieguez, F. and Vilella, M. (2006). Actin dynamics at the Golgi complex in mammalian cells. *Curr Opin Cell Biol* **18**, 168-78.

Ellies, L. G., Ditto, D., Levy, G. G., Wahrenbrock, M., Ginsburg, D., Varki, A., Le, D. T. and Marth, J. D. (2002). Sialyltransferase ST3Gal-IV operates as a dominant modifier of hemostasis by concealing asialoglycoprotein receptor ligands. *Proc Natl Acad Sci U S A* **99**, 10042-7.

Emeis, J. J., van den Eijnden-Schrauwen, Y., van den Hoogen, C. M., de Priester, W., Westmuckett, A. and Lupu, F. (1997). An endothelial storage granule for tissue-type plasminogen activator. *J Cell Biol* **139**, 245-56.

Ewenstein, B. M., Warhol, M. J., Handin, R. I. and Pober, J. S. (1987). Composition of the von Willebrand factor storage organelle (Weibel-Palade body) isolated from cultured human umbilical vein endothelial cells. *J Cell Biol* **104**, 1423-33.

Falcon-Perez, J. M., Nazarian, R., Sabatti, C. and Dell'Angelica, E. C. (2005). Distribution and dynamics of Lamp1-containing endocytic organelles in fibroblasts deficient in BLOC-3. *J Cell Sci* **118**, 5243-55.

Falcon-Perez, J. M., Starcevic, M., Gautam, R. and Dell'Angelica, E. C. (2002). BLOC-1, a novel complex containing the pallidin and muted proteins involved in the biogenesis of melanosomes and platelet-dense granules. *J Biol Chem* **277**, 28191-9.

Fath, K. R., Trimbur, G. M. and Burgess, D. R. (1994). Molecular motors are differentially distributed on Golgi membranes from polarized epithelial cells. *J Cell Biol* **126**, 661-75.

Federici, A. B., Bader, R., Pagani, S., Colibretti, M. L., De Marco, L. and Mannucci, P. M. (1989). Binding of von Willebrand factor to glycoproteins Ib and IIb/IIIa complex: affinity is related to multimeric size. *Br J Haematol* **73**, 93-9.

Feng, L., Seymour, A. B., Jiang, S., To, A., Peden, A. A., Novak, E. K., Zhen, L., Rusiniak, M. E., Eicher, E. M., Robinson, M. S. et al. (1999). The beta3A subunit gene (Ap3b1) of the AP-3 adaptor complex is altered in the mouse hypopigmentation mutant pearl, a model for Hermansky-Pudlak syndrome and night blindness. *Hum Mol Genet* **8**, 323-30.

Fiedler, U., Scharpfenecker, M., Koidl, S., Hegen, A., Grunow, V., Schmidt, J. M., Kriz, W., Thurston, G. and Augustin, H. G. (2004). The Tie-2 ligand angiopoietin-2 is stored in and rapidly released upon stimulation from endothelial cell Weibel-Palade bodies. *Blood* **103**, 4150-6.

Ford, M. G., Pearse, B. M., Higgins, M. K., Vallis, Y., Owen, D. J., Gibson, A., Hopkins, C. R., Evans, P. R. and McMahon, H. T. (2001). Simultaneous binding of PtdIns(4,5)P2 and clathrin by AP180 in the nucleation of clathrin lattices on membranes. *Science* **291**, 1051-5.

Fowler, W. E., Fretto, L. J., Hamilton, K. K., Erickson, H. P. and McKee, P. A. (1985). Substructure of human von Willebrand factor. *J Clin Invest* **76**, 1491-500.

Fu, J., Naren, A. P., Gao, X., Ahmmed, G. U. and Malik, A. B. (2005). Protease-activated receptor-1 activation of endothelial cells induces protein kinase Calpha-dependent phosphorylation of syntaxin 4 and Munc18c: role in signaling p-selectin expression. *J Biol Chem* **280**, 3178-84.

Gallop, J. L. and McMahon, H. T. (2005). BAR domains and membrane curvature: bringing your curves to the BAR. *Biochem Soc Symp*, 223-31.

Gautam, R., Chintala, S., Li, W., Zhang, Q., Tan, J., Novak, E. K., Di Pietro, S. M., Dell'Angelica, E. C. and Swank, R. T. (2004). The Hermansky-Pudlak syndrome 3 (cocoa) protein is a component of the biogenesis of lysosome-related organelles complex-2 (BLOC-2). *J Biol Chem* **279**, 12935-42.

Gautam, R., Novak, E. K., Tan, J., Wakamatsu, K., Ito, S. and Swank, R. T.

(2006). Interaction of Hermansky-Pudlak Syndrome genes in the regulation of lysosome-related organelles. *Traffic* **7**, 779-92.

Giddings, T. H. (2003). Freeze-substitution protocols for improved visualization of membranes in high-pressure frozen samples. *J Microsc* **212**, 53-61.

Godi, A., Di Campli, A., Konstantakopoulos, A., Di Tullio, G., Alessi, D. R., Kular, G. S., Daniele, T., Marra, P., Lucocq, J. M. and De Matteis, M. A. (2004). FAPPs control Golgi-to-cell-surface membrane traffic by binding to ARF and PtdIns(4)P. *Nat Cell Biol* **6**, 393-404.

Gotte, M. and von Mollard, G. F. (1998). A new beat for the SNARE drum. *Trends Cell Biol* **8**, 215-8.

Gralnick, H. R., Coller, B. S. and Sultan, Y. (1976). Carbohydrate deficiency of the factor VIII/von Willebrand factor Protein in von Willebrand's disease variants. *Science* **192**, 56-9.

Greider, M. H., Howell, S. L. and Lacy, P. E. (1969). Isolation and properties of secretory granules from rat islets of Langerhans. II. Ultrastructure of the beta granule. *J Cell Biol* **41**, 162-6.

Haberichter, S. L., Jacobi, P. and Montgomery, R. R. (2003). Critical independent regions in the VWF propeptide and mature VWF that enable normal VWF storage. *Blood* **101**, 1384-91.

Haberichter, S. L., Merricks, E. P., Fahs, S. A., Christopherson, P. A., Nichols, T. C. and Montgomery, R. R. (2005). Re-establishment of VWF-dependent Weibel-Palade bodies in VWD endothelial cells. *Blood* **105**, 145-52.

Hannah, M. J., Hume, A. N., Arribas, M., Williams, R., Hewlett, L. J., Seabra, M. C. and Cutler, D. F. (2003). Weibel-Palade bodies recruit Rab27 by a content-driven, maturation-dependent mechanism that is independent of cell type. *J Cell Sci* **116**, 3939-48.

Harrison-Lavoie, K. J., Michaux, G., Hewlett, L., Kaur, J., Hannah, M. J., Lui-Roberts, W. W., Norman, K. E. and Cutler, D. F. (2006). P-selectin and CD63 use different mechanisms for delivery to Weibel-Palade bodies. *Traffic* **7**, 647-62.

Hausser, A., Storz, P., Martens, S., Link, G., Toker, A. and Pfizenmaier, K. (2005). Protein kinase D regulates vesicular transport by phosphorylating and activating phosphatidylinositol-4 kinase IIIbeta at the Golgi complex. *Nat Cell Biol* **7**, 880-6.

Helip-Wooley, A., Westbroek, W., Dorward, H., Mommaas, M., Boissy, R. E., Gahl, W. A. and Huizing, M. (2005). Association of the Hermansky-Pudlak syndrome type-3 protein with clathrin. *BMC Cell Biol* **6**, 33.

Helip-Wooley, A., Westbroek, W., Dorward, H. M., Koshoffer, A., Huizing, M., Boissy, R. E. and Gahl, W. A. (2007). Improper trafficking of melanocyte-specific proteins in Hermansky-Pudlak syndrome type-5. *J Invest Dermatol* **127**, 1471-8.

Hemler, M. E. (2005). Tetraspanin functions and associated microdomains. *Nat Rev Mol Cell Biol* **6**, 801-11.

Hinshaw, J. E. and Schmid, S. L. (1995). Dynamin self-assembles into rings suggesting a mechanism for coated vesicle budding. *Nature* **374**, 190-2.

Hopkins, S. C., Vale, R. D. and Kuntz, I. D. (2000). Inhibitors of kinesin activity from structure-based computer screening. *Biochemistry* **39**, 2805-14.

Huang, L., Kuo, Y. M. and Gitschier, J. (1999). The pallid gene encodes a novel, syntaxin 13-interacting protein involved in platelet storage pool deficiency. *Nat Genet* **23**, 329-32.

Huber, D., Cramer, E. M., Kaufmann, J. E., Meda, P., Masse, J. M., Kruithof, E. K. and Vischer, U. M. (2002). Tissue-type plasminogen activator (t-PA) is stored in Weibel-Palade bodies in human endothelial cells both in vitro and in vivo. *Blood* **99**, 3637-45.

Huizing, M., Anikster, Y. and Gahl, W. A. (2000). Hermansky-Pudlak syndrome and related disorders of organelle formation. *Traffic* **1**, 823-35.

Huizing, M., Parkes, J. M., Helip-Wooley, A., White, J. G. and Gahl, W. A. (2007). Platelet alpha granules in BLOC-2 and BLOC-3 subtypes of Hermansky-Pudlak syndrome. *Platelets* **18**, 150-7.

Hume, A. N., Collinson, L. M., Rapak, A., Gomes, A. Q., Hopkins, C. R. and Seabra, M. C. (2001). Rab27a regulates the peripheral distribution of melanosomes in melanocytes. *J Cell Biol* **152**, 795-808.

Itoh, T., Erdmann, K. S., Roux, A., Habermann, B., Werner, H. and De Camilli, P. (2005). Dynamin and the actin cytoskeleton cooperatively regulate plasma membrane invagination by BAR and F-BAR proteins. *Dev Cell* **9**, 791-804.

Jones, S. M., Howell, K. E., Henley, J. R., Cao, H. and McNiven, M. A. (1998). Role of dynamin in the formation of transport vesicles from the trans-Golgi

network. *Science* **279**, 573-7.

Jordens, I., Marsman, M., Kuijl, C. and Neefjes, J. (2005). Rab proteins, connecting transport and vesicle fusion. *Traffic* **6**, 1070-7.

Jullien-Flores, V., Dorseuil, O., Romero, F., Letourneur, F., Saragosti, S., Berger, R., Tavitian, A., Gacon, G. and Camonis, J. H. (1995). Bridging Ral GTPase to Rho pathways. RLIP76, a Ral effector with CDC42/Rac GTPase-activating protein activity. *J Biol Chem* **270**, 22473-7.

Kakhlon, O., Sakya, P., Larijani, B., Watson, R. and Tooze, S. A. (2006). GGA function is required for maturation of neuroendocrine secretory granules. *Embo J* **25**, 1590-602.

Kakinuma, T., Ichikawa, H., Tsukada, Y., Nakamura, T. and Toh, B. H. (2004). Interaction between p230 and MACF1 is associated with transport of a glycosyl phosphatidyl inositol-anchored protein from the Golgi to the cell periphery. *Exp Cell Res* **298**, 388-98.

Kerkhoff, E., Simpson, J. C., Leberfinger, C. B., Otto, I. M., Doerks, T., Bork, P., Rapp, U. R., Raabe, T. and Pepperkok, R. (2001). The Spir actin organizers are involved in vesicle transport processes. *Curr Biol* **11**, 1963-8.

Klumperman, J., Kuliawat, R., Griffith, J. M., Geuze, H. J. and Arvan, P. (1998). Mannose 6-phosphate receptors are sorted from immature secretory granules via adaptor protein AP-1, clathrin, and syntaxin 6-positive vesicles. *J Cell Biol* **141**, 359-71.

Knop, M., Aareskjold, E., Bode, G. and Gerke, V. (2004). Rab3D and annexin A2 play a role in regulated secretion of vWF, but not tPA, from endothelial cells. *Embo J* **23**, 2982-92.

Knuehl, C. and Brodsky, F. M. (2003). The long and short of adaptor appendages. *Nat Struct Biol* **10**, 580-2.

Kosaka, T. and Ikeda, K. (1983a). Possible temperature-dependent blockage of synaptic vesicle recycling induced by a single gene mutation in Drosophila. *J Neurobiol* **14**, 207-25.

Kosaka, T. and Ikeda, K. (1983b). Reversible blockage of membrane retrieval and endocytosis in the garland cell of the temperature-sensitive mutant of Drosophila melanogaster, shibirets1. *J Cell Biol* **97**, 499-507.

Kovacs, M., Toth, J., Hetenyi, C., Malnasi-Csizmadia, A. and Sellers, J. R.

(2004). Mechanism of blebbistatin inhibition of myosin II. *J Biol Chem* **279**, 35557-63.

Kuliawat, R. and Arvan, P. (1992). Protein targeting via the "constitutive-like" secretory pathway in isolated pancreatic islets: passive sorting in the immature granule compartment. *J Cell Biol* **118**, 521-9.

Lalli, G., Gschmeissner, S. and Schiavo, G. (2003). Myosin Va and microtubule-based motors are required for fast axonal retrograde transport of tetanus toxin in motor neurons. *J Cell Sci* **116**, 4639-50.

Lazaro-Dieguez, F., Jimenez, N., Barth, H., Koster, A. J., Renau-Piqueras, J., Llopis, J. L., Burger, K. N. and Egea, G. (2006). Actin filaments are involved in the maintenance of Golgi cisternae morphology and intra-Golgi pH. *Cell Motil Cytoskeleton* **63**, 778-91.

Leung, K. F., Baron, R. and Seabra, M. C. (2006). Thematic review series: lipid posttranslational modifications. geranylgeranylation of Rab GTPases. *J Lipid Res* **47**, 467-75.

Li, W., Rusiniak, M. E., Chintala, S., Gautam, R., Novak, E. K. and Swank, R. T. (2004). Murine Hermansky-Pudlak syndrome genes: regulators of lysosome-related organelles. *Bioessays* **26**, 616-28.

Li, W., Zhang, Q., Oiso, N., Novak, E. K., Gautam, R., O'Brien, E. P., Tinsley, C. L., Blake, D. J., Spritz, R. A., Copeland, N. G. et al. (2003). Hermansky-Pudlak syndrome type 7 (HPS-7) results from mutant dysbindin, a member of the biogenesis of lysosome-related organelles complex 1 (BLOC-1). *Nat Genet* **35**, 84-9.

Liljedahl, M., Maeda, Y., Colanzi, A., Ayala, I., Van Lint, J. and Malhotra, V. (2001). Protein kinase D regulates the fission of cell surface destined transport carriers from the trans-Golgi network. *Cell* **104**, 409-20.

Lipschutz, J. H. and Mostov, K. E. (2002). Exocytosis: the many masters of the exocyst. *Curr Biol* **12**, R212-4.

Livak, K. J. and Schmittgen, T. D. (2001). Analysis of relative gene expression data using real-time quantitative PCR and the 2(-Delta Delta C(T)) Method. *Methods* **25**, 402-8.

Lollar, P. (1991). The association of factor VIII with von Willebrand factor. *Mayo Clin Proc* **66**, 524-34.

Lollar, P., Hill-Eubanks, D. C. and Parker, C. G. (1988). Association of the

factor VIII light chain with von Willebrand factor. *J Biol Chem* **263**, 10451-5.

Lopes, V. S., Wasmeier, C., Seabra, M. C. and Futter, C. E. (2007). Melanosome Maturation Defect in Rab38-deficient Retinal Pigment Epithelium Results in Instability of Immature Melanosomes during Transient Melanogenesis. *Mol Biol Cell* **18**, 3914-27.

Lorant, D. E., Topham, M. K., Whatley, R. E., McEver, R. P., McIntyre, T. M., Prescott, S. M. and Zimmerman, G. A. (1993). Inflammatory roles of P-selectin. *J Clin Invest* **92**, 559-70.

Lowenstein, C. J., Morrell, C. N. and Yamakuchi, M. (2005). Regulation of Weibel-Palade body exocytosis. *Trends Cardiovasc Med* **15**, 302-8.

Lui-Roberts, W. W., Collinson, L. M., Hewlett, L. J., Michaux, G. and Cutler, D. F. (2005). An AP-1/clathrin coat plays a novel and essential role in forming the Weibel-Palade bodies of endothelial cells. *J Cell Biol* **170**, 627-36.

Lyerla, T. A., Rusiniak, M. E., Borchers, M., Jahreis, G., Tan, J., Ohtake, P., Novak, E. K. and Swank, R. T. (2003). Aberrant lung structure, composition, and function in a murine model of Hermansky-Pudlak syndrome. *Am J Physiol Lung Cell Mol Physiol* **285**, L643-53.

Macia, E., Ehrlich, M., Massol, R., Boucrot, E., Brunner, C. and Kirchhausen, T. (2006). Dynasore, a cell-permeable inhibitor of dynamin. *Dev Cell* **10**, 839-50.

Manneville, J. B., Etienne-Manneville, S., Skehel, P., Carter, T., Ogden, D. and Ferenczi, M. (2003). Interaction of the actin cytoskeleton with microtubules regulates secretory organelle movement near the plasma membrane in human endothelial cells. *J Cell Sci* **116**, 3927-38.

Marks, M. S. and Seabra, M. C. (2001). The melanosome: membrane dynamics in black and white. *Nat Rev Mol Cell Biol* **2**, 738-48.

Martina, J. A., Moriyama, K. and Bonifacino, J. S. (2003). BLOC-3, a protein complex containing the Hermansky-Pudlak syndrome gene products HPS1 and HPS4. *J Biol Chem* **278**, 29376-84.

Matlin, K. S. and Simons, K. (1983). Reduced temperature prevents transfer of a membrane glycoprotein to the cell surface but does not prevent terminal glycosylation. *Cell* **34**, 233-43.

Matsuda, H. and Sugiura, S. (1970). Ultrastructure of "tubular body" in the endothelial cells of the ocular blood vessels. *Invest Ophthalmol* **9**, 919-25.

Matsushita, K., Morrell, C. N., Cambien, B., Yang, S. X., Yamakuchi, M., Bao, C., Hara, M. R., Quick, R. A., Cao, W., O'Rourke, B. et al. (2003). Nitric oxide regulates exocytosis by S-nitrosylation of N-ethylmaleimide-sensitive factor. *Cell* **115**, 139-50.

Matsushita, K., Yamakuchi, M., Morrell, C. N., Ozaki, M., O'Rourke, B., Irani, K. and Lowenstein, C. J. (2005). Vascular endothelial growth factor regulation of Weibel-Palade-body exocytosis. *Blood* **105**, 207-14.

Mayadas, T., Wagner, D. D. and Simpson, P. J. (1989). von Willebrand factor biosynthesis and partitioning between constitutive and regulated pathways of secretion after thrombin stimulation. *Blood* **73**, 706-11.

Mayadas, T. N. and Wagner, D. D. (1989). In vitro multimerization of von Willebrand factor is triggered by low pH. Importance of the propolypeptide and free sulfhydryls. *J Biol Chem* **264**, 13497-503.

Mayadas, T. N. and Wagner, D. D. (1992). Vicinal cysteines in the prosequence play a role in von Willebrand factor multimer assembly. *Proc Natl Acad Sci U S A* **89**, 3531-5.

McEver, R. P., Beckstead, J. H., Moore, K. L., Marshall-Carlson, L. and Bainton, D. F. (1989). GMP-140, a platelet alpha-granule membrane protein, is also synthesized by vascular endothelial cells and is localized in Weibel-Palade bodies. *J Clin Invest* **84**, 92-9.

Michaux, G., Abbitt, K. B., Collinson, L. M., Haberichter, S. L., Norman, K. E. and Cutler, D. F. (2006a). The physiological function of von Willebrand's factor depends on its tubular storage in endothelial Weibel-Palade bodies. *Dev Cell* **10**, 223-32.

Michaux, G. and Cutler, D. F. (2004). How to roll an endothelial cigar: the biogenesis of Weibel-Palade bodies. *Traffic* **5**, 69-78.

Michaux, G., Hewlett, L. J., Messenger, S. L., Goodeve, A. C., Peake, I. R., Daly, M. E. and Cutler, D. F. (2003). Analysis of intracellular storage and regulated secretion of 3 von Willebrand disease-causing variants of von Willebrand factor. *Blood* **102**, 2452-8.

Michaux, G., Pullen, T. J., Haberichter, S. L. and Cutler, D. F. (2006b). P-

selectin binds to the D'-D3 domains of von Willebrand factor in Weibel-Palade bodies. *Blood* **107**, 3922-4.

Millar, C. M. and Brown, S. A. (2006). Oligosaccharide structures of von Willebrand factor and their potential role in von Willebrand disease. *Blood Rev* **20**, 83-92.

Mori, T., Fukuda, Y., Kuroda, H., Matsumura, T., Ota, S., Sugimoto, T., Nakamura, Y. and Inazawa, J. (1999). Cloning and characterization of a novel Rab-family gene, Rab36, within the region at 22q11.2 that is homozygously deleted in malignant rhabdoid tumors. *Biochem Biophys Res Commun* **254**, 594-600.

Moriyama, K. and Bonifacino, J. S. (2002). Pallidin is a component of a multi-protein complex involved in the biogenesis of lysosome-related organelles. *Traffic* **3**, 666-77.

Moskalenko, S., Henry, D. O., Rosse, C., Mirey, G., Camonis, J. H. and White, M. A. (2002). The exocyst is a Ral effector complex. *Nat Cell Biol* **4**, 66-72.

Musch, A., Cohen, D. and Rodriguez-Boulan, E. (1997). Myosin II is involved in the production of constitutive transport vesicles from the TGN. *J Cell Biol* **138**, 291-306.

Nakata, T., Takemura, R. and Hirokawa, N. (1993). A novel member of the dynamin family of GTP-binding proteins is expressed specifically in the testis. *J Cell Sci* **105 (Pt 1)**, 1-5.

Nazarian, R., Falcon-Perez, J. M. and Dell'Angelica, E. C. (2003). Biogenesis of lysosome-related organelles complex 3 (BLOC-3): a complex containing the Hermansky-Pudlak syndrome (HPS) proteins HPS1 and HPS4. *Proc Natl Acad Sci U S A* **100**, 8770-5.

Neeft, M., Wieffer, M., de Jong, A. S., Negroiu, G., Metz, C. H., van Loon, A., Griffith, J., Krijgsveld, J., Wulffraat, N., Koch, H. et al. (2005). Munc13-4 is an effector of rab27a and controls secretion of lysosomes in hematopoietic cells. *Mol Biol Cell* **16**, 731-41.

Nguyen, T., Novak, E. K., Kermani, M., Fluhr, J., Peters, L. L., Swank, R. T. and Wei, M. L. (2002). Melanosome morphologies in murine models of hermansky-pudlak syndrome reflect blocks in organelle development. *J Invest Dermatol* **119**, 1156-64.

Nguyen, T. and Wei, M. L. (2004). Characterization of melanosomes in murine Hermansky-Pudlak syndrome: mechanisms of hypopigmentation. *J Invest Dermatol* **122**, 452-60.

Oh, J., Ho, L., Ala-Mello, S., Amato, D., Armstrong, L., Bellucci, S., Carakushansky, G., Ellis, J. P., Fong, C. T., Green, J. S. et al. (1998). Mutation analysis of patients with Hermansky-Pudlak syndrome: a frameshift hot spot in the HPS gene and apparent locus heterogeneity. *Am J Hum Genet* **62**, 593-8.

Oh, J., Liu, Z. X., Feng, G. H., Raposo, G. and Spritz, R. A. (2000). The Hermansky-Pudlak syndrome (HPS) protein is part of a high molecular weight complex involved in biogenesis of early melanosomes. *Hum Mol Genet* **9**, 375-85.

Oynebraten, I., Bakke, O., Brandtzaeg, P., Johansen, F. E. and Haraldsen, G. (2004). Rapid chemokine secretion from endothelial cells originates from 2 distinct compartments. *Blood* **104**, 314-20.

Park, J. B. (2001). Regulation of GTP-binding state in RalA through Ca2+ and calmodulin. *Exp Mol Med* **33**, 54-8.

Polishchuk, E. V., Di Pentima, A., Luini, A. and Polishchuk, R. S. (2003). Mechanism of constitutive export from the golgi: bulk flow via the formation, protrusion, and en bloc cleavage of large trans-golgi network tubular domains. *Mol Biol Cell* **14**, 4470-85.

Purvis, A. R. and Sadler, J. E. (2004). A covalent oxidoreductase intermediate in propeptide-dependent von Willebrand factor multimerization. *J Biol Chem* **279**, 49982-8.

Raposo, G. and Marks, M. S. (2007). Melanosomes--dark organelles enlighten endosomal membrane transport. *Nat Rev Mol Cell Biol* **8**, 786-97.

Reipert, S., Fischer, I. and Wiche, G. (2004). High-pressure freezing of epithelial cells on sapphire coverslips. *J Microsc* **213**, 81-5.

Rios, R. M. and Bornens, M. (2003). The Golgi apparatus at the cell centre. *Curr Opin Cell Biol* **15**, 60-6.

Robinson, M. S. and Kreis, T. E. (1992). Recruitment of coat proteins onto Golgi membranes in intact and permeabilized cells: effects of brefeldin A and G protein activators. *Cell* **69**, 129-38.

Rogalski, A. A. and Singer, S. J. (1984). Associations of elements of the Golgi

apparatus with microtubules. *J Cell Biol* **99**, 1092-100.

Romani de Wit, T., Rondaij, M. G., Hordijk, P. L., Voorberg, J. and van Mourik, J. A. (2003). Real-time imaging of the dynamics and secretory behavior of Weibel-Palade bodies. *Arterioscler Thromb Vasc Biol* **23**, 755-61.

Rondaij, M. G., Bierings, R., Kragt, A., van Mourik, J. A. and Voorberg, J. (2006). Dynamics and plasticity of Weibel-Palade bodies in endothelial cells. *Arterioscler Thromb Vasc Biol* **26**, 1002-7.

Rondaij, M. G., Sellink, E., Gijzen, K. A., ten Klooster, J. P., Hordijk, P. L., van Mourik, J. A. and Voorberg, J. (2004). Small GTP-binding protein Ral is involved in cAMP-mediated release of von Willebrand factor from endothelial cells. *Arterioscler Thromb Vasc Biol* **24**, 1315-20.

Rosenberg, J. B., Haberichter, S. L., Jozwiak, M. A., Vokac, E. A., Kroner, P. A., Fahs, S. A., Kawai, Y. and Montgomery, R. R. (2002). The role of the D1 domain of the von Willebrand factor propeptide in multimerization of VWF. *Blood* **100**, 1699-706.

Ruggeri, Z. M. (2007). Von Willebrand factor: looking back and looking forward. *Thromb Haemost* **98**, 55-62.

Sadler, J. E. and Gralnick, H. R. (1994). Commentary: a new classification for von Willebrand disease. *Blood* **84**, 676-9.

Sahlender, D. A., Roberts, R. C., Arden, S. D., Spudich, G., Taylor, M. J., Luzio, J. P., Kendrick-Jones, J. and Buss, F. (2005). Optineurin links myosin VI to the Golgi complex and is involved in Golgi organization and exocytosis. *J Cell Biol* **169**, 285-95.

Salazar, G., Craige, B., Styers, M. L., Newell-Litwa, K. A., Doucette, M. M., Wainer, B. H., Falcon-Perez, J. M., Dell'Angelica, E. C., Peden, A. A., Werner, E. et al. (2006). BLOC-1 complex deficiency alters the targeting of adaptor protein complex-3 cargoes. *Mol Biol Cell* **17**, 4014-26.

Samor, B., Mazurier, C., Goudemand, M., Debeire, P., Fournet, B. and Montreuil, J. (1982). Preliminary results on the carbohydrate moiety of factor VIII/von Willebrand factor (FVIII/vWf). *Thromb Res* **25**, 81-9.

Sarangarajan, R., Budev, A., Zhao, Y., Gahl, W. A. and Boissy, R. E. (2001). Abnormal translocation of tyrosinase and tyrosinase-related protein 1 in cutaneous

melanocytes of Hermansky-Pudlak Syndrome and in melanoma cells transfected with anti-sense HPS1 cDNA. *J Invest Dermatol* **117**, 641-6.

Schnyder-Candrian, S., Borsig, L., Moser, R. and Berger, E. G. (2000). Localization of alpha 1,3-fucosyltransferase VI in Weibel-Palade bodies of human endothelial cells. *Proc Natl Acad Sci U S A* **97**, 8369-74.

Sengel, A. and Stoebner, P. (1970). Golgi origin of tubular inclusions in endothelial cells. *J Cell Biol* **44**, 223-6.

Setty, S. R., Tenza, D., Truschel, S. T., Chou, E., Sviderskaya, E. V., Theos, A. C., Lamoreux, M. L., Di Pietro, S. M., Starcevic, M., Bennett, D. C. et al. (2007). BLOC-1 is required for cargo-specific sorting from vacuolar early endosomes toward lysosome-related organelles. *Mol Biol Cell* **18**, 768-80.

Simon, J. P., Shen, T. H., Ivanov, I. E., Gravotta, D., Morimoto, T., Adesnik, M. and Sabatini, D. D. (1998). Coatomer, but not P200/myosin II, is required for the in vitro formation of trans-Golgi network-derived vesicles containing the envelope glycoprotein of vesicular stomatitis virus. *Proc Natl Acad Sci U S A* **95**, 1073-8.

Sontag, J. M., Fykse, E. M., Ushkaryov, Y., Liu, J. P., Robinson, P. J. and Sudhof, T. C. (1994). Differential expression and regulation of multiple dynamins. *J Biol Chem* **269**, 4547-54.

Spudich, G., Chibalina, M. V., Au, J. S., Arden, S. D., Buss, F. and Kendrick-Jones, J. (2007). Myosin VI targeting to clathrin-coated structures and dimerization is mediated by binding to Disabled-2 and PtdIns(4,5)P2. *Nat Cell Biol* **9**, 176-83.

Stamnes, M. (2002). Regulating the actin cytoskeleton during vesicular transport. *Curr Opin Cell Biol* **14**, 428-33.

Starcevic, M. and Dell'Angelica, E. C. (2004). Identification of snapin and three novel proteins (BLOS1, BLOS2, and BLOS3/reduced pigmentation) as subunits of biogenesis of lysosome-related organelles complex-1 (BLOC-1). *J Biol Chem* **279**, 28393-401.

Starcevic, M., Nazarian, R. and Dell'Angelica, E. C. (2002). The molecular machinery for the biogenesis of lysosome-related organelles: lessons from Hermansky-Pudlak syndrome. *Semin Cell Dev Biol* **13**, 271-8.

Stephens, D. J. and Banting, G. (1999). Direct interaction of the trans-Golgi

network membrane protein, TGN38, with the F-actin binding protein, neurabin. *J Biol Chem* **274**, 30080-6.

Stinchcombe, J. C., Barral, D. C., Mules, E. H., Booth, S., Hume, A. N., Machesky, L. M., Seabra, M. C. and Griffiths, G. M. (2001). Rab27a is required for regulated secretion in cytotoxic T lymphocytes. *J Cell Biol* **152**, 825-34.

Stowell, M. H., Marks, B., Wigge, P. and McMahon, H. T. (1999). Nucleotide-dependent conformational changes in dynamin: evidence for a mechanochemical molecular spring. *Nat Cell Biol* **1**, 27-32.

Straight, A. F., Cheung, A., Limouze, J., Chen, I., Westwood, N. J., Sellers, J. R. and Mitchison, T. J. (2003). Dissecting temporal and spatial control of cytokinesis with a myosin II Inhibitor. *Science* **299**, 1743-7.

Studer, D., Graber, W., Al-Amoudi, A. and Eggli, P. (2001). A new approach for cryofixation by high-pressure freezing. *J Microsc* **203**, 285-94.

Tabb, J. S., Molyneaux, B. J., Cohen, D. L., Kuznetsov, S. A. and Langford, G. M. (1998). Transport of ER vesicles on actin filaments in neurons by myosin V. *J Cell Sci* **111 (Pt 21)**, 3221-34.

Takei, K., McPherson, P. S., Schmid, S. L. and De Camilli, P. (1995). Tubular membrane invaginations coated by dynamin rings are induced by GTP-gamma S in nerve terminals. *Nature* **374**, 186-90.

Thorlacius, H., Lindbom, L. and Raud, J. (1997). Cytokine-induced leukocyte rolling in mouse cremaster muscle arterioles in P-selectin dependent. *Am J Physiol* **272**, H1725-9.

Thyberg, J. and Moskalewski, S. (1999). Role of microtubules in the organization of the Golgi complex. *Exp Cell Res* **246**, 263-79.

Titani, K., Kumar, S., Takio, K., Ericsson, L. H., Wade, R. D., Ashida, K., Walsh, K. A., Chopek, M. W., Sadler, J. E. and Fujikawa, K. (1986). Amino acid sequence of human von Willebrand factor. *Biochemistry* **25**, 3171-84.

Tjernberg, P., Vos, H. L., Castaman, G., Bertina, R. M. and Eikenboom, J. C. (2004). Dimerization and multimerization defects of von Willebrand factor due to mutated cysteine residues. *J Thromb Haemost* **2**, 257-65.

Toivola, D. M., Tao, G. Z., Habtezion, A., Liao, J. and Omary, M. B. (2005). Cellular integrity plus: organelle-related and protein-targeting functions of intermediate

filaments. *Trends Cell Biol* **15**, 608-17.

Traub, L. M. (2005). Common principles in clathrin-mediated sorting at the Golgi and the plasma membrane. *Biochim Biophys Acta* **1744**, 415-37.

Tsai, H. M., Nagel, R. L., Hatcher, V. B., Seaton, A. C. and Sussman, II. (1991). The high molecular weight form of endothelial cell von Willebrand factor is released by the regulated pathway. *Br J Haematol* **79**, 239-45.

Valentijn, K. M., Valentijn, J. A., Jansen, K. A. and Koster, A. J. (2007). A new look at Weibel-Palade body structure in endothelial cells using electron tomography. *J Struct Biol.*

van der Bliek, A. M. and Meyerowitz, E. M. (1991). Dynamin-like protein encoded by the Drosophila shibire gene associated with vesicular traffic. *Nature* **351**, 411-4.

Vischer, U. M. and Wagner, D. D. (1993). CD63 is a component of Weibel-Palade bodies of human endothelial cells. *Blood* **82**, 1184-91.

Vischer, U. M. and Wagner, D. D. (1994). von Willebrand factor proteolytic processing and multimerization precede the formation of Weibel-Palade bodies. *Blood* **83**, 3536-44.

Vlot, A. J., Koppelman, S. J., Bouma, B. N. and Sixma, J. J. (1998). Factor VIII and von Willebrand factor. *Thromb Haemost* **79**, 456-65.

Voorberg, J., Fontijn, R., Calafat, J., Janssen, H., van Mourik, J. A. and Pannekoek, H. (1991). Assembly and routing of von Willebrand factor variants: the requirements for disulfide-linked dimerization reside within the carboxy-terminal 151 amino acids. *J Cell Biol* **113**, 195-205.

Wagner, D. D., Mayadas, T. and Marder, V. J. (1986). Initial glycosylation and acidic pH in the Golgi apparatus are required for multimerization of von Willebrand factor. *J Cell Biol* **102**, 1320-4.

Wagner, D. D., Mayadas, T., Urban-Pickering, M., Lewis, B. H. and Marder, V. J. (1985). Inhibition of disulfide bonding of von Willebrand protein by monensin results in small, functionally defective multimers. *J Cell Biol* **101**, 112-20.

Wagner, D. D., Olmsted, J. B. and Marder, V. J. (1982). Immunolocalization of von Willebrand protein in Weibel-Palade bodies of human endothelial cells. *J Cell Biol* **95**, 355-60.

Wagner, D. D., Saffaripour, S., Bonfanti, R., Sadler, J. E., Cramer, E. M., Chapman, B. and Mayadas, T. N. (1991). Induction of specific storage organelles by von Willebrand factor propolypeptide. *Cell* **64**, 403-13.

Wang, K. L., Khan, M. T. and Roufogalis, B. D. (1997). Identification and characterization of a calmodulin-binding domain in Ral-A, a Ras-related GTP-binding protein purified from human erythrocyte membrane. *J Biol Chem* **272**, 16002-9.

Warner, C. L., Stewart, A., Luzio, J. P., Steel, K. P., Libby, R. T., Kendrick-Jones, J. and Buss, F. (2003). Loss of myosin VI reduces secretion and the size of the Golgi in fibroblasts from Snell's waltzer mice. *Embo J* **22**, 569-79.

Wei, M. L. (2006). Hermansky-Pudlak syndrome: a disease of protein trafficking and organelle function. *Pigment Cell Res* **19**, 19-42.

Weibel, E. R. and Palade, G. E. (1964). New Cytoplasmic Components in Arterial Endothelia. *J Cell Biol* **23**, 101-12.

Weigert, R., Silletta, M. G., Spano, S., Turacchio, G., Cericola, C., Colanzi, A., Senatore, S., Mancini, R., Polishchuk, E. V., Salmona, M. et al. (1999). CtBP/BARS induces fission of Golgi membranes by acylating lysophosphatidic acid. *Nature* **402**, 429-33.

Wendler, F., Page, L., Urbe, S. and Tooze, S. A. (2001). Homotypic fusion of immature secretory granules during maturation requires syntaxin 6. *Mol Biol Cell* **12**, 1699-709.

Wilson, S. M., Yip, R., Swing, D. A., O'Sullivan, T. N., Zhang, Y., Novak, E. K., Swank, R. T., Russell, L. B., Copeland, N. G. and Jenkins, N. A. (2000). A mutation in Rab27a causes the vesicle transport defects observed in ashen mice. *Proc Natl Acad Sci U S A* **97**, 7933-8.

Wise, R. J., Dorner, A. J., Krane, M., Pittman, D. D. and Kaufman, R. J. (1991). The role of von Willebrand factor multimers and propeptide cleavage in binding and stabilization of factor VIII. *J Biol Chem* **266**, 21948-55.

Wise, R. J., Pittman, D. D., Handin, R. I., Kaufman, R. J. and Orkin, S. H. (1988). The propeptide of von Willebrand factor independently mediates the assembly of von Willebrand multimers. *Cell* **52**, 229-36.

Wixler, V., Laplantine, E., Geerts, D., Sonnenberg, A., Petersohn, D., Eckes, B., Paulsson, M. and Aumailley, M. (1999). Identification of novel interaction partners

for the conserved membrane proximal region of alpha-integrin cytoplasmic domains. *FEBS Lett* **445**, 351-5.

Wolff, B., Burns, A. R., Middleton, J. and Rot, A. (1998). Endothelial cell "memory" of inflammatory stimulation: human venular endothelial cells store interleukin 8 in Weibel-Palade bodies. *J Exp Med* **188**, 1757-62.

Wu, X., Bowers, B., Wei, Q., Kocher, B. and Hammer, J. A., 3rd. (1997). Myosin V associates with melanosomes in mouse melanocytes: evidence that myosin V is an organelle motor. *J Cell Sci* **110 (Pt 7)**, 847-59.

Wu, X., Rao, K., Bowers, M. B., Copeland, N. G., Jenkins, N. A. and Hammer, J. A., 3rd. (2001). Rab27a enables myosin Va-dependent melanosome capture by recruiting the myosin to the organelle. *J Cell Sci* **114**, 1091-100.

Yang, W., Li, C., Ward, D. M., Kaplan, J. and Mansour, S. L. (2000). Defective organellar membrane protein trafficking in Ap3b1-deficient cells. *J Cell Sci* **113 (Pt 22)**, 4077-86.

Yeaman, C., Ayala, M. I., Wright, J. R., Bard, F., Bossard, C., Ang, A., Maeda, Y., Seufferlein, T., Mellman, I., Nelson, W. J. et al. (2004). Protein kinase D regulates basolateral membrane protein exit from trans-Golgi network. *Nat Cell Biol* **6**, 106-12.

Zannettino, A. C., Holding, C. A., Diamond, P., Atkins, G. J., Kostakis, P., Farrugia, A., Gamble, J., To, L. B., Findlay, D. M. and Haynes, D. R. (2005). Osteoprotegerin (OPG) is localized to the Weibel-Palade bodies of human vascular endothelial cells and is physically associated with von Willebrand factor. *J Cell Physiol* **204**, 714-23.

Zenner, H. L., Collinson, L. M., Michaux, G. and Cutler, D. F. (2007). High-pressure freezing provides insights into Weibel-Palade body biogenesis. *J Cell Sci* **120**, 2117-25.

Zhang, Q., Zhao, B., Li, W., Oiso, N., Novak, E. K., Rusiniak, M. E., Gautam, R., Chintala, S., O'Brien, E. P., Zhang, Y. et al. (2003). Ru2 and Ru encode mouse orthologs of the genes mutated in human Hermansky-Pudlak syndrome types 5 and 6. *Nat Genet* **33**, 145-53.